René Corbet, BSc. MSc.

# Improvements to the Pipeline of Multiparameter Persistence

**Doctoral Thesis**

to achieve the university degree of

Doktor der technischen Wissenschaften

submitted to

**Graz University of Technology**

Supervisor

Univ.-Prof. Dr.-Ing. Michael Kerber

Institute of Geometry

Graz, May 2020

## Eidesstattliche Erklärung

Ich erkläre an Eides statt, dass ich die vorliegende Arbeit selbstständig verfasst, andere als die angegebenen Quellen/Hilfsmittel nicht benutzt, und die den benutzten Quellen wörtlich und inhaltlich entnommenen Stellen als solche kenntlich gemacht habe. Das in TUGRAZonline hochgeladene Textdokument ist mit der vorliegenden Dissertation identisch.

25.05.2020 — Datum

R. — Unterschrift

## Affidavit

I declare that I have authored this thesis independently, that I have not used other than the declared sources/resources, and that I have explicitly indicated all material which has been quoted either literally or by content from the sources used. The text document uploaded to TUGRAZonline is identical to the present thesis.

May 25, 2020 — Date

R. — Signature

# Acknowledgements

First and foremost, I am deeply grateful to my supervisor, Michael Kerber. His guidance was extremely valuable at every stage of my PhD studies. Michael shared many eye-opening ideas and practically uncountable hours of inspiring discussions with me. I tried my best to follow his patient and expedient advice to develop computational perspectives, to become better at coding, and to improve my scientific writing. He supported me anytime, gave an immense amount of freedom, and generated pressure only when necessary, which all helped me to make progress.

I would like to thank Wojciech Chachólski and Herbert Edelsbrunner for agreeing to evaluate my thesis.

I very much appreciate I had the chance to work with Michael Lesnick. When I visited him at SUNY Albany for three and a half months, I did not only learn about various intriguing mathematical approaches and techniques, but also that it makes sense to be a mathematical optimist.
Mike welcomed me very warmly in Albany. This is also true for Justin Curry, who was my landlord at that time. I also enjoyed talking to Robert Cardona and Jordan DeSha. These are further reasons why this time has become a great experience.

I would also like to thank my collaborators, Ulderico Fugacci, Claudia Landi, and Bei Wang. In our joint project it was especially instructive for me to understand how to focus on suitable solutions when the variety of options seems to be confusingly large.

Working at the Institute of Geometry at TU Graz was a pleasure. I thank Mickaël Buchet, Felix Dellinger, Bianca Dornelas, Ulderico Fugacci, Anton Gfrerrer, Svenja Hüning, Johann Lang, Alexander Rolle, Otto Röschel, and Johannes Wallner, and especially my office mates Leonardo Alese, Arnur Nigmetov, and Hannah Schreiber. The friendly and respectful atmosphere made good times be more fun and hard times be less hard.

I acknowledge all sources of funding I received. My position was funded by the Austrian Science Fund (FWF) grant number P 29984-N35. During

the last ten months of my studies I was an associated student in the the Doctoral Program “Discrete Mathematics” at TU Graz funded by the Austrian Science Fund (FWF) grant number W1230. My stay in Albany was partially funded by a scholarship granted by the Austrian Marshall Plan Foundation. I also thank the organizers of the Tutorial on Multiparameter Persistence at the IMA, the NSF-CBMS Conference on Topological Methods in Machine Learning and Artificial Intelligence at the College of Charleston, and the Summer Graduate School on Representation Stability at the MSRI, respectively, for allowing me to participate and for providing funding for the expenses.

Last but not least, I owe deep gratitude to my parents and grandparents for raising me plenty of years ago and supporting me throughout my studies.

Abstract. In the last two decades, persistent homology and its generalizations have grown to a substantial branch of mathematical research. It gives rise to various research problems in algebra, category theory, geometry, topology, and other areas. Moreover, since persistent homology has immediate applications in data science, efficient algorithms, computational and probabilistic methods, and concrete implementations deserve the same amount of attention. Multiparameter persistence is the generalization of persistence to multiple independent parameters taken into account at once. Since the theory of multiparameter persistence is provably much more complicated than the theory of ordinary persistence, new computational challenges arise as well. We give answers to questions for several different tasks in multiparameter persistence, including theoretical results, computational results, and results for novel approaches towards applications.

Zusammenfassung. Durch persistente Homologie und ihre Verallgemeinerungen wurde in den letzten zwei Jahrzehnten eine eigenständige mathematische Forschungsrichtung begründet. Es ergeben sich vielfältige Fragestellungen, unter anderem in Algebra, Kategorientheorie, Geometrie und Topologie. Da sich die Theorie direkt für Anwendungen in der Datenanalyse eignet, sind numerische und probabilistische Methoden sowie das Design von effizienten Algorithmen und nützlichen Implementierungen von derselben Wichtigkeit. Die gleichzeitige Betrachtung mehrerer unabhängiger Kenngrößen im Kontext der Persistenz nennt man Multiparameter Persistenz. Wie man leicht sieht, ist die mathematische Theorie in diesen Fällen deutlich komplizierter. Auch deshalb ergeben sich darüber hinaus im Zuge der Bereitstellung der Theorie für Anwendungen neue und schwierigere Problemstellungen. In dieser Arbeit lösen wir bislang offene Fragen, die sich über theoretische und numerische Aspekte sowie neue Ansätze für Anwendungen erstrecken.

# Contents

# 1 Introduction

*Persistence* is a multiscale extension of a functor. Formally, given a functor $H : \mathbf{C} \to \mathbf{D}$ and a totally ordered set $P$, persistence of $H$ can be defined to be the concatenation of $H$ with a reasonable functor $F : \mathbf{P} \to \mathbf{C}$, i.e.,

$$H \circ F : \mathbf{P} \to \mathbf{D}.$$

Hence, persistence gives rise to quite abstract research [33, 34]. It usually makes sense to restrict to an algebraic category as target category, however. This is sometimes called *algebraic persistence* [146]. The categories $\mathbf{Vect}_{\mathbb{K}}$ of vector spaces over a fixed field $\mathbb{K}$ and the category $R$-**Mod** of modules over a fixed ring $R$ make particular sense in this context.

Choosing the natural numbers as the totally ordered set, there is a correspondence between the category of functors $\mathbb{N} \to R$-**Mod** and the category of graded $R[t]$-modules. This is known as the *Representation Theorem* [176], a landmark theorem in the theory of persistence.

The importance of this result stems from the fact that the functors $\mathbb{N} \to R$-**Mod**, called *persistence modules* [176], can be understood under the lens of graded module theory. By a general result in commutative algebra it is well-known that if $R$ is a field, finitely generated graded modules over $R[t]$ permit a simple decomposition in free and torsion parts. This fact yields a complete discrete invariant for finitely generated functors $\mathbb{N} \to R$-**Mod**, which is also called *persistence diagram* [84] or *barcode* [44, 98] in the framework of persistence. The existence of this invariant shows that simple descriptors for persistence are available if the target category consists of vector spaces. Although the persistence diagram was defined along geometric and topological constructions before, one may define this invariant by means of pure algebra. Therefore, key objects and deep results in persistence can be defined, motivated, and obtained, respectively, by means of algebra. Furthermore, the theory of algebraic persistence is related to spectral sequences [81, 138] and sheaf theory [63], and gives rise to investigations of its homological algebra [32, 96].

# 1 Introduction

The idea of persistence goes back to Edelsbrunner et al. [84], Frosini and Landi [92], and Robins [151], constructing *persistent homology*. Here, $H$ : **Top** $\to$ **R-Mod** denotes a homology functor, and $F$ : **P** $\to$ **Top** a collection of nested topological spaces. In these cases, we call $F$ *filtration*. For instance, if $P$ equals the natural numbers, the persistence module $\mathbb{N} \to R$-**Mod** can be expressed as a sequence

$$H(F_0) \xrightarrow{F_{0,1}} H(F_1) \xrightarrow{F_{1,2}} H(F_2) \xrightarrow{F_{2,3}} H(F_3) \xrightarrow{F_{3,4}} \dots$$

tracking the homological changes along a sequence of inclusions of topological spaces. The idea is to quantify how homological features appear and disappear in a shape when a certain scale parameter increases. The persistence diagram captures this behavior. As a matter of fact, persistent homology can be viewed as a quantitative update of classical homology.
A prominent geometric construction of a filtration $F$ is the so-called *union-of-balls filtration*: given a (usually finite) input set in a metric space, the $F_i$ are defined to be the thickening of this set by increasing thickening radii $r_i$. In this setting, the parameter of persistent homology is the metric scale.

Remarkably, persistent homology does not only have a rich theory involving different areas of mathematics. In fact, it gives rise to numerous applications in data science having lead to the term *topological data analysis* (TDA). Many of these applications are in science and engineering [46, 49, 100, 104, 109, 134, 169, 173]. To name a few examples more concretely, TDA extracts in-depth geometric information in amorphous solids [109], determines robust topological properties of evolution from genomic data sets [49], and identifies distinct diabetes subgroups [134] and a new subtype of breast cancer [144] in high-dimensional clinical data sets. The various further applications of TDA in health science and life science include novel insights into the structure of the brain [15, 114, 126, 157], particularly in the context of diseases such as fibromyalgia [55], an automated sleep apnea diagnosis [108], a fast tumor segmentation of histology images [149], a visualization of disease clusters in asthma [29], and a better understanding of mutations of viruses [160]. Other examples of applications are a topological analysis of the performance of hockey teams [101], a topological representation of music using the Tonnetz [16], a classification

of texts [74] and RGB images [37], the shape of the space of natural images [41], and the extraction of topological patterns in political systems [105]. In the context of shape analysis, TDA techniques have been used in the reconstruction of manifolds [145] and algebraic varieties [28], the recognition, classification [133, 162], summarization [20], and clustering [158] of 2-dimensional and 3-dimensional shapes and surfaces. Oftentimes, such techniques capture and highlight structures in data that conventional techniques fail to treat [133, 158] or reveal properly [109].

A very important property in the light of TDA is the fact that persistent homology is *stable* [34, 57, 58]. The first step is to define a distance between persistence diagrams or even between persistence modules. Stability of such a distance is the formalization of the idea that small changes in the input data can only lead to small changes in the output. It ensures that measuring the persistent homology of datasets is robust against local noise. Such stable distances reasonably quantify the similarity of persistent homology of two input sets.

Recently, interfacing persistence with machine learning algorithms has grown interest. *Feature maps* [2, 31, 121, 150] have been defined on the set of persistence diagrams. These feature maps make the output of persistent homology become an input of kernel based machine learning algorithms. A conceptually different approach is to define *layers for deep learning* with the help of persistence diagrams [110].

Persistent homology has shown to be successful in applications because of constructions of discrete versions of filtrations $F$, the nicely working algebraic theory, and computationally feasible algorithms. This has lead to a smooth computational *pipeline* with efficient implementations [3, 11, 13, 14, 73, 90, 107, 136, 140, 142].

In *multiparameter persistence*, the totally ordered set is replaced by a product of totally ordered sets. For instance, one may replace $\mathbb{N}$ by $\mathbb{N}^k$, and the sequences as above are replaced by $k$-dimensional diagrams. Following the terminology of product posets, we have $(n_1, ..., n_k) \leq (m_1, ..., m_k)$ if and only if $n_i \leq m_i$ for all $i \in \{1, ..., k\}$. For instance, for $k = 2$, a functor $H \circ F : \mathbb{N}^2 \to \mathbf{D}$ can be written as a diagram of the form

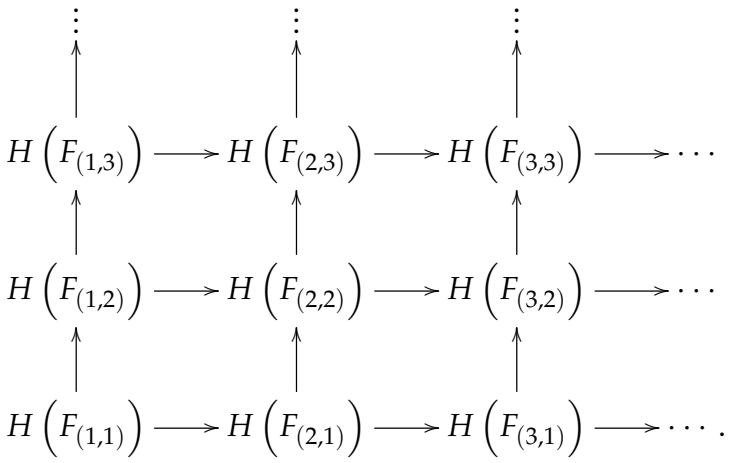

As in the setting of ordinary persistence, the restriction to an algebraic category as target category plays a major role. The Representation Theorem still holds in the sense that the category of functors $\mathbb{N}^k \to R\text{-}\mathbf{Mod}$, called *multiparameter persistence modules*, is isomorphic to the category of graded $R[t_1, ..., t_k]$-modules.

Unfortunately, if $k > 1$, the algebraic theory of such graded $R[t_1, ..., t_k]$-modules is substantially more complicated than the theory of $R[t]$-modules. Even under strong finiteness assumptions and if we restrict to vector space valued functors $\mathbb{N}^k \to \mathbf{Vect}_{\mathbb{K}}$, it is known that no complete discrete invariant can ever track the whole structural behavior of such multiparameter persistence modules [43]. That is why it is necessary to construct useful incomplete invariants. To do this, more advanced methods have shown to be helpful [95, 153, 161].

Multiparameter persistence has its roots in *multiparameter persistent homology*, first investigated by Carlsson and Zomorodian [43]. Analogously to the case of ordinary persistent homology, multiparameter persistent homology is the concatenation of a functor $F : \mathbf{P} \to \mathbf{Top}$ with a homology functor. Now, $\mathbf{P}$ denotes a product of totally ordered sets rather than a single totally ordered set. This generalization opens the door to more general frameworks enlarging the toolkit of TDA. Already existing applications include the shape of proteins [172] and drug discovery [115], partly supported by the use of the multiparameter persistence software RIVET [130].

More precisely, multiparameter persistence enables us to investigate $k$ independent parameters at once. For instance, additional parameters can capture local density, curvature [43], or parameters that arise from an applicational point of view [115]. This is formalized in the construction of a *multifiltration* $F : \mathbf{P} \to \mathbf{Top}$ where $\mathbf{P}$ is again the product of $k$ totally ordered sets.
Let us give a concrete geometric example. The union-of-balls filtration can be enriched by a second parameter measuring the local density of the input set. Consider the regions that are covered by a fixed number of multiple balls of a fixed radius at once. Letting the number of such balls decrease, the second parameter tracks the changes of the corresponding regions. Adding the variations in the radius, the resulting functor $F : \mathbb{R} \times \mathbb{N}^{op} \to \mathbf{Top}$ is called *multicover bifiltration*. In practice, it resolves the problem that persistent homology of the union-of-balls filtration is undesirably sensitive with respect to outliers.

Stability carries over to the multiparameter setting. Since no complete discrete invariant exists, the distances are usually defined directly on the level of multiparameter persistence modules. The main concept for this is called *interleavings* [129]. Unfortunately, the computation of the *interleaving distance* is NP-hard [21, 22]. Therefore, stable distances with better computational properties come into play [47].

Besides the new challenges arising from the more complicated algebraic theory, more involved computational methods are necessary as well. The main tasks include discrete models of reasonable multifiltrations, an efficient computation of useful invariants and distances, and understanding how connections to machine learning can be established. Consequently, the whole computational *pipeline of multiparameter persistence* demands much more effort and is not yet fully established.

## 1.1 Contributions

We give progress along the whole pipeline of multiparameter persistence.

We provide new mathematical insights into the process of discretizing multifiltrations. This is done in the strong context of the *multicover bifiltration*.

A nerve-based approach for a simplicial version of the multicover bifiltration is known to have beautiful mathematical properties but to be not computationally feasible [154]. The attempt of the more efficient Delaunay-based simplicial model causes a problematic issue, however: one does not get a multifiltration. A further construction gives a diagram of inclusions of simplicial complexes of the form

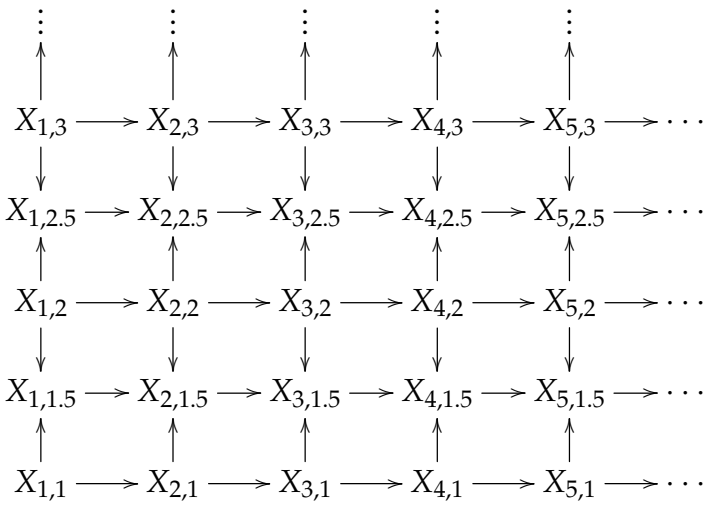


The problem in the vertical direction has been addressed and solved geometrically in prior work of Edelsbrunner and Osang [86]. We use topological methods to construct a diagram as above and construct a *simplicial bifiltration* $F : \mathbb{N} \times \mathbb{N}^{op} \to \mathbf{Simp}$ with the same multiparameter persistence as the multicover bifiltration $F : \mathbb{N} \times \mathbb{N}^{op} \to \mathbf{Top}$.

Secondly, we revisit and generalize the *Representation Theorem of persistence* stating the isomorphism of categories between functors in algebraic persistence and graded modules. We give a detailed and elementary proof of the classical version, and generalize this to a much more general index set, including the setting of multiparameter persistence as a special case. More precisely, we give a formulation of the Representation Theorem over a quite general class of *monoids* and specify the necessary finiteness conditions for more practical use. The corresponding graded modules are graded over monoid rings. Left-factorization of a given monoid yields a poset that is

not necessarily a product of totally ordered sets. Therefore, more generally indexed algebraic persistence modules can be analyzed via graded modules, including the cases $\mathbb{Q}^k_{\geq 0}$ , $\mathbb{R}^k_{\geq 0}$, and monoids with suitable congruences.

Finally, we give a construction of a *feature map* for multiparameter persistence. A feature map is defined to map an input set into a Hilbert space. Feature maps induce a *kernel*, which is the inner product of the images of two elements of the input set under the feature map. There are many useful algorithms in machine learning whenever a kernel is given, such as principle component analysis and support vector machines. To the best of our knowledge, we give the first such construction for multiparameter persistence. It opens the door to make multiparameter persistence become an instance of kernel-based machine learning algorithms. The main obstacle for an analogous construction of a feature map as in the case of persistence of one parameter is the lack of an analog of the persistence diagram. Our multiparameter feature map is defined along *slices* of multifiltrations. This approach is generic. Hence, a feature map from ordinary persistence gives rise to a feature map for multiparameter persistence. We show that stability of feature maps from ordinary persistence carries over to stability of multiparameter feature maps and give a polynomial approximation scheme for the case of two parameters.

## 1.2 Outline

We begin with preliminaries that are needed for the exposition of this thesis.

Then we provide a concise overview of the computational pipelines of persistence and multiparameter persistence.

We proceed to the contributions of this thesis. We also give references to related work and and ideas for future work.

Finally, we conclude with an outlook on some open questions on the pipeline of multiparameter persistence.

# 2 Preliminaries

## 2.1 Category theory

We review some basic definitions of category theory to make some aspects of the exposition more convenient. See [1, 135] for comprehensive introductions.

A *category* $\mathbf{C}$ is a class of *objects* and sets of *morphisms* between the objects, which have to satisfy associativity and identity axioms: for all morphisms $\alpha \in \hom(W,X)$, $\beta \in \hom(X,Y)$, $\gamma \in \hom(Y,Z)$ there are compositions $\beta \circ \alpha \in \hom(W,Y)$ and $\gamma \circ \beta \in \hom(X,Z)$ which ensure $(\gamma \circ \beta) \circ \alpha = \gamma \circ (\beta \circ \alpha)$. If it is not clear which category the morphisms belong to, one writes $\hom_{\mathbf{C}}$ to denote the category $\mathbf{C}$. Furthermore, for all objects $X$ in a category $\mathbf{C}$ there are identity morphisms $1_X \in \hom(X,X)$ such that $1_X \circ \alpha = \alpha$ and $\beta \circ 1_X = \beta$ for all $\alpha \in \hom(W,X)$, $\beta \in \hom(X,Y)$. One example of a category is the collection of all sets as objects and maps between sets as morphisms. Others are topological spaces and continuous maps, denoted by **Top**, simplicial complexes and simplicial maps, denoted by **Simp**, modules and module homomorphisms over a fixed ring $R$, denoted by $R$-**Mod**, and in particular vector spaces over a fixed field $\mathbb{K}$ and linear maps, denoted by $\mathbf{Vect}_{\mathbb{K}}$.

A category $\mathbf{C}$ is said to be *small* if its objects form a set. $\mathbf{C}$ is said to be *thin* if $\hom(X,Y)$ consists of at most one element for any two objects $X, Y$.

Given a category $\mathbf{C}$, then the *opposite category* $\mathbf{C}^{op}$ is defined to have the same objects as $\mathbf{C}$, and to have reserved morphisms, i.e. $\alpha \in \hom_{\mathbf{C}^{op}}(X,Y)$ if and only if $\alpha \in \hom_{\mathbf{C}}(Y,X)$, and $\beta \circ \alpha$ in $\mathbf{C}^{op}$ is defined to be $\alpha \circ \beta$ in $\mathbf{C}$.

A *functor* $F : \mathbf{C} \to \mathbf{D}$ carries the information from one category to another. It satisfies $F(\beta \circ \alpha) = F(\beta) \circ F(\alpha)$ and $F(1_X) = 1_{F(X)}$ for all $\alpha \in \hom_{\mathbf{C}}(W,X)$, $\beta \in \hom_{\mathbf{C}}(X,Y)$. It suffices to define functors on the morphisms only, but usually one also specifies $F(X)$ for clarity. For thin categories we may write $F_{X,Y}$ for the image of the unique morphism in $\hom_{\mathbf{C}}(Y,X)$. A simple example of a functor is the *identity functor* of a

category, which simply maps each object and each morphism on itself. As another example, homology is a functor from the category of topological spaces to the category of abelian groups **Ab**.

Functors describe similarities between two categories. Two categories $\mathbf{C}, \mathbf{D}$ are called *isomorphic* if there are functors $F : \mathbf{C} \to \mathbf{D}$, $G : \mathbf{D} \to \mathbf{C}$ such that $F \circ G$ is the identity functor on $\mathbf{D}$ and $G \circ F$ is the identity functor on $\mathbf{C}$.

A *natural transformation* can be understood as a functor of functors. Formally, given two functors $F, G : \mathbf{C} \to \mathbf{D}$ a natural transformation $\eta : F \to G$ is a family of morphisms indexed over the objects of $\mathbf{C}$. It has to satisfy $\eta_X : F(X) \to G(X)$ for all objects $X$ of $\mathbf{C}$, and $\eta_Y \circ F(\beta) = G(\beta) \circ \eta_X$ for all $\beta \in \hom_{\mathbf{C}}(X, Y)$.

## 2.2 Posets

A *poset*, also known as *partially ordered set*, is a tuple $(P, \leq)$, where $P$ is a set, and $\leq$ is a reflexive, anti-symmetric, transitive binary relation on $P$. I.e., for all $p, q, r \in P$ we have that $p \leq p$, and $p \leq q$, $q \leq p$ imply $p = q$, and $p \leq q$ and $q \leq r$ imply $p \leq r$. A poset $(P, \leq)$ always induces a *strict poset* $(P, <)$, where the binary relation $<$ is defined to be the irreflexive version of $\leq$, i.e., for all $p, q \in P$ we get $p < q$ if and only if $p \neq q$ and $p \leq q$.

A special class of posets is the class of *totally ordered sets*. In addition it satisfies the connexity axiom, i.e., for a totally ordered set $(P, \leq)$ we have $p \leq q$ or $q \leq p$ for all $p, q \in P$.

Given two posets $(P, \leq)$, $(Q, \preceq)$, the *product poset* $(P \times Q, \leq \times \preceq)$ satisfies the property that $(p_1, q_1) \leq \times \preceq (p_2, q_2)$ if and only if $p_1 \leq p_2$ and $q_1 \preceq q_2$. Whenever no confusion is possible, one avoids to write $\leq \times \preceq$ explicitly.

A poset $(P, \leq)$ always induces a *poset category* $\mathbf{P}$. It is defined to have the elements of $P$ as objects, and $\hom(p, q)$ to have one element if $p \leq q$, and to be empty if $p \not\leq q$.

So, poset categories are always small and thin. Hence, it may even be convenient to draw diagrams illustrating their global structure, particularly for finite posets. Even more convenient are Hasse diagrams. The *Hasse*

*diagram* of a finite poset $(P, \leq)$ is defined to be the finite directed graph with vertices $P$, and edges $(p, q)$ for each minimal relation $p < q$. $<$ is called *minimal* if there is no $r \in P$ such that $p < r < q$.

Given a poset $(P, \leq)$, the *opposite poset* $(P, \geq)$ is defined by letting $q \geq p$ if and only if $p \leq q$. It does not matter if one first takes the opposite of a poset, and then the induced category, or if one first takes the induced poset category, and takes the category theoretical opposite. Hence, one can just talk about the coinciding terminology of the opposite poset category $\mathbf{P}^{\mathbf{op}}$. Another simple observation is the fact that the Hasse diagram of $(P, \geq)$ is just the Hasse diagram of $(P, \leq)$ with reversed edges.

For further reading on basic aspects of posets, we recommend [143].

## 2.3 Topology

We assume basic knowledge in point-set topology and algebraic topology. There exist various well-written books for point-set topology [141, 167] and algebraic topology [27, 106]. To fix notation, we review some very basic concepts of homotopy theory, simplicial complexes, and homology. We also mention the important concept of nerves of covered spaces.

Homotopy. A *homotopy* is a family of maps $f_t : X \to Y$, $t \in [0, 1]$, such that the map $X \times [0, 1] \to Y$, $(x, t) \mapsto f_t(x)$ is continuous. Two maps $g, h$ are called *homotopic* if there is a homotopy $f_t$ such that $f_0 = g$ and $f_1 = h$. We write $g \simeq h$. A map $f : X \to Y$ is called *homotopy equivalence* if there is a map $g : Y \to X$ such that $gf \simeq \mathrm{id}_X$ and $fg \simeq \mathrm{id}_Y$. In this case we write $X \simeq Y$. If a map, denoted by an arrow, realizes a homotopy equivalence, we may just write $\xrightarrow{\simeq}$.

A special case of homotopies are *deformation retracts*. These have the additional property of being the identity on a subspace and having this subspace as the image of $f_1$. It is the formalization of a space shrinking continuously to a subspace without changing its topology.

**Simplicial complexes.** A(n) *(abstract) simplicial complex* $S$ is a family of finite subsets of a set such that every subset of an element of $S$ is itself an element of $S$. Elements of $S$ of cardinality 1 are called *vertices*. The elements of $S$ are called *simplices*, a *face* of a simplex is the convex hull of a nonempty subset of its vertices, and the *dimension* of a simplex $\sigma$ is defined to be $|\sigma| - 1$.

Given two simplicial complexes $S, T$, a map $S \to T$ is called *simplicial map* if it maps faces to faces and vertices to vertices.

When working with topology, one is interested in the *underlying space* $|S|$ of a simplicial complex $S$. It is the assignment of a canonical topological space to $S$. The underlying space enables us to talk about topological properties of a simplicial complex. The construction of the underlying space relies on a standard embedding of all given simplices into Euclidean space, and then glues the simplices together according to the rules of $S$. For a concise and formal exposition of this process, see [99], calling the underlying space geometric realization (which we find a bit misleading). In the rest of this thesis we omit writing $|S|$ even when it is formally necessary.

A *flag* in $S$ is an ordered subset of simplices $\{\sigma_1, ..., \sigma_m\}$ of $S$ such that $\sigma_1 \subset ... \subset \sigma_m$. The *barycentric subdivision* $\mathrm{Bary}(S)$ of a simplicial complex $S$ is another simplicial complex, defined to be the set of all flags of $S$. Note that $\mathrm{Bary}(S)$ and $S$ are homotopy equivalent. Intuitively speaking, this construction adjusts a simplicial complex in the sense that old simplices become additional vertices.

**Homology.** Informally, *homology* [148] was developed in the early 20th century to classify topological spaces by examining their topological features such as connected components, tunnels, voids, and holes of higher dimensions. An important property of homology is the fact that it is an invariant of homotopy theory, i.e., homotopy equivalent spaces have the same homology.

Building up on the Eilenberg-Steenrod axioms [88] there is the notion of *homology functors*. Among the variety of existing homology functors the most well known functor is called *singular homology*. Let us focus on the version of homology on simplicial complexes, *simplicial homology*.

Let $X$ be a simplicial complex, $p \in \mathbb{N}$. A *p-chain* is a formal sum of simplices of $X$ of dimension $p+1$. The set of all $p$-chains forms a group that we denote as $C_p$, the *p-chain group*. The *p-boundary map* $\partial_p$ maps $p$-chains onto a formal sum of $(p-1)$-chains. It is the group homomorphism generated by

$$\partial_p[u_0, ..., u_p] = \sum_{i=0}^{p} [u_0, ..., \hat{u_i}, ..., u_p]$$

where the hat indicates that the component is omitted.

The image of the $(p+1)$-boundary map is called *p-boundary group*. It is a subgroup of $C_p$. The subgroup of $C_p$ that gets mapped to $0 \in B_{p-1}$ is called *p-cycle group*. We denote these groups by $B_p$ and $Z_p$, respectively.

The *fundamental lemma of homology* expresses that $\partial_p \circ \partial_{p+1}(c) = 0$ for every $p \in \mathbb{N}$ and for every $(p+1)$-chain $c$. Hence, $B_p$ is a subgroup of $Z_p$. The *p-th simplicial homology group* $H_p$ is defined to be the quotient $Z_p / B_p$.

Simplicial homology can be understood as a functor $\mathbf{Simp} \to \mathbf{Ab}$, where $\mathbf{Ab}$ is the category of abelian groups. We rather view it as a functor $\mathbf{Simp} \to \mathbb{Z}\text{-}\mathbf{Mod}$, which is valid since $\mathbf{Ab}$ and $\mathbb{Z}\text{-}\mathbf{Mod}$ are isomorphic categories. The same holds true for general homology functors. In persistent homology, homology with field coefficients $\mathbb{K}$ are the canonical choice, sometimes even $\mathbb{K} = \mathbb{Z}_2$. We get a functor $\mathbf{Simp} \to \mathbf{Vect}_{\mathbb{K}}$. Choosing a field, we obtain a simpler theory and computational advantages.

Note that homology groups of simplicial complexes can be computed by a reduction of matrix representations of the boundary maps [82].

The Nerve Theorem. The *(Čech) nerve* is a classical construction of a simplicial complex for a covered space. It encodes all non-empty intersections of cover elements combinatorially.

A *cover* $\mathfrak{X}$ of a topological space $X \subseteq Z$ is a collection $\{\mathfrak{X}_i\}_{i \in I}$ of subsets of $Z$ such that $X \subseteq \bigcup_{i \in I} \mathfrak{X}_i$. We call $(X, \mathfrak{X})$ a *covered (topological) space*. Given a covered space $(X, \mathfrak{X})$, the nerve of $\mathfrak{X}$ is the abstract simplicial complex

$$\mathrm{Nrv}(\mathfrak{X}) := \left\{ \sigma \subseteq I \mid \bigcap_{i \in \sigma} \mathfrak{X}_i \neq \emptyset \right\}.$$

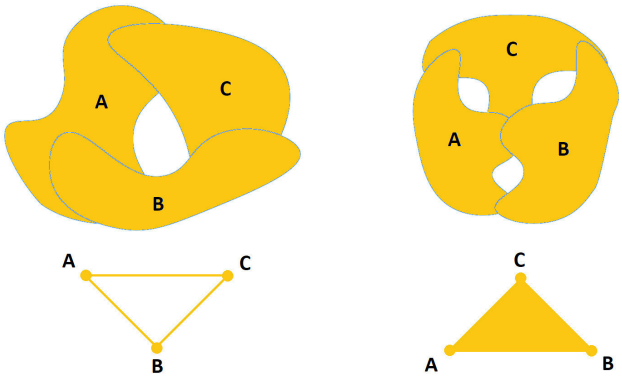


Figure 2.1: The nerve of the left cover preserves the homotopy type of the union of the cover elements. The nerve of the right cover does not.

The *Nerve Theorem* asserts that $X$ and (the underlying space of) $\mathrm{Nrv}(\mathfrak{X})$ are homotopy equivalent if the cover is sufficiently well behaved. See Figure 2.1 for simple examples. As for the structural description of covers with such a behavior, there exist many different variations [6, 23, 127, 171]. In each of these cases, the cover is simply called *good cover*. We will mostly use the versions of a finite cover of closed, convex sets in Euclidean space [82], and of an open cover of a paracompact space, with the property that all nonempty intersections of finitely many cover elements are contractible [6, 106].

**Theorem 1** (Nerve Theorem)**.** *Let $\mathfrak{X}$ be a good cover. Then $\mathrm{Nrv}(\mathfrak{X})$ is equivalent to the union of all cover elements.*

Let us sketch the idea of a proof of the Nerve Theorem. We follow the main arguments of Hatcher [106], rephrased e.g. in a paper by Botnan and Spreemann [26]. Later we use these insights to work with nerves along filtrations.

We assign a topological space $\Delta X_{\mathfrak{X}}$ to a cover $\mathfrak{X}$ of a space $X$:

$$\Delta X_{\mathfrak{X}} := \left( \bigsqcup_{S \in \mathrm{Nrv}(\mathfrak{X})} |S| \times \bigcap_{i \in S} \mathfrak{X}_i \right) / \sim,$$

where the equivalence relation $\sim$ is defined by $(s, x) \sim (t, y)$ if and only if $s \in |S|, t \in |T|, s = t$ and $x = y$.

There are canonical projections from $\Delta X_{\mathfrak{X}}$ to $\mathrm{Nrv}(\mathfrak{X})$, and from $\Delta X_{\mathfrak{X}}$ to $X$. These projections are homotopy equivalences. The homotopy equivalence of the projection onto $X$ can be shown with an argument using a partition of unity. This is where paracompactness comes into play. As for the homotopy equivalence of the projection onto $\mathrm{Nrv}(\mathfrak{X})$, the goodness of the cover is necessary.

For an inclusion of two covered spaces $(X, \mathfrak{X}) \subseteq (Y, \mathfrak{Y})$, i.e., $X \subseteq Y$ and element-wise inclusions $\mathfrak{X}_i \subseteq \mathfrak{Y}_i$ for all $i \in I$, we get an inclusion $\mathrm{Nrv}(\mathfrak{X}) \hookrightarrow \mathrm{Nrv}(\mathfrak{Y})$. If both covered spaces satisfy the assumptions of the Nerve Theorem, then there exist homotopy equivalences from the nerves to the corresponding spaces that commute with the canonical inclusions. I.e., we get a commuting diagram

$$\begin{array}{ccc} X & \longrightarrow & Y \\ \uparrow \simeq & & \uparrow \simeq \\ \mathrm{Nrv}(\mathfrak{X}) & \longrightarrow & \mathrm{Nrv}(\mathfrak{Y}). \end{array}$$

Consequently, we get a commuting diagram on homology

$$\begin{array}{ccc} H_*(X) & \longrightarrow & H_*(Y) \\ \downarrow \cong & & \downarrow \cong \\ H_*(\mathrm{Nrv}(\mathfrak{X})) & \longrightarrow & H_*(\mathrm{Nrv}(\mathfrak{Y})) \end{array}$$

where the horizontal maps are again induced by inclusion. The vertical arrows can be reversed in the second diagram, which we have done already.

This argumentation is known as the *Persistent Nerve Theorem* and its homological consequence, respectively. For details, see, e.g., [26, 54].

The above sketch of a proof of the Nerve Theorem is usually given for of open covers of a paracompact space such that nonempty intersections of finitely many cover elements are contractible. The same holds true for a proof of the Persistent Nerve Theorem. It is folklore that the Persistent Nerve Theorem also holds true for finite covers of closed, convex sets in Euclidean space. We expect to see a formal proof in the near future, using a variation of the sketched proof of the Nerve Theorem.

## 2.4 Algebra

Let us give some basic terminology on graded modules, also over monoid rings, as we need it later.

**Graded rings and modules.** We only consider rings with unity and usually denote them by $R$. A *left-ideal* $I$ of $R$ is an additive subgroup of $R$ such that $r \in R$ and $x \in I$ implies that $rx \in I$. Replacing $rx$ with $xr$ defines a *right-ideal*. A subgroup $I$ is called *ideal* if it is a left-ideal and a right-ideal.

An $R$-(left-)module $(M, +, \cdot)$ is an abelian group with a scalar multiplication (from the left), which is a bi-additive group action of $R$ on it. We usually denote modules by $M$. For example, every left-ideal of $R$ is also an $R$-module. An *$R$-module morphism* between $R$-modules $M$ and $N$ is a group homomorphism $f : M \to N$ that also satisfies $f(rx) = rf(x)$ for all $r \in R$ and $x \in M$.

A ring $S$ is $\mathbb{N}$-*graded*, or just *graded* if $S$ can be written as $S = \oplus_{i \in \mathbb{N}} S_i$ where each $S_i$ is an abelian group and $s_i \cdot s_j \in S_{i+j}$ whenever $s_i \in S_i$ and $s_j \in S_j$. If $R$ is a ring, the polynomial ring $R[t]$ is naturally graded with $R[t]_i$ being the $R$-module generated by $t^i$. While $R[t]$ might permit different gradings (e.g. if $R$ itself is a polynomial ring), we will always assume that $R[t]$ is graded in the above way.

If $S = \oplus S_i$ is a graded ring, an $S$-module $M$ is *graded* if there is a decomposition $M = \oplus_{i \in \mathbb{N}} M_i$ such that each $M_i$ is an abelian group and $s_i \cdot m_j \in M_{i+j}$ whenever $s_i \in S_i$ and $m_j \in M_j$. As a trivial example, $S$ is a graded $S$-module itself. By definition, every nonzero element of $M$ can be written as a finite sum

$$m = m_{i_1} + m_{i_2} + \ldots + m_{i_k}$$

with $k \geq 1$, $i_1 < i_2 < \ldots < i_k$, and $m_{i_j} \in M_{i_j}$. If $k = 1$, $m = m_{i_1}$ is called *homogeneous of degree* $i_1$.

A *graded morphism* $f : M \to N$ between graded $S$-modules is an $S$-module morphism such that $f(M_i) \subset N_i$ for all $i \in \mathbb{N}$. Fixing a ring $R$, the collection of all graded $R[t]$-modules together with graded morphisms yields another example of a category, which we will denote by R[t]-**Gr-Mod**.

MONOIDS. A *monoid* is a set $G$ with a binary associative operation $\star$ and a neutral element $e$, i.e., for all $g_1, g_2, g_3 \in G$ we have $g_1 \star g_2 \in G$, $(g_1 \star g_2) \star g_3 = g_1 \star (g_2 \star g_3)$ and $e \star g_1 = g_1 \star e = g_1$. A monoid is called *commutative* if $g_1 \star g_2 = g_2 \star g_1$ for all $g_1, g_2 \in G$. We usually denote a monoid by $G$ or $(G, \star)$. We sometimes omit denoting $\star$ if it clarifies the expression and no confusion is possible.

A monoid is called *right-cancellative* if $g_1 \star g_3 = g_2 \star g_3$ implies $g_1 = g_2$. Similarly, it is called *left-cancellative* if $g_1 \star g_2 = g_1 \star g_3$ implies $g_2 = g_3$. It is called *cancellative* if it is right-cancellative and left-cancellative. For commutative monoids these three properties are equivalent and in this case we simply call such a monoid cancellative. A (left-/right-)cancellative monoid $G$ admits (left-/right-)cancellativity on a monoid ring $R[G]$ with respect to multiplication by a monoid element (from the left/right).

Examples of non-cancellative monoids are $[0,1]$ with multiplication, square matrices with matrix multiplication, and $\mathbb{Z}_2 \times \mathbb{N} \cup \{\infty\}$ where $(x,n) \star (y,m) := (xy, \min(n,m))$ and $e = (0, \infty)$. An example of a right-cancellative monoid that is not left-cancellative is the monoid $\{e, g_1, g_2, g_3\}$ where $e$ is the neutral element and $g_i \star g_j := g_i$ for all $i \in \{1,2,3\}$.

MONOID GRADED RINGS AND MODULES. Let $(G, \star)$ be a monoid and $R$ be a ring with unity. The *monoid ring* $R[G]$ is defined as free $R$-module with basis $\{X^h\}_{h \in H}$ where ring multiplication of $R[G]$ is induced by its scalar multiplication as $R$-module and $X^{h_1} X^{h_2} := X^{h_1 \star h_2}$. It can be easily verified that with these operations $R[G]$ indeed becomes a ring with unity $X^e$. Note that both associativity of $\star$ and the existence of a neutral element in $G$ are required to guarantee a ring structure with unity on $R[G]$. Moreover, $R[G]$ is commutative if and only if both $R$ and $G$ are commutative. Furthermore, one can easily verify that $aX^g = X^g a$ in $R[G]$ whenever $a \in R$ and $g \in G$.

Monoid rings are a generalization of polynomial rings. For instance, with $R$ a ring, every $a \in R[t]$ has the form $\sum_{n \in \mathbb{N}} a_n t^n$ where almost all $a_n = 0$. By canonical identification of $t^n$ with $X^n \in R[\mathbb{N}]$, the two notions are isomorphic. Completely analogously, one can obtain $R[\mathbb{N}^n] \cong R[t_1, ..., t_n]$ for all $0 \neq n \in \mathbb{N}$. In general, we will often write elements of $R[G]$ in the form $\sum_{g \in G} a_g g$ with $a_g \in R$ and almost all $a_g = 0$.

The concept of gradings extends from natural numbers to arbitrary monoids without problems: a ring $S$ is called *$G$-graded ring* if $S = \oplus_{g \in G} S_g$ as abelian groups and $S_{g_1} S_{g_2} \subseteq S_{g_1 \star g_2}$ for all $g_1, g_2 \in G$. Monoid rings $R[G]$ are typical examples of $G$-graded rings. For a $G$-graded ring $S$, an $S$-module $M$ is called *$G$-graded module* if $M = \oplus_{g \in G} M_g$ as abelian groups and $S_{g_1} M_{g_2} \subseteq M_{g_1 \star g_2}$ for all $g_1, g_2 \in G$. A *$G$-graded module morphism* $f : M \to N$ between $G$-graded $S$-modules is a module morphism with $f\left(M_g\right) \subseteq N_g$ for all $g \in G$. Equivalently, one can think of $f$ as a family $\left(f_g\right)_{g \in G}$ of morphisms on the components with $f_g : M_g \to N_g$ for all $g \in G$. A $G$-graded module morphism is an isomorphism if each $f_g$ is an isomorphism. Given a ring $R$ and a monoid $G$, we denote the category of all $G$-graded modules over $R[G]$ and $G$-graded morphisms between $G$-graded $R[G]$-modules by R[$G$]-**Gr-Mod**.

Finiteness conditions for modules. An $R$-module $M$ is called *finitely generated* if there exist finitely many elements $\mathfrak{g}_1, \ldots, \mathfrak{g}_n$ in $M$ such that every $x \in M$ can be written as $x = \sum_{i=1}^{n} \lambda_i \mathfrak{g}_i$ with $\lambda_i \in R$. The set $\{\mathfrak{g}_1, \ldots, \mathfrak{g}_n\}$ is called the *generating set* of $M$. Equivalently, $M$ is finitely generated if and only if there exists a surjective module morphism

$$R^n \xrightarrow{\mu} M$$

where $R^n$ is just the free abelian $R$-module with $n$ generators $\mathfrak{e}_1, \ldots, \mathfrak{e}_n$. If $\mu$ maps $\mathfrak{e}_i$ to $\mathfrak{g}_i$, we call $\mu$ *associated* to the generating set $\{\mathfrak{g}_1, \ldots, \mathfrak{g}_n\}$.

In general, $\mu$ is not injective and there are relations between the generators (which are also sometimes called *syzygies*). $M$ is called *finitely presented* if it is finitely generated and the $R$-module $\ker \mu$ is finitely generated as well. Equivalently, finitely presented means that there exists an exact sequence

$$R^m \to R^n \xrightarrow{\mu} M \to 0.$$

Clearly, finitely presented modules are finitely generated, but the converse is not true as the example from the introduction shows. Note that morphisms between finitely presented modules always imply morphisms on the

corresponding free modules, such that the following diagram commutes:

$$\begin{array}{ccccc} R^{m_1} & \longrightarrow & R^{n_1} & \xrightarrow{\mu} & M \\ \downarrow{\scriptstyle \varphi_R} & & \downarrow{\scriptstyle \varphi_G} & & \downarrow{\scriptstyle \varphi} \\ R^{m_2} & \longrightarrow & R^{n_2} & \xrightarrow{\nu} & N \end{array}$$

So $\varphi$ can be represented as a matrix of two blocks, which describe how generators and relations are changing. For an easy proof, see Lemma 2.1.25 in [102] (which also holds for non-commutative rings).

A ring $R$ is called *(left-/right-)Noetherian* if every (left-/right-)ideal of $R$ is finitely generated. In particular, every principal ideal domain is Noetherian. We point out the following important statements on Noetherian rings:

**Lemma 1.** *Let $R$ be a Noetherian ring with unity. Then every finitely generated $R$-module is finitely presented. If $R$ is also commutative, then $R[t]$ is Noetherian.*

*Proof.* The second part is Hilbert's Basis Theorem (see [163], 15.1). For the first part, see [124] Proposition 4.29. □

We will mostly consider the case of finitely generated/presented graded modules. So, let $M$ be a finitely generated graded $S$-module (where $S$ is graded, but not necessarily Noetherian). It is not difficult to see that $M$ is also generated by a finite set of homogeneous elements in this case, which we will call a *homogeneous generating set*. With $\mu : S^n \to M$ associated to the homogeneous generating set $\{\mathfrak{g}_1, \ldots, \mathfrak{g}_n\}$, we define a grading on $S^n$ by setting $\deg(\mathfrak{e}_i)$ as the degree of $\mathfrak{g}_i$ in $M$ and $\deg(s_i) = i$ for $s_i \in S_i$ in the grading $\oplus S_i$ of $S$. Then again, each $x \in M$ decomposes into a finite sum of elements of pairwise distinct degrees, and we can talk about *homogeneous elements* of $S^n$ accordingly. If $M$ is finitely presented, the generating set of $\ker \mu$ can be chosen with homogeneous elements as well.

# 3 The pipelines of persistence and multiparameter persistence

We give a brief overview of the pipelines of persistence and multiparameter persistence, usually assuming the cases of persistent homology and multiparameter persistent homology. We emphasize the use of persistence towards topological data analysis.

## 3.1 The pipeline of persistence

In order to achieve a tool for data science, there is more to do than specifying the definitions and constructions of persistence or persistent homology only. It is necessary to bridge the gap between data as input and a computable output that describes the topological properties of this data robustly.

As shown in Figure 3.1, a few steps are necessary. Starting with data, one needs to construct a *filtration* that yields the desired multiscale approach. Usually applying homology, one gets the *persistence module*. Then, the *persistence diagram* has to be computed. Since it is a complete discrete invariant of the persistence module, it gives rise to meaningful *interpretations*. For instance, this can be done by introducing stable distances.

For more details on persistence, please consult the books [82, 146, 175] or the surveys [38, 81, 84, 85, 98, 116, 164].

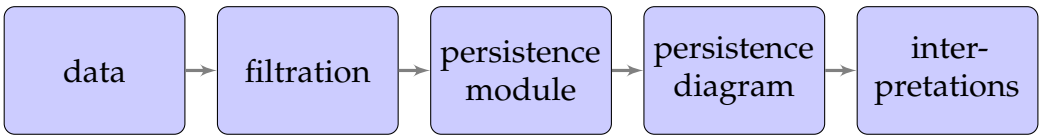


Figure 3.1: The pipeline of persistence

### 3.1.1 Filtrations

A filtration is a family of nested spaces along a totally ordered set. In the context of our introduction, it plays the role of the functor $F$. In the pipeline of persistent homology, it is the starting point of investigating the multiscale behavior of given input data.

**Definition 1.** [Filtration, topological version] Let $P$ be a totally ordered set. A *(mono-)filtration* is a functor $F : \mathbf{P} \to \mathbf{Top}$ such that each map $F_{p,q}$ is an inclusion.

Note that in practice a filtration needs to be discrete. By this we mean that the target category is actually the category of simplicial complexes **Simp** (or a subcategory of **Top** that only consists of underlying spaces of simplicial complexes). For this purpose, we rephrase the above definition:

**Definition 2.** [Filtration, simplicial version] Let $X$ be a simplicial complex, $P$ be a totally ordered set. A *simplicial (mono-)filtration* $\mathcal{X}$ of $X$ is a map that assigns to each $p \in P$ a subcomplex $\mathcal{X}(p)$ of $X$, with the property that whenever $p \leq q$, $\mathcal{X}(p) \subseteq \mathcal{X}(q)$.

It is clear that this definition describes a functor $\mathbf{P} \to \mathbf{Simp}$ where each simplicial complex $\mathcal{X}(p)$ is included in a fixed simplicial complex $X$.
Usually, the natural numbers or the real numbers play the role of the totally ordered set $P$. If $P \subseteq \mathbb{R}$, we can immediately state some important definitions: Let us call the number of simplices of $X$ the *size* of $\mathcal{X}$. Since $X$ is finite, $\mathcal{X}(p)$ changes at only finitely many places when $p$ grows from $-\infty$ to $+\infty$. We call these values *critical*. More formally, $p$ is *critical* if there exists no open neighborhood of $p$ such that the filtration assigns the identical subcomplex to each value in the neighborhood. For a simplex $\sigma$ of $X$, we call the *critical value* of $\sigma$ the infimum over all $p$ for which $\sigma \in \mathcal{X}(p)$. For simplicity, we may assume that this infimum is a minimum, so every simplex has a unique critical value where it is included in the simplicial filtration.

For practical purposes, given a filtration $F : \mathbf{P} \to \mathbf{Top}$, it is important to construct a simplicial filtration $\mathcal{X} : \mathbf{P} \to \mathbf{Simp}$. The simplicial filtration has to capture the same topological information as the filtration. We may call simplicial filtrations just filtrations if and only if no confusion is possible.

EXAMPLES. Let us mention two common constructions of filtrations indexed over the real numbers.

The *sublevel set filtration* is a quite general concept. For a topological space $X$ and a (not necessarily continuous) map $f : X \to \mathbb{R}$, the *sublevel set filtration* of $f$ is defined by

$$F^f(r) := \{x \in X | f(x) \leq r\}.$$

If $\leq$ is replaced by $\geq$, this defines the *superlevel set filtration*.

In many practical cases, the *union-of-balls filtration* is of importance. For a (usually finite) subspace $X$ of a metric space it is given by

$$F^X(r) := \bigcup_{x \in X} B(x, r)$$

where $B(x, t)$ denotes the ball around $x$ of radius $r$.

FROM A FILTRATION TO A SIMPLICIAL FILTRATION. When constructing a simplicial filtration for a given filtration, its computational properties are important. Its size may depend on several properties of the input data (e.g., its size) or the input space (e.g., its dimension).

We give some examples of how to get simplicial filtrations for the union-of-balls filtration, assuming that $X$ is a finite subset of $\mathbb{R}^d$. We write $n := |X|$.

The probably most intuitive simplicial proxy of the union-of-balls filtration is the *Čech filtration*. It is defined by

$$\mathcal{X}(r) := \mathrm{Nrv}(\{B(x, r) | x \in X\}).$$

Hence, the Čech filtration at $r$ consists of $d$-simplices for all $d$-fold intersections of balls around points of $X$ with radius $r$. If $n$ is large, the size of the Čech filtration is huge and its computation is very slow since all subsets of $X$ may create a simplex.

A good workaround for low dimensions is given by the *Delaunay filtration* [67, 77], which is sometimes also called *alpha filtration*. The difference to the Čech filtration lies in restricting the balls to the so-called *Voronoi regions*. The Voronoi region $\mathrm{Vor}(x)$ of $x \in X$ consists of all points in $\mathbb{R}^d$ that have

$x$ as closest point among all points of $X$. Now, the Delaunay filtration is defined by

$$\mathcal{X}(r) := \mathrm{Nrv}(\{B(x,r) \cap \mathrm{Vor}(x) | x \in X\})$$

for all $r \in \mathbb{R}$.

It has the advantage that only those points can create a simplex whose Voronoi regions have a common intersection. Therefore, if the space dimension $d$ is low, say, 2 or 3, the Delaunay filtration can be computed much more efficiently than the Čech filtration. The computation of Voronoi regions is very expensive, however, when the space dimension increases.

Another example is the *Vietoris-Rips filtration*, which goes back to an old paper of Vietoris [165]. We replace the Čech complex at radius $r$ by the *Vietoris-Rips complex*

$$\mathrm{VR}(r) := \{A \subset X | \mathrm{diam}(A) \leq 2r\}.$$

Čech complexes are subcomplexes of the corresponding Vietoris-Rips complexes. Since only pairwise distances of points have to be taken into account, the computations are less expensive than in the case of Čech complexes. In addition, this construction is computationally feasible for any metric space. On the other hand, Vietoris-Rips complexes cannot be understood as the nerve of a cover and therefore have no direct geometric interpretation.

### 3.1.2 Persistence modules

Persistence modules are they key objects towards an understanding of algebraic persistence. Here we restrict to vector space valued persistence modules.

**Definition 3.** Let $P$ be a totally ordered set, $\mathbb{K}$ a field. A functor $\mathbf{P} \to \mathbf{Vect}_{\mathbb{K}}$ is called *persistence module* (over $P$ with respect to $\mathbb{K}$).

Given a filtration $F : \mathbf{P} \to \mathbf{Top}$ (or a simplicial filtration $\mathcal{X} : \mathbf{P} \to \mathbf{Simp}$), we just need to decompose it with a functor $H : \mathbf{Top} \to \mathbf{Vect}_{\mathbb{K}}$ (or $H : \mathbf{Simp} \to \mathbf{Vect}_{\mathbb{K}}$) to get a persistence module $H \circ F$ (or $H \circ \mathcal{X}$). In persistent homology, $H$ is given by (simplicial) homology, usually with field coefficients.

We call a persistence module indexed over $\mathbb{N}$ *of finitely generated type* if all vector spaces are finitely generated and the sequence consists of only finitely many non-isomorphic maps. We can expect that only persistence modules of finitely generated type arise in practice.

### 3.1.3 Persistence diagrams

By the Representation Theorem of Zomorodian and Carlsson [176], the category of functors $\mathbf{N} \to \mathbf{Vect}_{\mathbb{K}}$ with the corresponding natural transformations are isomorphic to the category of graded $\mathbb{K}[t]$-modules. Furthermore, the subcategory of persistence modules of finitely generated type is isomorphic to the category of finitely generated graded $\mathbb{K}[t]$-modules. Since furthermore $\mathbb{K}[t]$ is a principle ideal domain, we can use the following theorem from commutative algebra.

**Theorem 2.** *Any finitely generated graded $\mathbb{K}[t]$-module permits a decomposition*

$$\left(\bigoplus_{i=1}^{n} \Sigma^{\alpha_i}\mathbb{K}[t]\right) \oplus \left(\bigoplus_{j=1}^{m} \Sigma^{\beta_j}\mathbb{K}[t] \,/\, (t^{n_j})\right)$$

*where $\Sigma^{\cdot}$ denotes a shift in the grading.*

The integers $\alpha_i, \beta_j, n_j$ give rise to a *complete discrete invariant*. Intuitively speaking, these numbers describe (homological) features that are born at indices $\alpha_i$, and (homological) features that are born at indices $\beta_j$ and die at indices $n_j$. Hence, we talk about *birth* and *death* of features. As pairs, birth and death values of features can be interpreted as a point in $\mathbb{R}^2$. The finite multiset of all such points is known as the *persistence diagram* of a persistence module [84]. For an illustration, see Figure 3.2. An alternative description is the so-called *barcode* in which the multiset of points is replaced by a multiset of intervals. For a barcode-based overview on persistence, see [98].

Finite totally ordered sets of the form $\{1, ..., n\}$ may arise in practice. These sets can of course be embedded into $\mathbb{N}$ and yield a persistence module of finitely generated type if and only if each individual vector space is

finitely dimensional. More complicatedly, the totally ordered set $\mathbb{R}$ naturally arise from certain filtrations. Usually, the restriction to finitely many critical values is possible, yet not necessarily simple. Algebraically, it is known to be possible under mild finiteness assumptions with the use of methods from representation theory [62]. For an illustration of the computation of the persistence diagram from the union-of-balls filtration, see Figure 3.2.

Persistence diagrams can also be constructed by means of quiver representation theory [146]. A main role plays Gabriel's Theorem [94].

COMPUTATION OF PERSISTENCE DIAGRAMS. Remarkably, the persistence diagram of a simplicial filtration can be computed by a single matrix reduction. Briefly sketched, for computing the $i$-th persistent homology over $\mathbb{Z}_2$, the initial matrix $A$ is the $i$-boundary matrix: its columns are indexed by the critical values of the $(i+1)$-simplices and its rows are indexed by the critical values of the $i$-simplices. $A$ has an entry 1 iff the corresponding $i$-simplex is a subset of the corresponding $(i+1)$-simplex. Then, $A$ has to be reduced by left-to-right column additions: while there exist two columns with same pivot (the largest row index which contains a 1), the left column has to be added to the right one. In the end, the persistence diagram is obtained by the pivots of the resulting matrix. For a detailed description of this algorithm, see [82]. There also exists an algorithm that computes the persistence diagram of a persistence module of finitely generated type [176].

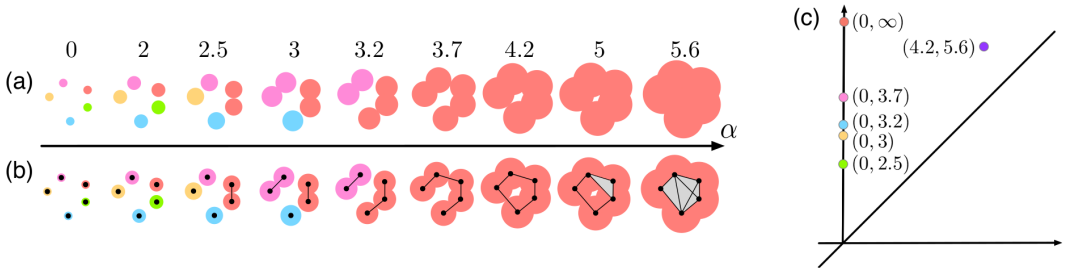


Figure 3.2: Computing persistent homology of a point cloud in $\mathbb{R}^2$. (a) The union-of-balls filtration with respect to a certain sequence of increasing parameter values. (b) The Čech filtration of (a). (c) Persistence diagrams of 0-dimensional and 1-dimensional homology combined.

### 3.1.4 Interpretations

**Distances between persistence diagrams.** Given two sets of input data, we may want to understand their topological similarity using persistence. Such a similarity measure is the Bottleneck distance on the set of persistence diagrams. Let $D$, $D'$ be two persistence diagrams. For technical reasons, we assume that both contain infinitely many copies of the points on the diagonal. The *bottleneck distance* between $D$ and $D'$ is defined as

$$d_B(D, D') := \inf_{\gamma} \sup_{x \in D} \|x - \gamma(x)\|_\infty \tag{3.1}$$

where $\gamma$ ranges over all bijections from $D$ to $D'$. We will also use the notation $d_B(\mathcal{X}, \mathcal{Y})$ for two simplicial filtrations instead of $d_B(D(\mathcal{X}), D(\mathcal{Y}))$.

Crucial results for persistent homology are *stability theorems*. We rephrase the version for the simplicial sublevel set filtration proven in [57]: Given two functions $f, g : X \to \mathbb{R}$ whose sublevel sets form two filtrations of a finite simplicial complex $X$, the induced persistence diagrams $D_f, D_g$ satisfy

$$d_B(D_f, D_g) \leq \|f - g\|_\infty := \sup_{\sigma \in X} |f(\sigma) - g(\sigma)|. \tag{3.2}$$

The bottleneck distance can also be defined via *interleavings* [50]. These are defined on the level of persistence modules. If the bottleneck distance is redefined via interleavings, it is called *interleaving distance* [129], and denoted by $d_I$. Remarkably, it is also the universal choice among all stable distances. This means that every stable distance $d$ on the set of persistence modules over a prime field satisfies $d \leq d_I$ [129].

**Connections to machine learning algorithms.** In order to make persistence diagrams become an instance of *machine learning algorithms*, several feature maps aimed at the construction of a *kernel* for filtrations have been proposed in the literature [34, 121, 123, 150]. A *feature map* assigns to a filtration $\mathcal{X}$ an $L^2$-function $\phi_{\mathcal{X}}$ (usually) defined on $\Delta^{(1)} := \{(x_1, x_2) \in \mathbb{R}^2 \mid x_1 < x_2\}$. The main idea behind most of such constructions of $\phi_{\mathcal{X}}$ is to define a sum of possibly weighted Gaussian peaks, with each

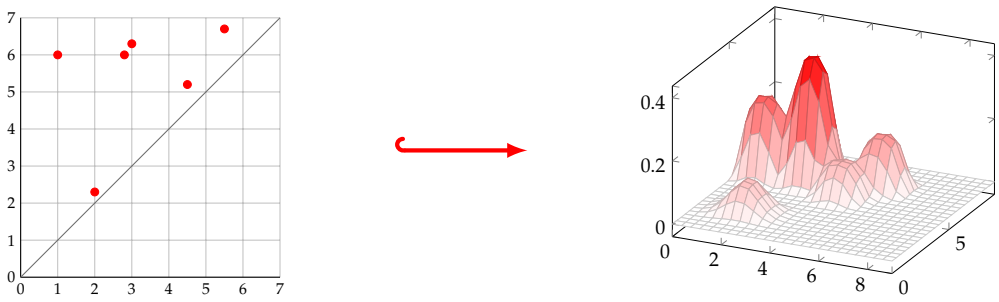


Figure 3.3: A feature map applied to a persistence diagram.

peak centered at one finite off-diagonal point of the persistence diagram of $\mathcal{X}$. See Figure 3.3 for an illustration of a transformation of a persistence diagram to the function $\phi_{\mathcal{X}}$. The induced kernel is given by the $L^2$-scalar product of the feature map of two instances.

A different connection between persistence and machine learning is given by an integration of persistence in deep neural networks. In this approach, persistence diagrams give rise to an additional input layer to already existing deep learning architectures. For details, see [111].

## 3.2 The pipeline of multiparameter persistence

We proceed with describing how the pipeline of persistence generalizes to the setting of multiparameter persistence. The theory of algebraic multiparameter persistence is known to be substantially more difficult than the theory of algebraic persistence. Therefore, new and mathematically imperfect choices have to be made, and the pipeline of multiparameter persistence consists of more options. See Figure 3.4 for a schematic overview.
The pipeline of multiparameter persistence is partly research in progress. As of now, no monograph on multiparameter persistence exists. Publicly available lecture notes on multiparameter persistence by Michael Lesnick [128] are a good source for more detailed insights.

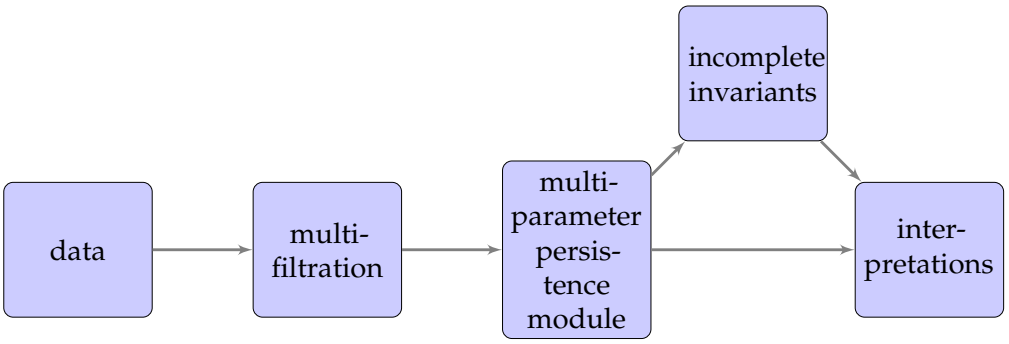


Figure 3.4: The pipeline of multiparameter persistence

### 3.2.1 Multifiltrations

In multiparameter persistence, filtrations are replaced by multifiltrations. These are families of nested spaces along a product of totally ordered sets. In other words, one allows the spaces to grow in multiple directions independently.

**Definition 4.** [Multifiltration, topological version] Let $P$ be the product of $k$ totally ordered sets. A *(k-/)multifiltration* is a functor $F : \mathbf{P} \to \mathbf{Top}$ such that each morphism $F_{p,q}$ is an inclusion.

Analogously to the setting of filtrations, we state a simplicial version:

**Definition 5.** [Multifiltration, simplicial version] Let $X$ be a simplicial complex, $P$ be the product of $k$ totally ordered sets. A *simplicial (k-/)multifiltration* $\mathcal{X}$ of $X$ is a map that assigns to each number $p \in P$ a subcomplex $\mathcal{X}(p)$ of $X$, with the property that whenever $p \leq q$, $\mathcal{X}(p) \subseteq \mathcal{X}(q)$.

This definition clearly induces a functor $\mathcal{X} : \mathbf{P} \to \mathbf{Simp}$.

We may call simplicial multifiltrations just multifiltrations if and only if no confusion is possible. If $k = 2$, we call (simplicial) multifiltrations *(simplicial) bifiltrations*.
As we will see later, constructing an efficient simplicial proxy of a multifiltration may require more subtle tools than in the case of ordinary persistence.

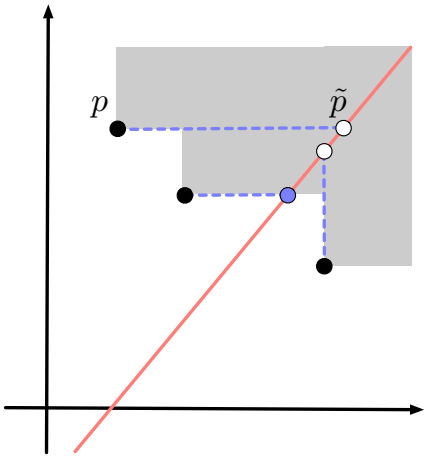


Figure 3.5: The three black points mark the three critical points of some simplex $\sigma$ in $X$. The shaded area denotes the positions at which $\sigma$ is present in the bifiltration. Along the given slice (red line), the dashed lines denote the first position where the corresponding critical point "affects" the slice. This position is either the upper-vertical, or right-horizontal projection of the critical point onto the slice, depending on whether the critical point is below or above the line. For $\sigma$, we see that it enters the slice at the position marked by the blue point.

Let us fix some useful definitions. A point $p = (p_1, ..., p_k) \in P$ is called *critical* for $\mathcal{X}$ if for all $\varepsilon > 0$, all $\mathcal{X}(p_1 - \varepsilon, ..., p_k), ..., \mathcal{X}(p_1, ..., p_k - \varepsilon)$ are not equal to $\mathcal{X}(p)$. Unlike in the monofiltration case, the set of critical points might not be finite: a single simplex might be born at infinitely many pairwise incomparable points. We call a multifiltration *tame* if it has only finitely many critical points. $p \in \mathbb{R}^k$ is called *critical for a simplex* $\sigma$ if for all $\varepsilon > 0$, $\sigma$ is in neither of $\mathcal{X}(p_1 - \varepsilon, ..., p_k), ..., \mathcal{X}(p_1, ..., p_k - \varepsilon)$, whereas $\sigma$ is in all $\mathcal{X}(p_1 + \varepsilon, ..., p_k), ..., \mathcal{X}(p_1, ..., p_k + \varepsilon)$. For simplicity, we assume that $\sigma \in \mathcal{X}(p)$ in this case. A consequence of tameness is that each simplex has a finite number of critical points. Therefore, we can represent a tame multifiltration of a finite simplicial complex $X$ by specifying the set of critical points for each simplex in $X$. We call a multifiltration 1-*critical* if each simplex has a unique critical point. The sum of the number of critical points over all simplices of $X$ is called the *size* of the multifiltration. We may henceforth assume that simplicial multifiltrations are always represented in this form and particularly assume tameness in practice.

EXAMPLES. We give two examples of important multifiltrations.

Given a simplicial complex $X$ and a map $f : X \to \mathbb{R}^k$ with the property that if $\tau \subset \sigma$ are two simplices of $X$, $f(\tau) \leq f(\sigma)$, we define the *sublevel set multifiltration* by

$$\mathcal{X}^f(p) := \{\sigma \in X \mid F(\sigma) \leq p\},$$

It is easy to verify that $\mathcal{X}^f$ yields a (tame) bifiltration and $F(\sigma)$ is the unique critical value of $\sigma$ in the bifiltration. The sublevel set multifiltration can of course be defined on the level of topological spaces as well.

The canonical generalization of the union-of-balls filtration to the setting of two parameters is the *multicover bifiltration*. The second parameter captures the local density of points. This importance of the multicover bifiltration stems from the fact that it solves the problem of the union-of-balls filtration being not robust to outliers. See Section 4.2 for a more thorough introduction of this bifiltration.

See [128] for more examples of multifiltrations and a discussion of their criticality, viewed on the level of topological spaces.

SLICES OF A MULTIFILTRATION. A multifiltration $\mathcal{X} : \mathbb{R}^k \to \mathbf{Top}$ contains an infinite collection of monofiltrations. Let $\mathcal{L}$ be the set of all non-vertical lines in $\mathbb{R}^k$ with positive slope, i.e., its direction has to be nonnegative in all components, and at least one of them has to be strictly positive. Fixing any line $\ell \in \mathcal{L}$, we observe that when traversing this line in positive direction, the subcomplexes of the multifiltration are nested in each other.

Note that $\ell$ intersects the hyperplane $\Sigma_{i=1}^k x_i = 0$ in a unique base point $b$. Parameterizing $\ell$ as $b + \lambda \cdot a$, where $a$ is the (positive) unit direction vector of $\ell$, we obtain a monofiltration: the *slice* $\mathcal{X}_\ell$ of $\mathcal{X}$ along $\ell$

$$\mathcal{X}_\ell(\alpha) := \mathcal{X}(b + \alpha \cdot a).$$

Sometimes we also call $\ell$ itself the slice, however, abusing notation.

The critical values of a slice can be inferred by the critical points of the multifiltration in a computationally straightforward way. Instead of a formal description, we refer to Figure 3.5 for a graphical description. Also, if the multifiltration is of size $n$, each of its slices is of size at most $n$.

From a multifiltration to a simplicial multifiltration. If a multifiltration is appropriately covered, i.e., the cover elements systematically grow in all directions, nerves directly yield simplicial multifiltrations. Unfortunately, we cannot always expect this friendly behavior of covers. Even if such an appropriately covered multifiltration is given, it might be computationally unfeasible. A well-known example for this problem is the multicover bifiltration [154].

As we outline in Section 4.3, nerves can be used for a more general class of covered multifiltrations. Later in Chapter 4, we use these techniques for the construction of a computationally feasible simplicial proxy for the multicover bifiltration.

### 3.2.2 Multiparameter persistence modules

In algebraic multiparameter persistence, we investigate multiparameter persistence modules.

**Definition 6.** Let $P$ be a product of $k$ totally ordered sets, $\mathbb{K}$ a field. A functor $\mathbf{P} \to \mathbf{Vect}_{\mathbb{K}}$ is called *(k-)persistence module* (over $P$ with respect to $\mathbb{K}$). 2-persistence modules are also called *bipersistence modules*.

If $k > 1$, even in the most simple formulation, namely, if $P = \mathbb{N}^k$, no discrete complete invariant for multiparameter persistence modules exists. Hence, there is no full analog of a persistence diagram. This can either be validated from investigating algebro-geometric properties of graded modules over the non-PID $\mathbb{K}[t_1, ..., t_k]$ [43], or by using the wildness of the quiver representation theory of multiparameter persistence modules [94]. The latter has lead to more abstract persistence-related research in quiver representation theory [24, 25, 35, 36].

Completely analogously to the case of one parameter, we obtain multiparameter persistence modules from multifiltrations by applying a homology functor to a multifiltration.

### 3.2.3 Invariants for multiparameter persistence

Since for more than one parameter no complete discrete invariant for multiparameter persistence exists, there are more choices to make on the level of invariants.

Let us have a brief look at simple formulations of invariants and show their incompleteness along minimal examples.

The *Hilbert function* is a standard object in commutative algebra. For a $k$-persistence module $M : \mathbf{P} \to \mathbf{Vect}_{\mathbb{K}}$, it is defined by

$$\begin{aligned} \mathrm{hf} : P &\to \mathbb{N} \cup \infty, \\ p &\mapsto \mathrm{rank} M_p. \end{aligned}$$

In a sense dual to Hilbert functions, the *rank invariant* tracks how the rank changes along the morphisms. For a $k$-persistence module $M : \mathbf{P} \to \mathbf{Vect}_{\mathbb{K}}$, writing $P^2_{\leq}$ for the set of all pairs $(p, q) \in P^2$ with $p \leq q$, the rank invariant is defined as

$$\begin{aligned} \mathrm{rk} : P^2_{\leq} &\to \mathbb{N} \cup \infty, \\ (p, q) &\mapsto \mathrm{rank} M_{p,q}. \end{aligned}$$

The rank invariant captures the same information as the persistence diagram if $k = 1$ [43]. Therefore, it can be viewed as a straight-forward generalization of persistence diagrams. If $k > 1$, the rank invariant is not a complete invariant, however [43]. See Figure 3.6 for an example. Remarkably, the rank invariant captures the same information as the collection of persistence diagrams along all slices, including the vertical and horizontal ones [18].

One usually considers *pointwise finitely dimensional* multiparameter persistence modules, i.e., persistence modules such that the Hilbert function (and, consequently, also the rank invariant) maps to $\mathbb{N}$ instead of $\mathbb{N} \cup \infty$. This is implied if the corresponding graded module is finitely generated.

For more complicated invariants, please consult [95, 132, 153, 161].

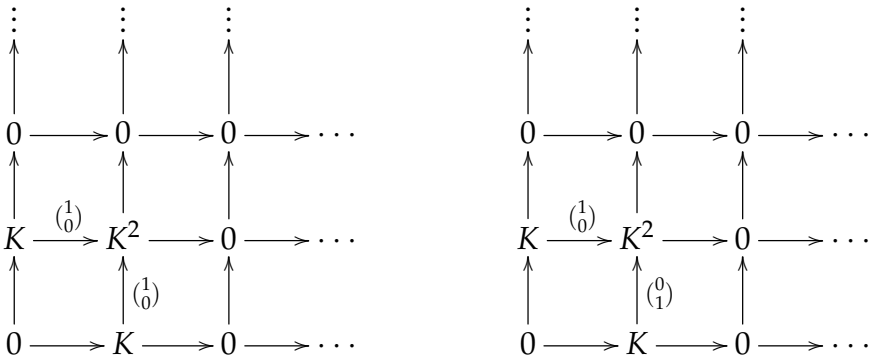


Figure 3.6: Two non-isomorphic persistence modules with same Hilbert function and same rank invariant.

**Computations of invariants.** There exists a useful tool for persistence of 2 parameters called RIVET [130]. It features the computation of the invariants mentioned before and an interactive visualization of 2-parameter persistent homology [131]. In particular, RIVET has an interface that displays the persistence diagram along a slice while this slice can be chosen interactively. In addition to that, it can compute minimal presentations of 2-persistence modules efficiently [132]. RIVET has shown to be useful in applications [115].

### 3.2.4 Interpretations

**Distances between multiparameter persistence modules.** The multiparameter version of the *interleaving distance* [129] can be seen as a generalization of the Bottleneck distance. It is defined on multiparameter persistence modules $\mathbb{R}^k \to \mathbf{Vect}_{\mathbb{K}}$. For such a $k$-persistence module $M$ and $\varepsilon \in [0, \infty)$, define $\overrightarrow{\varepsilon} := (\varepsilon, ..., \varepsilon) \in \mathbb{R}^k$. Now, the *$\varepsilon$-shift* $M(\varepsilon)$ of $M$ is given by $M(\varepsilon)_p := M_{p+\overrightarrow{\varepsilon}}$ on vector spaces and $M(\varepsilon)_{p,q} := M_{p+\overrightarrow{\varepsilon},q+\overrightarrow{\varepsilon}}$ on linear transformations for all $p \leq q \in \mathbb{R}^k$. Note that for any morphism of $k$-persistence modules $\xi : M \to N$, an $\varepsilon$-shift induces a morphism $\xi(\varepsilon) : M(\varepsilon) \to N(\varepsilon)$. Furthermore, the maps $M_{p,p+\varepsilon}$ induce a morphism $\varepsilon^M : M \to M(\varepsilon)$. Now, an *$\varepsilon$-interleaving* between $M$ and $N$ is defined to be a

pair of morphisms $\xi : M \to N$, $\eta : N \to M$ such that

$$\eta(\varepsilon) \circ \xi = (2\varepsilon)^M,$$
$$\xi(\varepsilon) \circ \eta = (2\varepsilon)^N.$$

Note that if $\varepsilon = 0$, this just rephrases the condition of two $k$-persistence modules being isomorphic. The *interleaving distance* $d_I$ on $k$-persistence modules is defined by

$$d_I(M, N) := \inf\{\varepsilon \mid \text{There exists an } \varepsilon\text{-interleaving between } M \text{ and } N\}.$$

Remarkably, the universality of the interleaving distance generalizes to the multiparameter setting. That means that the interleaving distance is stable and every stable distance $d$ on $k$-persistence modules over a prime field satisfies $d \leq d_I$ [129].

Recently it was proved that it is NP-hard to compute the interleaving distance [21, 22]. It is an interesting topic to find and investigate subclasses of multiparameter persistence modules on which the interleaving distance has a better computational performance [69, 70]. A computationally more feasible alternative of a stable distance on $k$-persistence modules is given by the *matching distance* [47]. It is known to be computable in polynomial time for $k = 2$ [117, 118].

Alternatively, distances can also be introduced on incomplete invariants [161].

Connections to machine learning algorithms. As for applications to machine learning, the problem of defining kernels for multiparameter persistence is a recent task. In Chapter 6 we give a generic and stable construction of such a kernel. Recently, a preprint on a concrete construction of a kernel called *multiparameter persistent landscapes* [166] has been published as well.

## 3.3 Generalizations

*Zigzag persistence* [39] is a generalization of persistence that allows spaces to both grow and shrink. Also in this case, we are interested in understanding

the topological changes along that process. Formally, in zigzag persistence we are given a diagram of inclusions of spaces

$$X_1 \hookleftarrow X_2 \hookleftarrow X_3 \hookleftarrow X_4 \hookleftarrow \cdots \hookleftarrow X_N = X_{N+1} = \cdots,$$

where the two-sided arrows represent the fact that *one* of these directions is an inclusion. Now, *zigzag persistent homology* tracks homology along the given diagram. The resulting diagram is called *(zigzag) persistence module*. As in the case of ordinary persistent homology, a complete discrete invariant exists for zigzag persistence, analogously to persistence diagrams. This can for instance be defined with the use of quiver representation theory [25, 94]. Note that are many well-working algorithms for computing zigzag persistent homology [40, 137, 119].

It is an active field of research to consider more general versions of persistence. These include persistence over general posets [25, 34, 139], directed acyclic graphs [48], and, as exposed in Section 5, monoids [61].

# 4 Paper 1: Computing the multicover bifiltration

This is joint work with Michael Kerber and Michael Lesnick. By the date of the publication of this thesis, a version of this work is submitted but not yet published.

Abstract. Given a finite set $A \subset \mathbb{R}^d$, let $\mathrm{Cov}_{r,k}$ denote the set of all points within distance $r$ to at least $k$ points of $A$. Allowing $r$ and $k$ to vary, the spaces $\mathrm{Cov}_{r,k}$ form a 2-parameter family of spaces that grow larger when $r$ increases or $k$ decreases, known as the *multicover bifiltration*. We introduce a simplicial bifiltration S-$\mathrm{Cov}_{r,k}$ which is topologically equivalent (in the sense of persistent homology) to the multicover bifiltration and far smaller than a Čech-based construction considered in prior work of Sheehy. Our construction uses the nerve of covers of the $\mathrm{Cov}_{r,k}$ by higher-order Voronoi cells. For $d = 2$, we describe an algorithm to compute S-$\mathrm{Cov}_{r,k}$, and present some experimental results.

## 4.1 Introduction

In this work, we study a natural density-sensitive 2-parameter persistence construction, the *multicover bifiltration* [52, 86, 154], with a view towards practical data analysis computations. The multicover bifiltration extends the usual union-of-balls filtration and is well suited to the study of noisy data. Given a fixed radius $r \geq 0$ (the *scale*) and $k \in \mathbb{N}$ (the *local density*), the *k-fold cover* of a finite set $A \subset \mathbb{R}^d$ consists of all points in $\mathbb{R}^d$ that are covered by $k$ or more closed balls of radius $r$ centered at points in $A$. Equivalently, the $k$-fold cover is defined to be the set of all points that are within distance $r$ to at least $k$ points of $A$. See Figure 4.1 for an example. The parameterized family of all such spaces, as $k$ and $r$ vary, is called the multicover bifiltration. If $r$ increases or $k$ decreases, the corresponding space grows, giving the multicover the structure of a bifiltration.

Regardless of which invariants of the multicover bifiltration we wish to consider, to handle this bifiltration computationally, the natural first step is to find a reasonably sized *simplicial model* for the bifiltration, i.e., a bifiltration of simplicial complexes which preserves the homology modules of the multicover bifiltration, up to isomorphism.

In the 1-parameter setting, the *Čech filtration* is a standard simplicial model for the union-of-balls filtration, given at each scale by the nerve of the balls. For large point sets, this is too large to be used in practical computations of full persistence diagrams. However, a subfiltration of the Čech filtration called the *Delaunay filtration* (also known as the alpha filtration) [77, 82] also is a simplicial model for the union-of-balls filtration, and is much smaller. The Delaunay filtration is given at each scale by intersecting each ball with the Voronoi cell [168] of its center, and then taking the nerve of the resulting regions. For $d$ small (say $d \leq 3$), the Delaunay filtration is readily computed in practice for many thousands of points.

As observed by Sheehy [154], the multicover bifiltration also has a Čech-based simplicial model, obtained by filtering the barycentric subdivision of each Čech complex. While this construction is mathematically appealing, the resulting bifiltration has exponentially many vertices in the size of the input, making it even more unsuitable for computational purposes than the ordinary Čech filtration.

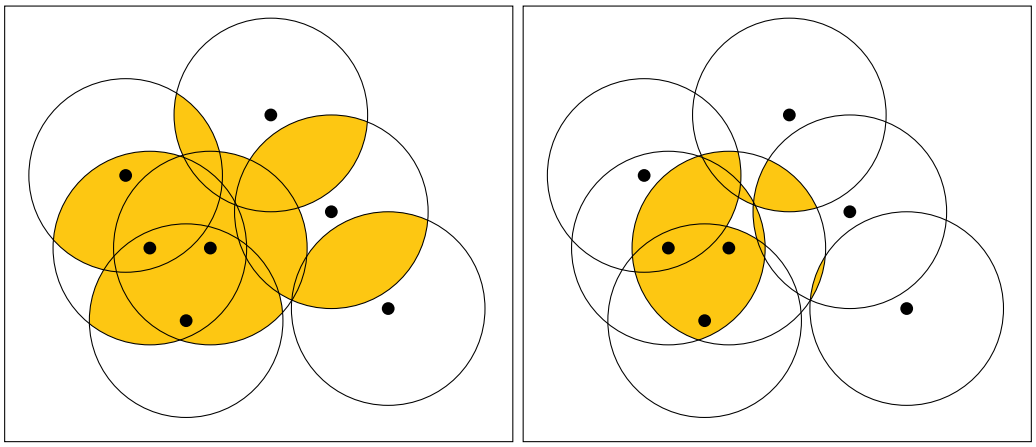

Figure 4.1: In yellow: the 2-, and 3-fold cover of a few points with respect to a certain radius. The first homology of the 2-fold cover is trivial, while the first homology of the 3-fold cover is non-trivial.

Recent work of Edelsbrunner and Osang [86] thus seeks to develop the computational theory of the multicover bifiltration using *higher-order Delaunay complexes* [78, 120], taking the alpha filtration as inspiration. That work provides a polynomial time algorithm to compute the persistence diagrams of a horizontal or vertical slice of the multicover bifiltration. (By this, we mean the single-parameter filtration obtained by fixing either one of the two parameters $k, r$ in the bifiltration.) For fixed local density $k$ and varying scale $r$, this is straightforward, using the fact that the $k$-th order Delaunay complexes form a filtration. On the other hand, for fixed $r$ and varying $k$, the $k$-th order Delaunay complexes do not form a filtration. Thus, to compute a persistence diagram of a linear slice of the multicover bifiltration, of varying density and fixed scale, [86] considers a zigzag construction. It is defined in terms of a polyhedral cell decomposition of $\mathbb{R}^{d+1}$ which contains all higher-order Delaunay complexes as planar sections.

A simplicial model of the full multicover bifiltration is not provided in [86], and indeed the question of how to handle the full 2-parameter setting is left as an open question in [86].

Contributions. Our first contribution is a different way to assemble the Delaunay complexes over all orders into a zigzag diagram, which is conceptually simpler than the approach of [86], yet sufficient to encode the homology of the multicover bifiltration. Our approach uses the interpretation of Delaunay complexes as nerves of a cover of Voronoi regions, and includes the Delaunay complexes of order $k$ and $k+1$ into the nerve of the common refinement of the covers. This leads to a zigzag of filtered simplicial complexes along the parameter $k$. Applying homology to this zigzag and then inverting certain isomorphisms yields a bipersistence module (without zigzags) isomorphic to the bipersistence module of the multicover.
For our second contribution, we straighten out this zigzag to a simplicial bifiltration. Since it is simplicial, existing algorithms and implementations from persistence [71, 93, 130, 131, 132] can be used directly to efficiently compute the homology of this bifiltration or invariants thereof. The straightening technique is the same as in a paper by Sheehy on an approximation of the Vietoris-Rips filtration [155]: just take the union of all simplices that get included in the zigzag. We show the equivalence of the zigzag and its straightening under slightly weaker conditions than in [155].
Our third contribution is an efficient algorithm for the computation of our bifiltration in the plane. In particular, we use Delaunay triangulations and geometric properties of higher-order Voronoi diagrams. Fixing a maximal density index $K$, we show that the size of the bifiltration is $O(K^2n)$, its time complexity is $O(K^2n(K+\log n))$, and its space complexity is $O(K^2n)$.
Our final contribution is an implementation of this algorithm, together with experimental results. We experimentally show how the size of the bifiltration scales when the input set or the scale parameter increases, and how the running time scales along these lines.

## 4.2 Background on the multicover bifiltration

Multicovers. Let $A$ be a finite subset of $\mathbb{R}^d$. Its *k-fold cover of radius r* is defined as

$$\mathrm{Cov}_{r,k} := \left\{ b \in \mathbb{R}^d \mid \; ||b-a|| \leq r \text{ for at least } k \text{ points } a \in A \right\}.$$

In other words, the multicover $\mathrm{Cov}_{r,k}$ describes the space given by the union of all points that are covered by $k$ or more closed balls of radius $r$. With respect to topological terminology, multicovers are actually the *union* of all multiply covered spaces with respect to a certain value of $r$ and $k$, respectively. Hence, multicovers are rather the covered space itself. In order to be in accordance with the existing literature, we stick to the above terminology, however.

SIMPLICIAL COMPLEXES FOR MULTICOVERS. A first step towards constructing a simplicial model for $\mathrm{Cov}_{r,k}$ is to decompose the multicover into a cover in the topological sense. For $\widetilde{A} \subseteq A$ we define

$$\mathrm{Cov}_r(\widetilde{A}) := \left\{ b \in \mathbb{R}^d \mid \; ||b - \tilde{a}|| \leq r \text{ for all } \tilde{a} \in \widetilde{A} \right\}.$$

Clearly, $\mathrm{Cov}_{r,k}$ is the union of all $\mathrm{Cov}_r(\widetilde{A})$ such that $\widetilde{A} \subseteq A$ and $|\widetilde{A}| = k$, and each $\mathrm{Cov}_r(\widetilde{A})$ is closed and convex. Hence, $\mathrm{Cov}_{r,k}$ is homotopy equivalent to the nerve of all $\mathrm{Cov}_r(\widetilde{A})$:

$$\mathrm{Nrv}\left( \left\{ \mathrm{Cov}_r(\widetilde{A}) \mid \widetilde{A} \subseteq A, |\widetilde{A}| = k \right\} \right).$$

For fixed $k$ and increasing $r$, we get inclusions on the nerve level. On the other hand, using the barycentric subdivision, fixing $r$ and letting $k$ decrease, we get inclusions, too [154]. However, there is no hope for applying this construction of a simplicial bifiltration to large point sets: for order $k$, it contains $\binom{n}{k}$ vertices.

Towards constructions of computationally more feasible simplicial complexes, we use *higher-order Delaunay complexes* [78, 120]. First we need to define *higher-order Voronoi diagrams* [8, 87]. These give a decomposition of the space into closed convex subsets having the same $k$ closest points of $A$ in common. Formally, for a subset $\tilde{A} \subseteq A$ with $|\tilde{A}| = k$, define its *Voronoi region* as

$$\mathrm{Vor}(\tilde{A}) := \left\{ b \in \mathbb{R}^d \mid \; ||b - \tilde{a}|| \leq ||b - a|| \text{ for all } \tilde{a} \in \tilde{A}, a \in A \right\}.$$

The set of all Voronoi regions of subsets with cardinality $k$ yields a decomposition of $\mathbb{R}^d$.

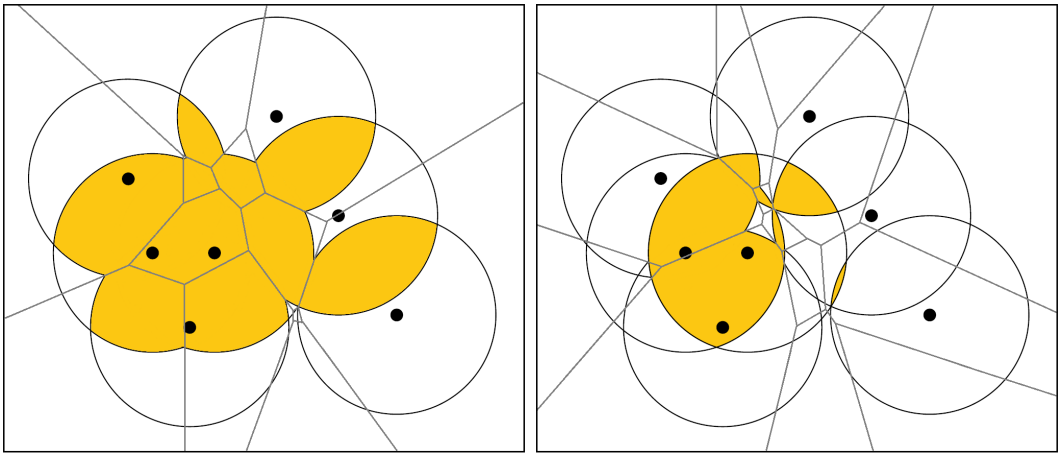

Figure 4.2: *Left:* The 2-fold cover of some points with respect to a certain radius overlapped with its Voronoi diagram of order 2. Vor-Cov$_{r,2}$ is combinatorially simpler than $\{\mathrm{Cov}_r(\tilde{A}) \mid \tilde{A} \subseteq A, |\tilde{A}| = 2\}$. *Right:* The corresponding 3-fold cover overlapped with its Voronoi diagram of order 3.

The *k-th order Voronoi diagram* of $A$ is the subdivision of $\mathbb{R}^d$ induced by the Voronoi regions of subsets $\tilde{A} \subseteq A$ with $|\tilde{A}| = k$. For $d = 2$ and arbitrary $k$, the space gets subdivided by a planar graph (with some edges being unbounded). We call its vertices *(k-th order) Voronoi vertices*, and its edges *(k-th order) Voronoi edges*.
Now, we restrict the multicovers of fixed radius to the corresponding Voronoi regions:

$$\text{Vor-Cov}_{r,k} := \left\{ \mathrm{Cov}_r(\tilde{A}) \cap \mathrm{Vor}(\tilde{A}) \mid \tilde{A} \subseteq A, |\tilde{A}| = k \right\}.$$

For an illustration, see Figure 4.2. Its nerve is the *k-th order Delaunay complex (of radius r)*:

$$\mathrm{Del}_{r,k} := \mathrm{Nrv}\left(\text{Vor-Cov}_{r,k}\right).$$

When $r = \infty$, the $k$-th order Delaunay complex is equal to the *Delaunay triangulation* [67, 79], which we denote by $\mathrm{Del}_k$. Note that $\mathrm{Del}_{r,1}$ is the *alpha complex* of radius $r$ [77, 82].

## 4.3 Methodological overview

Before we describe our construction of an efficient simplicial version of the multicover bifiltration in details, we give an overview on the methods. Since we apply these methods to a bifiltration, we restrict to bifiltrations in this section as well. Note that the rest of the paper can be read without a consultation of this section.

### Jointly well covered filtrations.

**Definition 7.** Given an $\mathbb{N}^{op}$-filtration that we denote by $(X_i)_{i\in\mathbb{N}}$. We call $(\mathfrak{X}_i)_{i\in\mathbb{N}}$ *jointly good covers for* $(X_i)_{i\in\mathbb{N}}$ if $(\mathfrak{X}_i)$ is a good cover of $X_i$ for all $i \in \mathbb{N}$ and $\mathfrak{X}_i \cup \mathfrak{X}_{i+1}$ is a good cover of $X_i$ for all $i \in \mathbb{N}$. In this situation we call $((X_i)_{i\in\mathbb{N}}, (\mathfrak{X}_i)_{i\in\mathbb{N}})$ a *jointly well covered filtration*. If in addition the inclusions of covers $\mathfrak{X}_i \hookrightarrow \mathfrak{X}_i \cup \mathfrak{X}_{i+1}$ induce homotopy equivalences $\mathrm{Nrv}(\mathfrak{X}_i) \hookrightarrow \mathrm{Nrv}(\mathfrak{X}_i \cup \mathfrak{X}_{i+1})$ for all $i \in \mathbb{N}$, we call $(\mathfrak{X}_i)_{i\in\mathbb{N}}$ *strong jointly good covers* and $((X_i)_{i\in\mathbb{N}}, (\mathfrak{X}_i)_{i\in\mathbb{N}})$ a *strong jointly well covered filtration*.

This definition can also be stated for other totally ordered sets such as $\mathbb{N}$ and $\mathbb{Z}$. In these two cases, one has to change the conditions such that $\mathfrak{X}_i \cup \mathfrak{X}_{i+1}$ is a good cover of $X_{i+1}$ for all $i \in \mathbb{N}$ or all $i \in \mathbb{Z}$, respectively. For strong jointly good covers, all induced maps $\mathrm{Nrv}(\mathfrak{X}_{i+1}) \hookrightarrow \mathrm{Nrv}(\mathfrak{X}_i \cup \mathfrak{X}_{i+1})$ have to be homotopy equivalences. The direction of the total orders induce opposite directions in the conditions.

For jointly well covered filtrations, it is not difficult to see that all unions of the form $\bigcup_{j=i}^{l} \mathfrak{X}_j$ are good covers of $X_i$. This gives rise to even define jointly well covered filtrations over an arbitrary totally ordered set. Here, we demand that the union of all covers between two elements have to be good. The assumptions in this alternative definition are still relatively weak. For instance, one could also demand that arbitrary unions of good covers build good covers. Although this might be true in various use cases, we do not need this stronger condition.

**Example 1.** $(i)$ Vor-Cov, *the restrictions of multicovers of Euclidean balls to the corresponding Voronoi regions, induce jointly well covered filtrations along the density parameter for an arbitrary radius: Letting $X_k$ denote the k-fold covers of some radius r, we do not only have inclusions $X_1 \supseteq X_2 \supseteq X_3 \supseteq \cdots$, but also that the covers* $\text{Vor-Cov}_{r,k}$ *are finite closed convex covers of $X_k$. The union of two finite closed convex covers of subsets of $\mathbb{R}^n$ is again a finite closed convex cover of the union of the corresponding subsets of $\mathbb{R}^n$. Hence, the covers* $(\text{Vor-Cov}_{r,k})_{k\in\mathbb{N}}$ *are jointly good covers.*

$(ii)$ *A special case of jointly well covered filtrations are those filtrations that are covered by nested good covers. This includes many standard cases such as the union-of-balls filtration. Also, fixing a density parameter, multicovers of Euclidean balls induce strong jointly well covered filtrations along the radius, even when the covers are restricted to the corresponding Voronoi regions.*

Let $((X_i)_{i\in\mathbb{N}}, (\mathfrak{X}_i)_{i\in\mathbb{N}})$ be a jointly well covered filtration. Consider the diagram of canonical inclusions and canonical projections

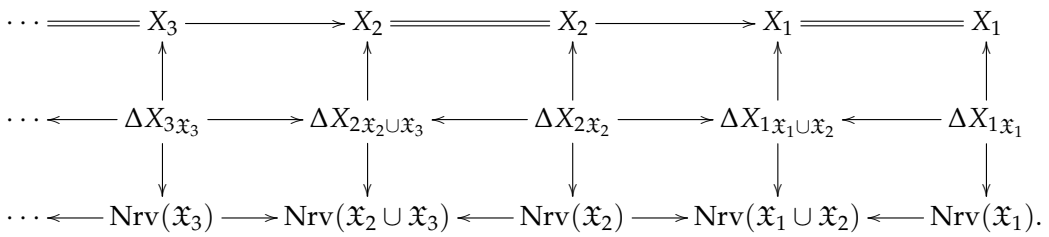


Recall that the maps are defined to be as follows. $X_{i+1} \hookrightarrow X_i$ is the inclusion induced by the subset relation $X_{i+1} \subseteq X_i$. We get the canonical inclusions $\text{Nrv}(\mathfrak{X}_i) \hookrightarrow \text{Nrv}(\mathfrak{X}_i \cup \mathfrak{X}_{i+1})$ and $\text{Nrv}(\mathfrak{X}_{i+1}) \hookrightarrow \text{Nrv}(\mathfrak{X}_i \cup \mathfrak{X}_{i+1})$. As for the vertical arrows $\Delta X_{i\mathfrak{X}_i} \to X_i$ and $\Delta X_{i\mathfrak{X}_i} \to \text{Nrv}(\mathfrak{X}_i)$, the maps are the projections coming from the construction of $\Delta X_{\mathfrak{X}}$ as seen in the proof of the Nerve Theorem. The same holds true for $\Delta X_{i\mathfrak{X}_i\cup\mathfrak{X}_{i+1}} \to \text{Nrv}(\mathfrak{X}_i \cup \mathfrak{X}_{i+1})$ and $\Delta X_{i\mathfrak{X}_i\cup\mathfrak{X}_{i+1}} \to X_i$, since $\mathfrak{X}_i \cup \mathfrak{X}_{i+1}$ is a good cover and $X_i = X_i \cup X_{i+1}$. Finally, the maps $\Delta X_{i\mathfrak{X}_i} \hookrightarrow \Delta X_{i\mathfrak{X}_i\cup\mathfrak{X}_{i+1}}$ and $\Delta X_{i+1\mathfrak{X}_{i+1}} \hookrightarrow \Delta X_{i\mathfrak{X}_i\cup\mathfrak{X}_{i+1}}$ are given by the products of the maps on space level and nerve level defined before. It is not difficult to show that this diagram commutes. More remarkably, many of these maps are homotopy equivalences.

**Lemma 2.** *In the above diagram, all maps of the forms* $\Delta X_{i\mathfrak{X}_i} \to X_i$, $\Delta X_{i\mathfrak{X}_i} \to \mathrm{Nrv}(\mathfrak{X}_i)$, $\Delta X_{i\mathfrak{X}_i \cup \mathfrak{X}_{i+1}} \to \mathrm{Nrv}(\mathfrak{X}_i \cup \mathfrak{X}_{i+1})$, $\Delta X_{i\mathfrak{X}_i \cup \mathfrak{X}_{i+1}} \to X_i$, *are homotopy equivalences. If the filtration is a strong jointly well covered filtration, then also* $\Delta X_{i\mathfrak{X}_i} \hookrightarrow \Delta X_{i\mathfrak{X}_i \cup \mathfrak{X}_{i+1}}$ *and* $\mathrm{Nrv}(\mathfrak{X}_i) \hookrightarrow \mathrm{Nrv}(\mathfrak{X}_i \cup \mathfrak{X}_{i+1})$ *are homotopy equivalences. Hence, we can write*

$$\begin{array}{ccccccccccc}
\cdots & = & X_3 & \longrightarrow & X_2 & = & X_2 & \longrightarrow & X_1 & = & X_1 \\
 & & \simeq\uparrow & & \simeq\uparrow & & \simeq\uparrow & & \simeq\uparrow & & \simeq\uparrow \\
\cdots & \longleftarrow & \Delta X_{3\mathfrak{X}_3} & \longrightarrow & \Delta X_{2\mathfrak{X}_2\cup\mathfrak{X}_3} & \longleftarrow & \Delta X_{2\mathfrak{X}_2} & \longrightarrow & \Delta X_{1\mathfrak{X}_1\cup\mathfrak{X}_2} & \longleftarrow & \Delta X_{1\mathfrak{X}_1} \\
 & & \simeq\downarrow & & \simeq\downarrow & & \simeq\downarrow & & \simeq\downarrow & & \simeq\downarrow \\
\cdots & \longleftarrow & \mathrm{Nrv}(\mathfrak{X}_3) & \longrightarrow & \mathrm{Nrv}(\mathfrak{X}_2 \cup \mathfrak{X}_3) & \longleftarrow & \mathrm{Nrv}(\mathfrak{X}_2) & \longrightarrow & \mathrm{Nrv}(\mathfrak{X}_1 \cup \mathfrak{X}_2) & \longleftarrow & \mathrm{Nrv}(\mathfrak{X}_1),
\end{array}$$

*and for strong jointly well covered filtrations* $\mathrm{Nrv}(\mathfrak{X}_i) \hookrightarrow \mathrm{Nrv}(\mathfrak{X}_i \cup \mathfrak{X}_{i+1})$ *and* $\Delta X_{i\mathfrak{X}_i} \hookrightarrow \Delta X_{i\mathfrak{X}_i \cup \mathfrak{X}_{i+1}}$ *are homotopy equivalences. So, in this case we can write*

$$\begin{array}{ccccccccccc}
\cdots & = & X_3 & \longrightarrow & X_2 & = & X_2 & \longrightarrow & X_1 & = & X_1 \\
 & & \simeq\uparrow & & \simeq\uparrow & & \simeq\uparrow & & \simeq\uparrow & & \simeq\uparrow \\
\cdots & \xleftarrow{\simeq} & \Delta X_{3\mathfrak{X}_3} & \longrightarrow & \Delta X_{2\mathfrak{X}_2\cup\mathfrak{X}_3} & \xleftarrow{\simeq} & \Delta X_{2\mathfrak{X}_2} & \longrightarrow & \Delta X_{1\mathfrak{X}_1\cup\mathfrak{X}_2} & \xleftarrow{\simeq} & \Delta X_{1\mathfrak{X}_1} \\
 & & \simeq\downarrow & & \simeq\downarrow & & \simeq\downarrow & & \simeq\downarrow & & \simeq\downarrow \\
\cdots & \xleftarrow{\simeq} & \mathrm{Nrv}(\mathfrak{X}_3) & \longrightarrow & \mathrm{Nrv}(\mathfrak{X}_2 \cup \mathfrak{X}_3) & \xleftarrow{\simeq} & \mathrm{Nrv}(\mathfrak{X}_2) & \longrightarrow & \mathrm{Nrv}(\mathfrak{X}_1 \cup \mathfrak{X}_2) & \xleftarrow{\simeq} & \mathrm{Nrv}(\mathfrak{X}_1).
\end{array}$$

*Proof.* The maps of the form $\Delta X_{i\mathfrak{X}_i} \to X_i$ and $\Delta X_{i\mathfrak{X}_i} \to \mathrm{Nrv}(\mathfrak{X}_i)$ are homotopy equivalences because the covers were assumed to be good. Since the union of two consecutive covers is still assumed to be good, the maps $\Delta X_{i\mathfrak{X}_i \cup \mathfrak{X}_{i+1}} \to \mathrm{Nrv}(\mathfrak{X}_i \cup \mathfrak{X}_{i+1})$ and $\Delta X_{i\mathfrak{X}_i \cup \mathfrak{X}_{i+1}} \to X_i$ are homotopy equivalences as well.
If the filtration is strong jointly well covered, then we are also given homotopy equivalence $\mathrm{Nrv}(\mathfrak{X}_i) \hookrightarrow \mathrm{Nrv}(\mathfrak{X}_i \cup \mathfrak{X}_{i+1})$. The maps of the form $\Delta X_{i\mathfrak{X}_i} \hookrightarrow \Delta X_{i\mathfrak{X}_i \cup \mathfrak{X}_{i+1}}$ are homotopy equivalences as well since such maps consist of the product of a homotopy equivalence and the identity map, which is a homotopy equivalence. □

In this lemma we see a difference between jointly well covered filtrations and strong jointly well covered filtrations. The strongness assumption is

necessary to give a homotopical proxy of the given filtration of spaces. In other words, the zigzag filtrations

$$\cdots = X_3 \longrightarrow X_2 = X_2 \longrightarrow X_1 = X_1$$

and

$$\cdots \longleftarrow \mathrm{Nrv}(\mathfrak{X}_3) \longrightarrow \mathrm{Nrv}(\mathfrak{X}_2 \cup \mathfrak{X}_3) \longleftarrow \mathrm{Nrv}(\mathfrak{X}_2) \longrightarrow \mathrm{Nrv}(\mathfrak{X}_1 \cup \mathfrak{X}_2) \longleftarrow \mathrm{Nrv}(\mathfrak{X}_1)$$

are homotopically equivalent if we are given a strong jointly well covered filtration. When going over to homology, however, strongness is not necessary:

**Theorem 3.** *Let $((X_i)_{i\in\mathbb{N}}, (\mathfrak{X}_i)_{i\in\mathbb{N}})$ be a jointly well covered filtration. Then the zigzags*

$$\cdots = X_3 \longrightarrow X_2 = X_2 \longrightarrow X_1 = X_1$$

*and*

$$\cdots \longleftarrow \mathrm{Nrv}(\mathfrak{X}_3) \longrightarrow \mathrm{Nrv}(\mathfrak{X}_2 \cup \mathfrak{X}_3) \longleftarrow \mathrm{Nrv}(\mathfrak{X}_2) \longrightarrow \mathrm{Nrv}(\mathfrak{X}_1 \cup \mathfrak{X}_2) \longleftarrow \mathrm{Nrv}(\mathfrak{X}_1)$$

*induce isomorphic persistence modules on homology.*

*Proof.* Using that homotopy equivalences induce isomorphisms on homology, we obtain the diagram

$$\begin{array}{ccccccc}
\cdots & \longrightarrow & H_*(X_2) & = & H_*(X_2) & \longrightarrow & H_*(X_1) & = & H_*(X_1) \\
 & & \cong\uparrow & & \cong\uparrow & & \cong\uparrow & & \cong\uparrow \\
\cdots & \longrightarrow & H_*(\Delta X_{2\mathfrak{X}_2\cup\mathfrak{X}_3}) & \longleftarrow & H_*(\Delta X_{2\mathfrak{X}_2}) & \longrightarrow & H_*(\Delta X_{1\mathfrak{X}_1\cup\mathfrak{X}_2}) & \longleftarrow & H_*(\Delta X_{1\mathfrak{X}_1}) \\
 & & \cong\downarrow & & \cong\downarrow & & \cong\downarrow & & \cong\downarrow \\
\cdots & \longrightarrow & H_*(\mathrm{Nrv}(\mathfrak{X}_2\cup\mathfrak{X}_3)) & \longleftarrow & H_*(\mathrm{Nrv}(\mathfrak{X}_2)) & \longrightarrow & H_*(\mathrm{Nrv}(\mathfrak{X}_1\cup\mathfrak{X}_2)) & \longleftarrow & H_*(\mathrm{Nrv}(\mathfrak{X}_1)).
\end{array}$$

Applying the homology functor preserves the commutativity of diagrams. Chasing the diagram, all maps of the form $H_*(\Delta X_{i\mathfrak{X}_i}) \to H_*(\Delta X_{i\mathfrak{X}_i\cup\mathfrak{X}_{i+1}})$ and, consequently, $H_*(\mathrm{Nrv}(\mathfrak{X}_i)) \to H_*(\mathrm{Nrv}(\mathfrak{X}_i \cup \mathfrak{X}_{i+1}))$ have to be isomorphisms.

Therefore, the persistence modules on space level and nerve level are connected by a commuting diagram of index-wise isomorphisms

$$\begin{array}{ccccccccc}
\cdots & \longrightarrow & H_*(X_2) & = & H_*(X_2) & \longrightarrow & H_*(X_1) & = & H_*(X_1) \\
 & & \downarrow\cong & & \downarrow\cong & & \downarrow\cong & & \downarrow\cong \\
\cdots & \longrightarrow & H_*(\mathrm{Nrv}(\mathfrak{X}_2 \cup \mathfrak{X}_3)) & \xleftarrow{\cong} & H_*(\mathrm{Nrv}(\mathfrak{X}_2)) & \longrightarrow & H_*(\mathrm{Nrv}(\mathfrak{X}_1 \cup \mathfrak{X}_2)) & \xleftarrow{\cong} & H_*(\mathrm{Nrv}(\mathfrak{X}_1)).
\end{array}$$

Thus, the desired persistence modules are isomorphic. □

As a matter of fact, for all jointly well covered filtrations, we denote the maps of the form $H_*(\mathrm{Nrv}(\mathfrak{X}_{i+1})) \to H_*(\mathrm{Nrv}(\mathfrak{X}_i))$ by the concatenation of $H_*(\mathrm{Nrv}(\mathfrak{X}_{i+1})) \to H_*(\mathrm{Nrv}(\mathfrak{X}_i \cup \mathfrak{X}_{i+1}))$ with the inverse of $H_*(\mathrm{Nrv}(\mathfrak{X}_i)) \to H_*(\mathrm{Nrv}(\mathfrak{X}_i \cup \mathfrak{X}_{i+1}))$. Now, the sequence

$$\cdots \longrightarrow H_*(\mathrm{Nrv}(\mathfrak{X}_4)) \longrightarrow H_*(\mathrm{Nrv}(\mathfrak{X}_3)) \longrightarrow H_*(\mathrm{Nrv}(\mathfrak{X}_2)) \longrightarrow H_*(\mathrm{Nrv}(\mathfrak{X}_1)).$$

is the desired simplicial version of the persistence module

$$\cdots \longrightarrow H_*(X_4) \longrightarrow H_*(X_3) \longrightarrow H_*(X_2) \longrightarrow H_*(X_1).$$

**Essentially one-way zigzags and straightened out filtrations.** Let us outline how we can compute persistent homology of jointly well covered filtrations.

Note that the persistence module

$$\cdots \longrightarrow H_*(\mathrm{Nrv}(\mathfrak{X}_4)) \longrightarrow H_*(\mathrm{Nrv}(\mathfrak{X}_3)) \longrightarrow H_*(\mathrm{Nrv}(\mathfrak{X}_2)) \longrightarrow H_*(\mathrm{Nrv}(\mathfrak{X}_1))$$

is induced by a zigzag quiver

$$\cdots \longrightarrow \mathrm{Nrv}(\mathfrak{X}_2 \cup \mathfrak{X}_3) \longleftarrow \mathrm{Nrv}(\mathfrak{X}_2) \longrightarrow \mathrm{Nrv}(\mathfrak{X}_1 \cup \mathfrak{X}_2) \longleftarrow \mathrm{Nrv}(\mathfrak{X}_1).$$

So, a persistence diagram obtained from a zigzag filtration yields a persistence diagram of the sequence we are actually interested in.

Our zigzag filtrations have the property that all arrows going to the left are isomorphisms. Therefore, for this case of *essentially one-way zigzags*, the algorithms for zigzag persistent homology should be revisited and improved. More concretely, one should express the maps on homology in terms of a consistent system of bases. In particular, this has to be done for the reversed isomorphisms. Strong jointly covered filtrations may give some useful additional structure.

An alternative solution is the technique of *straightening out* the zigzag quiver to a simplicial filtration. This technique has been used by Sheehy [155] for an approximation of the Vietoris-Rips filtration.

**Definition 8.** Let $((X_i)_{i\in\mathbb{N}}, (\mathfrak{X}_i)_{i\in\mathbb{N}})$ be a jointly well covered $\mathbb{N}^{op}$-filtration. Its *straightened out simplicial filtration* $((\text{S-}X_i)_{i\in\mathbb{N}})$ is defined as

$$\text{S-}X_i := \bigcup_{\ell\geq i} \text{Nrv}(\mathfrak{X}_\ell \cup \mathfrak{X}_{\ell+1})$$

It is clear that straightened out simplicial filtrations are in fact simplicial filtrations. Moreover, the straightening technique preserves persistent homology on jointly well covered filtrations:

**Theorem 4.** *Let $((X_i)_{i\in\mathbb{N}}, (\mathfrak{X}_i)_{i\in\mathbb{N}})$ be a jointly well covered $\mathbb{N}^{op}$-filtration. Then the persistence modules $H_*((X_i)_{i\in\mathbb{N}})$ and $H_*((\text{S-}X_i)_{i\in\mathbb{N}})$ are isomorphic.*

*Proof (sketch).* The fact that the homology groups $H_*(X_i)$ and $H_*(\text{S-}X_i)$ at each individual scale $i$ are isomorphic can be seen using excision and Theorem 3. □

We will do a detailed proof for straightening out our simplicial multicover bifiltration along the density parameter. We use excision in Lemma 6. Its proof readily generalizes to the setting of this theorem.

JOINTLY WELL COVERED BIFILTRATIONS. Let us build up a simplicial framework for covered multifiltrations, too. We focus on bifiltrations along $\mathbb{N} \times \mathbb{N}^{op}$. Writing down the commutative diagram of spaces and canonical inclusions, we have

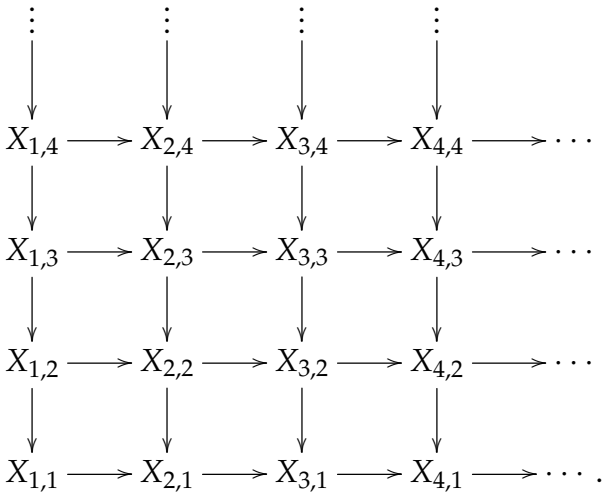

We assume that we have jointly well covered filtrations along all horizontal and vertical slices:

**Definition 9.** Given an $\mathbb{N} \times \mathbb{N}^{op}$-bifiltration $(X_{i,j})_{i,j\in\mathbb{N}}$. We call a family $(\mathfrak{X}_{i,j})_{i,j\in\mathbb{N}}$ *(strong) jointly good covers* for $(X_{i,j})_{i,j\in\mathbb{N}}$ if $\mathfrak{X}_{i,j}$ is a cover for $X_{i,j}$ for all $i, j \in \mathbb{N}$, and any horizontally and vertically embedded filtration in $(X_{i,j})_{i,j\in\mathbb{N}}$ is (strong) jointly well covered with the corresponding covers $\mathfrak{X}_{i,j}$. In this case we call $\big((X_{i,j})_{i,j\in\mathbb{N}}, (\mathfrak{X}_{i,j})_{i,j\in\mathbb{N}}\big)$ *(strong) jointly well covered bifiltration*.

Without any problems, one can also consider the same definition along $\mathbb{N} \times \mathbb{N}$, $\mathbb{N}^{op} \times \mathbb{N}$, or $\mathbb{N}^{op} \times \mathbb{N}^{op}$, or replacing any $\mathbb{N}$ by a $\mathbb{Z}$. This framework can easily be generalized to multifiltrations of more than two parameters. Under slightly stronger assumptions, an analogous version can even be defined for multifiltrations over general posets. To formulate this, the slicewise definition has to be replaced by the property that all unions of the form $\bigcup_{\hat{p}\leq q\leq p} \mathfrak{X}_q$ have to be good covers of $X_p$. Using Example 1, we see that

multicovers of Euclidean balls and their Voronoi-restricted covers Vor-Cov induce a jointly well covered bifiltration over $\mathbb{R} \times \mathbb{N}^{op}$.

The process of going over from a bifiltration to a simplicial bifiltration should preserve the 2-persistence module. We show that this holds true if we use the slice-wise nerve construction of jointly well covered filtrations.

An important step for proving this result is an issue of well-definedness.

**Lemma 3.** *Let* $\left((X_{i,j})_{i,j\in\mathbb{N}}, (\mathfrak{X}_{i,j})_{i,j\in\mathbb{N}}\right)$ *be a jointly well covered bifiltration. Let* $i, j \in \mathbb{N}$*. Then, the diagram of maps obtained from the horizontally and vertically embedded jointly well covered filtrations commutes:*

$$\begin{array}{ccc} H_*\left(\mathrm{Nrv}(\mathfrak{X}_{i,j+1})\right) & \longrightarrow & H_*\left(\mathrm{Nrv}(\mathfrak{X}_{i+1,j+1})\right) \\ \downarrow & & \downarrow \\ H_*\left(\mathrm{Nrv}(\mathfrak{X}_{i,j})\right) & \longrightarrow & H_*\left(\mathrm{Nrv}(\mathfrak{X}_{i+1,j})\right). \end{array}$$

*Proof.* We show that $H_*\left(\mathrm{Nrv}(\mathfrak{X}_{i,j+1})\right) \to H_*\left(\mathrm{Nrv}(\mathfrak{X}_{i,j})\right) \to H_*\left(\mathrm{Nrv}(\mathfrak{X}_{i+1,j})\right)$ and $H_*\left(\mathrm{Nrv}(\mathfrak{X}_{i,j+1})\right) \to H_*\left(\mathrm{Nrv}(\mathfrak{X}_{i+1,j+1})\right) \to H_*\left(\mathrm{Nrv}(\mathfrak{X}_{i+1,j})\right)$ are equal. By construction, the first expression is the concatenation of

$$H_*\left(\mathrm{Nrv}(\mathfrak{X}_{i,j+1})\right) \to H_*\left(\mathrm{Nrv}(\mathfrak{X}_{i,j} \cup \mathfrak{X}_{i,j+1})\right) \xrightarrow{\cong} H_*\left(\mathrm{Nrv}(\mathfrak{X}_{i,j})\right)$$

and

$$H_*\left(\mathrm{Nrv}(\mathfrak{X}_{i,j})\right) \to H_*\left(\mathrm{Nrv}(\mathfrak{X}_{i,j} \cup \mathfrak{X}_{i+1,j})\right) \xrightarrow{\cong} H_*\left(\mathrm{Nrv}(\mathfrak{X}_{i+1,j})\right).$$

By the commutativity of the corresponding diagrams along these filtrations, it is the same as the concatenation of

$$H_*\left(\mathrm{Nrv}(\mathfrak{X}_{i,j+1})\right) \xrightarrow{\cong} H_*\left(X_{i,j+1}\right) \to H_*\left(X_{i,j}\right) \xrightarrow{\cong} H_*\left(\mathrm{Nrv}(\mathfrak{X}_{i,j})\right)$$

and

$$H_*\left(\mathrm{Nrv}(\mathfrak{X}_{i,j})\right) \xrightarrow{\cong} H_*\left(X_{i,j}\right) \to H_*\left(X_{i+1,j}\right) \xrightarrow{\cong} H_*\left(\mathrm{Nrv}(\mathfrak{X}_{i+1,j})\right).$$

Now, this concatenation can be expressed as

$$H_*\left(\mathrm{Nrv}(\mathfrak{X}_{i,j+1})\right) \xrightarrow{\cong} H_*\left(X_{i,j+1}\right) \to H_*\left(X_{i,j}\right) \to H_*\left(X_{i+1,j}\right) \xrightarrow{\cong} H_*\left(\mathrm{Nrv}(\mathfrak{X}_{i+1,j})\right).$$

The analogous procedure for $H_*\left(\mathrm{Nrv}(\mathfrak{X}_{i,j+1})\right) \to H_*\left(\mathrm{Nrv}(\mathfrak{X}_{i+1,j+1})\right) \to H_*\left(\mathrm{Nrv}(\mathfrak{X}_{i+1,j})\right)$ yields the expression

$$H_*\left(\mathrm{Nrv}(\mathfrak{X}_{i,j+1})\right) \xrightarrow{\cong} H_*\left(X_{i,j+1}\right) \to H_*\left(X_{i+1,j+1}\right) \to H_*\left(X_{i+1,j}\right) \xrightarrow{\cong} H_*\left(\mathrm{Nrv}(\mathfrak{X}_{i+1,j})\right).$$

These expressions denote exactly the same map since the diagram

$$\begin{array}{ccc} H_*\left(X_{i,j+1}\right) & \longrightarrow & H_*\left(X_{i+1,j+1}\right) \\ \downarrow & & \downarrow \\ H_*\left(X_{i,j}\right) & \longrightarrow & H_*\left(X_{i+1,j}\right) \end{array}$$

commutes. Therefore, as we wanted to show, the desired homology diagram on nerve level commutes as well. □

Let us see that the pieces fall into place quite smoothly.

**Theorem 5.** *Let* $\left((X_{i,j})_{i,j\in\mathbb{N}}, (\mathfrak{X}_{i,j})_{i,j\in\mathbb{N}}\right)$ *be a jointly well covered bifiltration. Then, applying the homology functor, its bipersistence module*

$$\begin{array}{ccccccc}
\vdots & & \vdots & & \vdots & & \vdots \\
\downarrow & & \downarrow & & \downarrow & & \downarrow \\
H_*\left(X_{1,4}\right) & \longrightarrow & H_*\left(X_{2,4}\right) & \longrightarrow & H_*\left(X_{3,4}\right) & \longrightarrow & H_*\left(X_{4,4}\right) \longrightarrow \cdots \\
\downarrow & & \downarrow & & \downarrow & & \downarrow \\
H_*\left(X_{1,3}\right) & \longrightarrow & H_*\left(X_{2,3}\right) & \longrightarrow & H_*\left(X_{3,3}\right) & \longrightarrow & H_*\left(X_{4,3}\right) \longrightarrow \cdots \\
\downarrow & & \downarrow & & \downarrow & & \downarrow \\
H_*\left(X_{1,2}\right) & \longrightarrow & H_*\left(X_{2,2}\right) & \longrightarrow & H_*\left(X_{3,2}\right) & \longrightarrow & H_*\left(X_{4,2}\right) \longrightarrow \cdots \\
\downarrow & & \downarrow & & \downarrow & & \downarrow \\
H_*\left(X_{1,1}\right) & \longrightarrow & H_*\left(X_{2,1}\right) & \longrightarrow & H_*\left(X_{3,1}\right) & \longrightarrow & H_*\left(X_{4,1}\right) \longrightarrow \cdots .
\end{array}$$

*is isomorphic to the bipersistence module*

$$\begin{array}{ccccccc}
\vdots & & \vdots & & \vdots & & \vdots \\
\downarrow & & \downarrow & & \downarrow & & \downarrow \\
H_*\left(\mathrm{Nrv}(\mathfrak{X}_{1,4})\right) & \longrightarrow & H_*\left(\mathrm{Nrv}(\mathfrak{X}_{2,4})\right) & \longrightarrow & H_*\left(\mathrm{Nrv}(\mathfrak{X}_{3,4})\right) & \longrightarrow & H_*\left(\mathrm{Nrv}(\mathfrak{X}_{4,4})\right) \longrightarrow \cdots \\
\downarrow & & \downarrow & & \downarrow & & \downarrow \\
H_*\left(\mathrm{Nrv}(\mathfrak{X}_{1,3})\right) & \longrightarrow & H_*\left(\mathrm{Nrv}(\mathfrak{X}_{2,3})\right) & \longrightarrow & H_*\left(\mathrm{Nrv}(\mathfrak{X}_{3,3})\right) & \longrightarrow & H_*\left(\mathrm{Nrv}(\mathfrak{X}_{4,3})\right) \longrightarrow \cdots \\
\downarrow & & \downarrow & & \downarrow & & \downarrow \\
H_*\left(\mathrm{Nrv}(\mathfrak{X}_{1,2})\right) & \longrightarrow & H_*\left(\mathrm{Nrv}(\mathfrak{X}_{2,2})\right) & \longrightarrow & H_*\left(\mathrm{Nrv}(\mathfrak{X}_{3,2})\right) & \longrightarrow & H_*\left(\mathrm{Nrv}(\mathfrak{X}_{4,2})\right) \longrightarrow \cdots \\
\downarrow & & \downarrow & & \downarrow & & \downarrow \\
H_*\left(\mathrm{Nrv}(\mathfrak{X}_{1,1})\right) & \longrightarrow & H_*\left(\mathrm{Nrv}(\mathfrak{X}_{2,1})\right) & \longrightarrow & H_*\left(\mathrm{Nrv}(\mathfrak{X}_{3,1})\right) & \longrightarrow & H_*\left(\mathrm{Nrv}(\mathfrak{X}_{4,1})\right) \longrightarrow \cdots .
\end{array}$$

*in which all maps are defined by the maps of the slice-wise jointly well covered filtrations.*

*Proof.* The bipersistence modules are isomorphic if and only if they are connected by index-wise isomorphisms and all arising diagrams commute. Because of Lemma 3, the second bipersistence module itself is well-defined and thus commutes. Using Theorem 3, the restrictions of the two diagrams to an arbitrary vertical or horizontal line are isomorphic. It is only left to show that all diagrams of the form

$$\begin{array}{ccc}
H_*\left(X_{i,j+1}\right) & \longrightarrow & H_*\left(X_{i,j}\right) \\
\cong\downarrow & & \cong\downarrow \\
H_*\left(\mathrm{Nrv}(\mathfrak{X}_{i,j+1})\right) & \longrightarrow & H_*\left(\mathrm{Nrv}(\mathfrak{X}_{i,j})\right)
\end{array}$$

and

$$\begin{array}{ccc}
H_*\left(X_{i,j}\right) & \longrightarrow & H_*\left(X_{i+1,j}\right) \\
\cong\downarrow & & \cong\downarrow \\
H_*\left(\mathrm{Nrv}(\mathfrak{X}_{i,j})\right) & \longrightarrow & H_*\left(\mathrm{Nrv}(\mathfrak{X}_{i+1,j})\right)
\end{array}$$

commute. But this is clear: as we have already seen in the proof of Lemma 3, the map $H_*\left(\mathrm{Nrv}(\mathfrak{X}_{i,j+1})\right) \to H_*\left(\mathrm{Nrv}(\mathfrak{X}_{i,j})\right)$ can be expressed as

$$H_*\left(\mathrm{Nrv}(\mathfrak{X}_{i,j+1})\right) \xrightarrow{\cong} H_*\left(X_{i,j+1}\right) \to H_*\left(X_{i,j}\right) \xrightarrow{\cong} H_*\left(\mathrm{Nrv}(\mathfrak{X}_{i,j})\right),$$

and the map $H_*\left(\mathrm{Nrv}(\mathfrak{X}_{i,j})\right) \to H_*\left(\mathrm{Nrv}(\mathfrak{X}_{i+1,j})\right)$ can be expressed as

$$H_*\left(\mathrm{Nrv}(\mathfrak{X}_{i,j})\right) \xrightarrow{\cong} H_*\left(X_{i,j}\right) \to H_*\left(X_{i+1,j}\right) \xrightarrow{\cong} H_*\left(\mathrm{Nrv}(\mathfrak{X}_{i+1,j})\right).$$

Thus, the two bipersistence modules are isomorphic. □

For the multicover bifiltration and its restricted cover Vor-Cov, the above framework applies. We will use a slightly different approach, however. Using the straightened out filtration along the density parameter, we construct a simplicial bifiltration that preserves the bipersistence module.

## 4.4 A simplicial zigzag for multicovers

For an arbitrary $r \in \mathbb{R}$, we have inclusions

$$\cdots \hookrightarrow \mathrm{Cov}_{r,5} \hookrightarrow \mathrm{Cov}_{r,4} \hookrightarrow \mathrm{Cov}_{r,3} \hookrightarrow \mathrm{Cov}_{r,2} \hookrightarrow \mathrm{Cov}_{r,1},$$

but there are no inclusions between consecutive higher-order Delaunay complexes $\mathrm{Del}_{r,k}$ along decreasing $k \in \mathbb{N}$. The reason is that the Voronoi regions of consecutive higher-order Voronoi diagrams are not included in each other.

Let us bridge this gap. Recall that Del is defined as the nerve of its underlying cover Vor-Cov. We replace higher-order Delaunay complexes Del by the nerve of the union of two consecutive Vor-Cov. For an illustration of the outcome, see Figure 4.3. Formally, we define

$$\widetilde{\mathrm{Del}}_{r,k} := \mathrm{Nrv}\left(\text{Vor-Cov}_{r,k} \cup \text{Vor-Cov}_{r,k+1}\right).$$

For any choice of $r \in \mathbb{R}$ and $k \in \mathbb{N}$ we get a zigzag

$$\mathrm{Del}_{r,k+1} \hookrightarrow \widetilde{\mathrm{Del}}_{r,k} \hookleftarrow \mathrm{Del}_{r,k}.$$

**Lemma 4.** *For any $r \in \mathbb{R}$ and $k \in \mathbb{N}$, the induced map on homology,*

$$H_*\left(\mathrm{Del}_{r,k}\right) \to H_*(\widetilde{\mathrm{Del}}_{r,k}),$$

*is an isomorphism.*

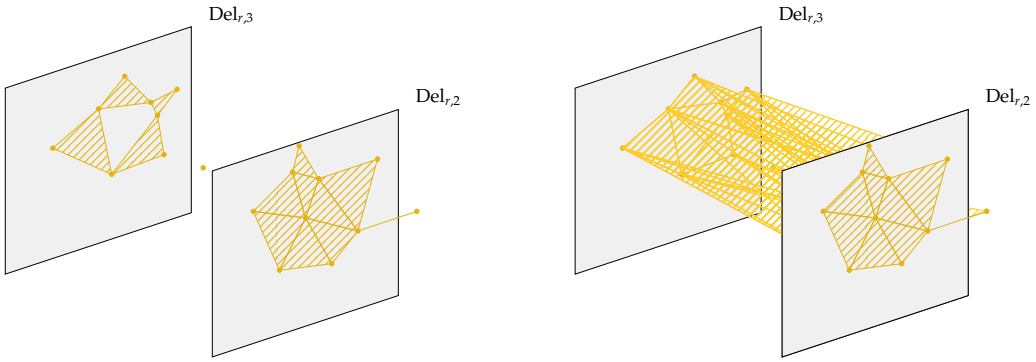


Figure 4.3: *Left:* The Delaunay complexes of order 2 and 3 of our running example. *Right:* The construction of the simplicial complex $\widetilde{\mathrm{Del}}_{r,2}$. $\widetilde{\mathrm{Del}}_{r,2}$ consists of the Delaunay complexes $\mathrm{Del}_{r,2}$ and $\mathrm{Del}_{r,3}$, and additional mixed simplices connecting these. This connection arises from intersections of the 2-, and 3-fold covers restricted to their Voronoi diagrams of order 2 and 3, respectively.

*Proof.* For all $k \in \mathbb{N}$, Vor-$\mathrm{Cov}_{r,k}$ and Vor-$\mathrm{Cov}_{r,k} \cup$ Vor-$\mathrm{Cov}_{r,k+1}$ are finite covers of closed, convex sets in Euclidean space. Hence, the Nerve Theorem (Theorem 1) induces all vertical isomorphisms in the diagram

$$\begin{array}{ccccccccc}
\cdots & = & H_*\left(\mathrm{Cov}_{r,k+1}\right) & \longrightarrow & H_*\left(\mathrm{Cov}_{r,k}\right) & = & H_*\left(\mathrm{Cov}_{r,k}\right) & \longrightarrow & \cdots \\
 & & \downarrow\cong & & \downarrow\cong & & \downarrow\cong & & \\
\cdots & \longleftarrow & H_*(\mathrm{Del}_{r,k+1}) & \longrightarrow & H_*\left(\widetilde{\mathrm{Del}}_{r,k}\right) & \longleftarrow & H_*\left(\mathrm{Del}_{r,k}\right) & \longrightarrow & \cdots .
\end{array}$$

Since these isomorphisms commute with the maps on homology induced by inclusion, the diagram commutes and $H_*\left(\mathrm{Del}_{r,k}\right) \to H_*(\widetilde{\mathrm{Del}}_{r,k})$ is an isomorphism. □

Hence, for all $k \in \mathbb{N}$, we can reverse the arrow $H_*\left(\mathrm{Del}_{r,k}\right) \xrightarrow{\cong} H_*(\widetilde{\mathrm{Del}}_{r,k})$ and define a map

$$H_*\left(\widetilde{\mathrm{Del}}_{r,k+1}\right) \to H_*\left(\widetilde{\mathrm{Del}}_{r,k}\right)$$

by the concatenation of the isomorphism $H_*(\widetilde{\mathrm{Del}}_{r,k+1}) \xrightarrow{\cong} H_*\left(\mathrm{Del}_{r,k+1}\right)$ and the map $H_*\left(\mathrm{Del}_{r,k+1}\right) \to H_*(\widetilde{\mathrm{Del}}_{r,k})$.

Consequently, we get a persistence module

$$\cdots \to H_*\left(\widetilde{\mathrm{Del}}_{r,k+1}\right) \to H_*\left(\widetilde{\mathrm{Del}}_{r,k}\right) \to H_*\left(\widetilde{\mathrm{Del}}_{r,k-1}\right) \to \cdots \to H_*\left(\widetilde{\mathrm{Del}}_{r,1}\right).$$

We get a filtration $(\widetilde{\mathrm{Del}}_{r,k})_{r\in\mathbb{R}}$ for any fixed $k$ when the radius $r$ increases. Combining the induced persistence modules with the persistence modules along $k$ yields a bipersistence module $H_*(\widetilde{\mathrm{Del}}_{r,k})_{r\in\mathbb{R},k\in\mathbb{N}}$.

**Lemma 5.** *$H_*(\widetilde{\mathrm{Del}}_{r,k})_{r\in\mathbb{R},k\in\mathbb{N}}$ is a bipersistence module.*

*Proof.* Let $r \leq s$. We have to show that all squares of the form

$$\begin{array}{ccc} H_*\left(\widetilde{\mathrm{Del}}_{r,k+1}\right) & \longrightarrow & H_*\left(\widetilde{\mathrm{Del}}_{s,k+1}\right) \\ \downarrow & & \downarrow \\ H_*\left(\widetilde{\mathrm{Del}}_{r,k}\right) & \longrightarrow & H_*\left(\widetilde{\mathrm{Del}}_{s,k}\right) \end{array}$$

commute.

Let us have a closer look at the definition of the concatenations of maps

$$H_*\left(\widetilde{\mathrm{Del}}_{r,k+1}\right) \to H_*\left(\widetilde{\mathrm{Del}}_{r,k}\right) \to H_*\left(\widetilde{\mathrm{Del}}_{s,k}\right)$$

and

$$H_*\left(\widetilde{\mathrm{Del}}_{r,k+1}\right) \to H_*\left(\widetilde{\mathrm{Del}}_{s,k+1}\right) \to H_*\left(\widetilde{\mathrm{Del}}_{s,k}\right).$$

By construction, the first sequence is the concatenation of the following maps:

$$H_*\left(\widetilde{\mathrm{Del}}_{r,k+1}\right) \xrightarrow{\cong} H_*\left(\mathrm{Del}_{r,k+1}\right) \to H_*\left(\widetilde{\mathrm{Del}}_{r,k}\right) \to H_*\left(\widetilde{\mathrm{Del}}_{s,k}\right)$$

where the last two maps are induced by an inclusion. The second sequence is given by

$$H_*\left(\widetilde{\mathrm{Del}}_{r,k+1}\right) \to H_*\left(\widetilde{\mathrm{Del}}_{s,k+1}\right) \xrightarrow{\cong} H_*\left(\mathrm{Del}_{s,k+1}\right) \to H_*\left(\widetilde{\mathrm{Del}}_{s,k}\right)$$

where the first and the last map is induced by an inclusion. Therefore, we can use commutativity of homological nerve diagrams. We can replace the above diagrams by

$$H_*\left(\widetilde{\mathrm{Del}}_{r,k+1}\right) \xrightarrow{\cong} H_*\left(\mathrm{Cov}_{r,k+1}\right) \to H_*\left(\mathrm{Cov}_{r,k}\right) \to H_*\left(\mathrm{Cov}_{s,k}\right) \xrightarrow{\cong} H_*\left(\widetilde{\mathrm{Del}}_{s,k}\right)$$

and

$$H_*\left(\widetilde{\mathrm{Del}}_{r,k+1}\right) \xrightarrow{\cong} H_*\left(\mathrm{Cov}_{r,k+1}\right) \to H_*\left(\mathrm{Cov}_{s,k+1}\right) \to H_*\left(\mathrm{Cov}_{s,k}\right) \xrightarrow{\cong} H_*\left(\widetilde{\mathrm{Del}}_{s,k}\right).$$

Since clearly the compositions of maps induced by canonical inclusions

$$H_*\left(\mathrm{Cov}_{r,k+1}\right) \to H_*\left(\mathrm{Cov}_{r,k}\right) \to H_*\left(\mathrm{Cov}_{s,k}\right)$$

and

$$H_*\left(\mathrm{Cov}_{r,k+1}\right) \to H_*\left(\mathrm{Cov}_{s,k+1}\right) \to H_*\left(\mathrm{Cov}_{s,k}\right)$$

are equal, the desired diagram commutes. □

**Theorem 6.** *The bipersistence modules* $H_*(\widetilde{\mathrm{Del}}_{r,k})_{r\in\mathbb{R},k\in\mathbb{N}}$ *and* $H_*(\mathrm{Cov}_{r,k})_{r\in\mathbb{R},k\in\mathbb{N}}$ *are isomorphic.*

*Proof.* Since the diagram in the proof of Lemma 4 commutes on space level, the induced diagram on homology also commutes. Therefore, the isomorphisms between $H_*(\widetilde{\mathrm{Del}}_{r,k})$ and $H_*\left(\mathrm{Cov}_{r,k}\right)$ commute with the maps in the persistence module. Hence, for any fixed radius $r$ the persistence modules $H_*(\widetilde{\mathrm{Del}}_{r,k})_{k\in\mathbb{N}}$ and $H_*(\mathrm{Cov}_{r,k})_{k\in\mathbb{N}}$ along decreasing $k$ are isomorphic. Analogously, fixing $k \in \mathbb{N}$, the persistence modules $H_*(\widetilde{\mathrm{Del}}_{r,k})_{r\in\mathbb{R}}$ and $H_*(\mathrm{Cov}_{r,k}(r,k))_{r\in\mathbb{R}}$ along increasing radii are isomorphic. Therefore, all diagrams of the forms

$$\begin{array}{ccc} H_*\left(\widetilde{\mathrm{Del}}_{r,k+1}\right) & \longrightarrow & H_*\left(\widetilde{\mathrm{Del}}_{r,k}\right) \\ \downarrow\cong & & \downarrow\cong \\ H_*\left(\mathrm{Cov}_{r,k+1}\right) & \longrightarrow & H_*\left(\mathrm{Cov}_{r,k}\right), \end{array} \qquad \begin{array}{ccc} H_*\left(\widetilde{\mathrm{Del}}_{r,k}\right) & \longrightarrow & H_*\left(\widetilde{\mathrm{Del}}_{s,k}\right) \\ \downarrow\cong & & \downarrow\cong \\ H_*\left(\mathrm{Cov}_{r,k}\right) & \longrightarrow & H_*\left(\mathrm{Cov}_{s,k}\right) \end{array}$$

commute for $r \leq s$. Using Lemma 5, all squares commute, and so do the bipersistence modules $H_*(\widetilde{\mathrm{Del}}_{r,k})_{r\in\mathbb{R},k\in\mathbb{N}}$ and $H_*(\mathrm{Cov}_{r,k})_{r\in\mathbb{R},k\in\mathbb{N}}$ with the index-wise isomorphisms $H_*(\widetilde{\mathrm{Del}}_{r,k}) \to H_*(\mathrm{Cov}_{r,k})$. □

Using Lemma 4, we could also consider the persistence module

$$\cdots \to H_*\left(\mathrm{Del}_{r,k+1}\right) \to H_*\left(\mathrm{Del}_{r,k}\right) \to H_*\left(\mathrm{Del}_{r,k-1}\right) \to \cdots \to H_*\left(\mathrm{Del}_{r,1}\right).$$

It is isomorphic to $H_*(\widetilde{\mathrm{Del}}_{r,k})_{k\in\mathbb{N}}$. The subcomplexes Del of $\widetilde{\mathrm{Del}}$ are obviously much smaller. Consequently, the persistence module $H_*(\mathrm{Del}_{r,k})_{k\in\mathbb{N}}$ would be a better choice for zigzag algorithms along $k$. We focus on the complexes $\widetilde{\mathrm{Del}}$, however, since they will be useful for the construction of a simplicial bifiltration in the next section.

## 4.5 A simplicial bifiltration for multicovers

In the previous section we showed how to construct a proxy for persistence of multicovers on the level of bipersistence modules. However, most algorithms for persistent homology and 2-parameter persistent homology use a simplicial bifiltration as input, and not a general bipersistence module [71, 131, 132]. In order to define such a bifiltration, let $n := |A|$, $r \in \mathbb{R}$, and define the filtration

$$\mathrm{Del}_{r,n} = \widetilde{\mathrm{Del}}_{r,n} \hookrightarrow \widetilde{\mathrm{Del}}_{r,n-1} \hookrightarrow \left(\widetilde{\mathrm{Del}}_{r,n-2} \cup \widetilde{\mathrm{Del}}_{r,n-1}\right) \hookrightarrow \cdots \hookrightarrow \bigcup_{i=1}^{n-1} \widetilde{\mathrm{Del}}_{r,i}.$$

Since $\mathrm{Del}_{r,k} = \emptyset$ for all $k > n$, we can denote this filtration by

$$\text{S-Cov}_{r,k} := \bigcup_{i\geq k} \widetilde{\mathrm{Del}}_{r,i}$$

for all $k \in \mathbb{N}$.

In other words, at each position we add all $\widetilde{\mathrm{Del}}_{r,i}$ with $i$ greater than $k$. Note that $\text{S-Cov}_{r,k}$ is *not* equal to the nerve of the union of all $\text{Vor-Cov}_{r,i}$, $i \geq k$, which would result in a much larger object. We show that $\text{S-Cov}_{r,k}$ yields the same homology as $\widetilde{\mathrm{Del}}_{r,k}$: To carry out the proof, only the equivalence on the level of homology is necessary. This is different from the proof in [155], using deformation retracts and contiguity arguments.

**Lemma 6.** *Let $r \in \mathbb{R}, k \in \mathbb{N}$. The canonical inclusion $\widetilde{\mathrm{Del}}_{r,k} \hookrightarrow \text{S-Cov}_{r,k}$ induces an isomorphism on homology.*

*Proof.* Let $r \in \mathbb{R}, k \in \mathbb{N}$. We have to prove that $\widetilde{\mathrm{Del}}_{r,k} \hookrightarrow \bigcup_{i\geq k} \widetilde{\mathrm{Del}}_{r,i}$ induces an isomorphism on homology. By excision, the inclusion $\widetilde{\mathrm{Del}}_{r,n-1} \hookrightarrow \widetilde{\mathrm{Del}}_{r,n-2} \cup \widetilde{\mathrm{Del}}_{r,n-1}$ induces an isomorphism on homology. Inductively, this holds for all inclusions of the form $\bigcup_{i\geq n-j+1} \widetilde{\mathrm{Del}}_{r,i} \hookrightarrow \bigcup_{i\geq n-j} \widetilde{\mathrm{Del}}_{r,i}$. Concatenating the isomorphisms yields the claim. For an illustration of this concept, see Figure 4.4. Let us check the details:

If $k \geq n-1$, the corresponding simplicial complexes $\widetilde{\mathrm{Del}}_{r,k}$ and $\text{S-Cov}_{r,k}$ are equal. Otherwise, namely, if $k < n-1$, we need to prove that $\widetilde{\mathrm{Del}}_{r,k} \hookrightarrow \bigcup_{i\geq k} \widetilde{\mathrm{Del}}_{r,i}$ induces an isomorphism on homology. To do this, we make heavy use of the excision property of homology.

Consider the sequence

$$H_*\left(\widetilde{\mathrm{Del}}_{r,k}\right) \to H_*\left(\widetilde{\mathrm{Del}}_{r,k} \cup \bigcup_{i\geq k+1} \widetilde{\mathrm{Del}}_{r,i}\right) \to H_*\left(\widetilde{\mathrm{Del}}_{r,k} \cup \bigcup_{i\geq k+1} \widetilde{\mathrm{Del}}_{r,i}, \widetilde{\mathrm{Del}}_{r,k}\right)$$

where the first map is induced by the canonical inclusion and the second map is the canonical projection onto relative homology of the union $\widetilde{\mathrm{Del}}_{r,k} \cup \bigcup_{i\geq k+1} \widetilde{\mathrm{Del}}_{r,i}$ modulo $\widetilde{\mathrm{Del}}_{r,k}$. By construction, this sequence is a short exact sequence. We will show that this relative homology is trivial. Then, by exactness, $H_*(\widetilde{\mathrm{Del}}_{r,k}) \to H_*(\widetilde{\mathrm{Del}}_{r,k} \cup \bigcup_{i\geq k+1} \widetilde{\mathrm{Del}}_{r,i}) = H_*(\bigcup_{i\geq k} \widetilde{\mathrm{Del}}_{r,i})$ must be an isormorphism. Since $(\widetilde{\mathrm{Del}}_{r,k} \cup \bigcup_{i\geq k+1} \widetilde{\mathrm{Del}}_{r,i}, \widetilde{\mathrm{Del}}_{r,k})$ is a pair of simplicial complexes, it is a good pair. Hence, by excision, the map

$$H_*\left(\bigcup_{i\geq k+1} \widetilde{\mathrm{Del}}_{r,i}, \widetilde{\mathrm{Del}}_{r,k} \cap \bigcup_{i\geq k+1} \widetilde{\mathrm{Del}}_{r,i}\right) \to H_*\left(\widetilde{\mathrm{Del}}_{r,k} \cup \bigcup_{i\geq k+1} \widetilde{\mathrm{Del}}_{r,i}\right)$$

is an isomorphism. For a detailed argumentation on excision and exact sequences, see Section 2.1 and particularly Corollary 2.24 in [106].
We need to show that the relative homology group

$$H_*\left(\bigcup_{i\geq k+1} \widetilde{\mathrm{Del}}_{r,i}, \widetilde{\mathrm{Del}}_{r,k} \cap \bigcup_{i\geq k+1} \widetilde{\mathrm{Del}}_{r,i}\right)$$

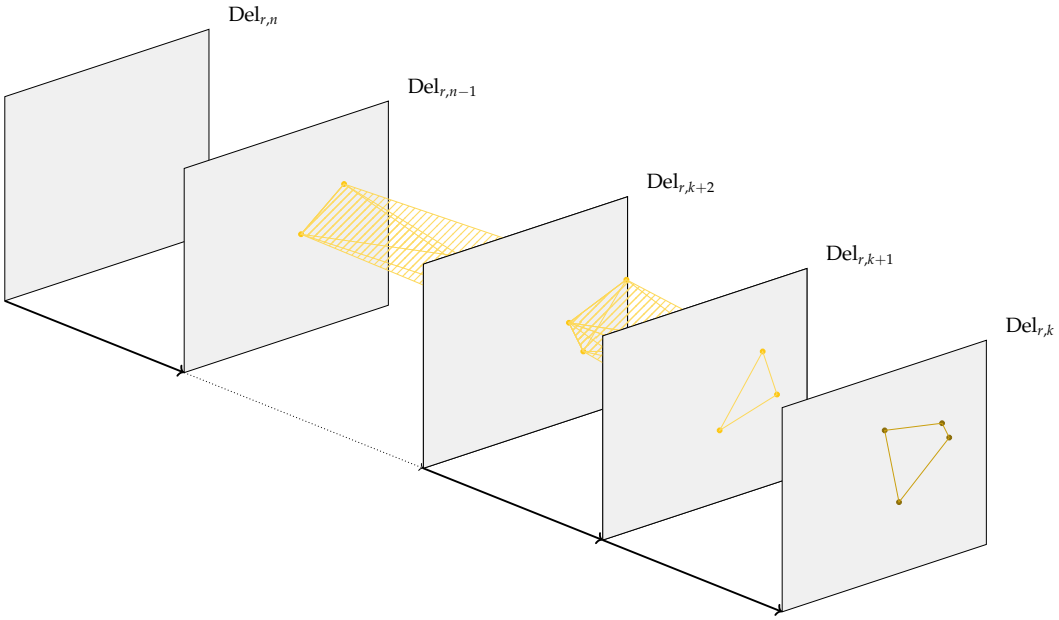


Figure 4.4: An illustration of the idea of the proof of Lemma 6: We use excision of all Delaunay complexes of order higher than $k$ along the union-cover construction of $\widetilde{\mathrm{Del}}$. An arbitrary chain in $\text{S-Cov}_{r,k}$ (in this case, a chain living between the levels $k+1$ and $n-1$; brighter color) is homologous to a chain in $\widetilde{\mathrm{Del}}_{r,k}$. By Lemma 4, it is even homologous to a chain in $\mathrm{Del}_{r,k}$ (darker color).

is trivial. Note that $\widetilde{\mathrm{Del}}_{r,k} \cap \bigcup_{i\geq k+1} \widetilde{\mathrm{Del}}_{r,i} = \mathrm{Del}_{r,k+1}$. Now, the sequence

$$H_*\left(\mathrm{Del}_{r,k+1}\right) \to H_*\left(\bigcup_{i\geq k+1} \widetilde{\mathrm{Del}}_{r,i}\right) \to H_*\left(\bigcup_{i\geq k+1} \widetilde{\mathrm{Del}}_{r,i}, \mathrm{Del}_{r,k+1}\right)$$

is a short exact sequence. Therefore, it suffices to show that its first map is an isomorphism. This map is the same as the concatenation of maps induces by inclusion

$$H_*\left(\mathrm{Del}_{r,k+1}\right) \xrightarrow{\cong} H_*\left(\widetilde{\mathrm{Del}}_{r,k+1}\right) \to H_*\left(\bigcup_{i\geq k+1} \widetilde{\mathrm{Del}}_{r,i}\right)$$

where the isomorphism in the first part comes from Lemma 4. Hence it is only left to show that $H_*(\widetilde{\mathrm{Del}}_{r,k+1}) \to H_*(\bigcup_{i\geq k+1} \widetilde{\mathrm{Del}}_{r,i})$ is an isomorphism. But this is just the statement we want to show for $k+1$.

For $k = n-2$ we arrive at

$$H_*\left(\mathrm{Del}_{r,n-1}\right) \xrightarrow{\cong} H_*\left(\widetilde{\mathrm{Del}}_{r,n-1}\right) \xrightarrow{=} H_*\left(\bigcup_{i\geq n-1} \widetilde{\mathrm{Del}}_{r,i}\right).$$

So, by induction we showed that $\widetilde{\mathrm{Del}}_{r,k} \hookrightarrow \bigcup_{i\geq k} \widetilde{\mathrm{Del}}_{r,i}$ induces an isomorphism on homology for any $k < n-1$. □

The bifiltration $(\text{S-Cov}_{r,k})_{r\in\mathbb{R},k\in\mathbb{N}}$ constitutes the desired simplicial version for multicovers:

**Theorem 7.** *$H_*(\text{S-Cov}_{r,k})_{r\in\mathbb{R},k\in\mathbb{N}}$ and $H_*(\mathrm{Cov}_{r,k})_{r\in\mathbb{R},k\in\mathbb{N}}$ are isomorphic bipersistence modules.*

*Proof.* Because of Theorem 6, we only have to show that the bipersistence modules $H_*(\text{S-Cov}_{r,k})_{r\in\mathbb{R},k\in\mathbb{N}}$ and $H_*(\widetilde{\mathrm{Del}}_{r,k})_{r\in\mathbb{R},k\in\mathbb{N}}$ are isomorphic. It suffices to show that there exist isomorphisms $H_*(\widetilde{\mathrm{Del}}_{r,k}) \to H_*(\text{S-Cov}_{r,k})$ for each $r, k$ such that the diagram

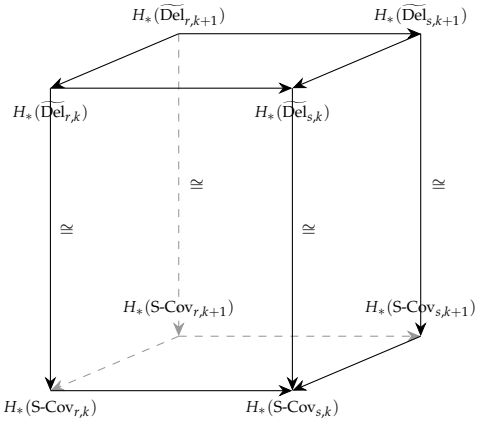


commutes, whenever $r \leq s$. These isomorphisms are induced by the canonical inclusions $\widetilde{\mathrm{Del}}_{r,k} \hookrightarrow \text{S-Cov}_{r,k}$. By Lemma 6, we already know that these maps are isomorphisms. In Lemma 5, we showed that the top face commutes. Note that the bottom face and the front/back faces of the cube are induced by commuting diagrams of inclusions on the level of simplicial

complexes and therefore commute as well. We are left to show that the left and right faces commute. Consider the commuting diagram of canonical inclusions

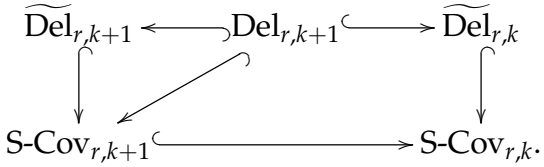

When applying the homology functor, the corresponding diagram also commutes. The map $H_*(\widetilde{\mathrm{Del}}_{r,k+1}) \to H_*(\widetilde{\mathrm{Del}}_{r,k})$ is defined to be the top row of the resulting diagram when reversing the arrow of the isomorphism $H_*(\mathrm{Del}_{r,k+1}) \xrightarrow{\cong} H_*(\widetilde{\mathrm{Del}}_{r,k+1})$. Therefore, the concatenation of maps $H_*(\widetilde{\mathrm{Del}}_{r,k+1}) \to H_*(\widetilde{\mathrm{Del}}_{r,k}) \xrightarrow{\cong} H_*(\text{S-Cov}_{r,k})$ is equal to $H_*(\widetilde{\mathrm{Del}}_{r,k+1}) \xrightarrow{\cong} H_*(\text{S-Cov}_{r,k+1}) \to H_*(\text{S-Cov}_{r,k})$, which we needed to show. In total, the bipersistence modules commute with index-wise isomorphisms and thus are isomorphic. □

## 4.6 Computations

We describe an algorithm to compute the simplicial bifiltration S-Cov as defined in Section 4.5. As input, we take a finite point set $A \subset \mathbb{R}^2$, called *sites* from now, and assume it to be in generic position (no 3 sites collinear, no 4 sites cocircular). We also take some $K$ as input and compute S-Cov only up to level $K$. The output is a sequence of lines of the form

$$\texttt{id} \quad r \quad k \quad \partial_1 \quad \partial_2 \quad \ldots \quad \partial k$$

where each line defines a simplex with unique identifier `id`, which enters the bifiltration at radius $r$ and level $k$. $\partial_1, \ldots, \partial_k$ specifies the boundary of the simplex, listing the identifiers of the facets of the simplex. Since the bifiltration is 1-critical, this sequence of graded simplices describes S-Cov completely. Since we know that S-Cov has only homology in dimensions 0 and 1, we can restrict our attention to simplices in dimension $\leq 2$.

Every vertex $v$ of S-Cov is a vertex of $\mathrm{Del}_k$, with $k \in \{1, \ldots, K\}$. That means, a vertex of $\mathrm{Del}_k$ is associated to a $k$-subset $\{a_1, \ldots, a_k\}$ of sites, denoting the

$k$ nearest neighbors of the dual Voronoi region. In what follows, we will frequently identify a vertex, its associated $k$-subset of sites, and the dual Voronoi region.

By construction of S-Cov, every simplex is spanned by vertices that are either all on the same level, or of two consecutive levels (see Figure 4.3). We call a simplex *pure* in the first case, and *mixed* in the second case. The level of a mixed simplex is the smaller of the two levels of its boundary vertices. Both for mixed and pure simplices, we define the *critical value* of a simplex $\sigma$ to be the minimal $r$ such that $\sigma \in \text{S-Cov}_{r,k}$, with $k$ the level of $\sigma$, that is, with $\sigma = [v_0, \dots, v_d]$, the critical value is the smallest $r$ for which

$$\text{Cov}_{r,k} \cap \text{Vor}(v_0) \cap \dots \cap \text{Vor}(v_d) \neq \emptyset.$$

To rephrase, let $\delta_k(p)$ denote the distance to the $k$-th nearest neighbor of $p$. Then, $\text{Cov}_{r,k}$ is just the sublevel set of $\delta_k$ for value $r$. The critical value of $\sigma$ is then the minimum of $\delta_k$ within the intersection of the Voronoi regions $\text{Vor}(v_0), \dots, \text{Vor}(v_d)$.

THE STRUCTURE OF VORONOI DIAGRAMS. The structure of $k$-th order Voronoi diagrams (and the dual Delaunay triangulation) in the plane is well understood [68]. We recall a few properties important for our algorithm, with an emphasis on the relation of the Voronoi regions of order $k$ and $k+1$. Note that the assumption of generic position is crucial for most of these properties.

Every edge $v_1v_2$ of $\text{Del}_k$ is between subsets of the form $v_1 = \{a_1, \dots, a_{k-1}, x\}$ and $v_2 = \{a_1, \dots, a_{k-1}, y\}$. The Voronoi edge dual to $v_1v_2$ is part of the bisector between the sites $x$ and $y$. In particular, locally around this Voronoi edge, $x$ and $y$ are $k$-th nearest neighbor of $v_1$ and of $v_2$, respectively. The vertex $w = \{a_1, \dots, a_{k-1}, x, y\}$ of $\text{Del}_{k+1}$ has a dual Voronoi regions that contains the dual of $v_1v_2$.

Every triangle $v_1v_2v_3$ of $\text{Del}_k$ is of one of the following types. The first type is $v_1 = \{a_1, \dots, a_{k-1}, x\}$, $v_2 = \{a_1, \dots, a_{k-1}, y\}$, and $v_3 = \{a_1, \dots, a_{k-1}, z\}$. The second type is $v_1 = \{a_1, \dots, a_{k-2}, x, y\}$, $v_2 = \{a_1, \dots, a_{k-2}, x, z\}$, and $v_3 = \{a_1, \dots, a_{k-2}, y, z\}$. In both cases, the three dual Voronoi regions meet in a single point, which is the center $p$ of the circle through $x$, $y$, and

$z$. For the first type, $p$ is also dual to a triangle of $\mathrm{Del}_{k+1}$, namely the triangle spanned by $w_1 = \{a_1, \ldots, a_{k-1}, x, y\}$, $w_2 = \{a_1, \ldots, a_{k-1}, x, z\}$, and $w_3 = \{a_1, \ldots, a_{k-1}, y, z\}$. For the second type, the point $p$ lies in the interior of the Voronoi region dual to $w = \{a_1, \ldots, a_{k-2}, x, y, z\}$.

Computing the Delaunay triangulations. The pure simplices of S-Cov are the simplices of $\mathrm{Del}_k$, for $k = 1, \ldots, K$. The computation of $\mathrm{Del}_k$ can be reduced to the computation of a *weighted Delaunay triangulation* (with $k = 1$) [9]. For that, we create for every $k$-subset $\{a_1, \ldots, a_k\}$ the weighted point $(b, w)$ with $b$ the barycenter of $a_1, \ldots, a_k$, and

$$w := \frac{1}{k^2} \sum_{1 \le i < j \le k} \|a_i - a_j\|^2.$$

Then, the weighted Voronoi region of $(b, w)$ coincides with the Voronoi region of $\{a_1, \ldots, a_k\}$, which implies that also the dual Delaunay triangulations are equal.

Applying the above algorithm on all $k$-subsets results in a large number of *hidden vertices*, that is, $k$-subsets with an empty Voronoi region. It is beneficial to filter out these hidden vertices beforehand. And indeed, when computing the Delaunay triangulations incrementally in $k$, we can compute all visible (=non-hidden) vertices for $k+1$ from the Delaunay triangulation of $k$: traverse all edges of $\mathrm{Del}_k$. Each of them is dual to the intersection of two Voronoi regions of subsets $\{a_1, \ldots, a_{k-1}, x\}$ and $\{a_1, \ldots, a_{k-1}, y\}$. It follows that in the interior of the edge, each point belongs to the Voronoi region of $\{a_1, \ldots, a_{k-1}, x, y\}$. Also the converse is true: each visible subset $\{a_1, \ldots, a_{k+1}\}$ can be split in two $k$-subsets $\{a_1, \ldots, a_k\}$ and $\{a_1, \ldots, a_{k-1}, a_{k+1}\}$ that are connected by an edge in $\mathrm{Del}_k$. With that, we can incrementally compute all Delaunay triangulations efficiently.

Simplices of S-Cov. The pure simplices of S-Cov are precisely the Delaunay simplices computed in the previous step. It remains to find all mixed simplices. Note that a mixed edge corresponds to an intersection of a $k$-region and a $(k+1)$-region, and a mixed triangle to an intersection of two $k$-regions and a $(k+1)$-region, or vice versa.

We traverse the edges of $\mathrm{Del}_k$. For any edge $v_1v_2$ with $v_1 = \{a_1, \ldots, a_{k-1}, x\}$, $v_2 = \{a_1, \ldots, a_{k-1}, y\}$, both $k$-regions of $v_1$ and $v_2$ overlap with the $(k+1)$-region $\{a_1, \ldots, a_{k-1}, x, y\}$, and we add the mixed edges $v_1w$, $v_2w$, and the mixed triangle $v_1v_2w$.

The astute reader might realize that there are more mixed edges and triangles than the ones above: the three regions of $v_1 = \{a_1, \ldots, a_{k-1}, x\}$, $v_2 = \{a_1, \ldots, a_{k-1}, y\}$, and $v_3 = \{a_1, \ldots, a_{k-1}, z\}$ meet in a common point (the circumcenter of $x, y, z$), and at this point, also the three regions $w_1 = \{a_1, \ldots, a_{k-1}, x, y\}$, $w_2 = \{a_1, \ldots, a_{k-1}, x, z\}$, and $w_3 = \{a_1, \ldots, a_{k-1}, y, z\}$ meet. This would lead to another 3 mixed edges and 12 mixed triangles that were not previously detected. However, let us see that all these mixed simplices can be disregarded without changing the persistence module in dimensions 0 or 1. To do this, consider the $k$-regions of $v_1 = \{a_1, \ldots, a_{k-1}, x\}$, $v_2 = \{a_1, \ldots, a_{k-1}, y\}$, and $v_3 = \{a_1, \ldots, a_{k-1}, z\}$ meeting in a common point $p$. Also the three regions $w_1 = \{a_1, \ldots, a_{k-1}, x, y\}$, $w_2 = \{a_1, \ldots, a_{k-1}, x, z\}$, and $w_3 = \{a_1, \ldots, a_{k-1}, y, z\}$ meet at $p$. There are 3 edges that intersect only at $p$, namely $v_1w_3$, $v_2w_2$ and $v_3w_1$. Also, there are 12 triangles that only meet at $p$, for instance $v_1v_2w_2$ and $v_1v_2w_3$, but not $v_1v_2w_1$ because the latter intersects along the edge $v_1v_2$. Note that all these edges and triangles have the same critical value, namely the circumradius of $xyz$. Writing down the triangle in some order, and adding them one by one, we observe that for 9 of them, the addition of the triangle leads to an empty tetrahedron in the complex. In other words, these 9 triangles create a generator in $H_2$, and hence not inserting them will not affect $H_0$ or $H_1$. However, not adding these 9 triangles makes the 3 mixed edges free facets of the remaining 3 triangles. It is well-known [82] that removing a maximal simplex and a free facet does not change the homotopy type of the complex. Doing so leaves us without any of the mixed edges and triangles caused by an intersection at $p$.

Critical values. We have to determine the critical value of each vertex, edge, and triangle of S-Cov. The case of triangles is the simplest to describe: for pure triangles, the dual Voronoi vertex is the circumcenter of three sites $x$, $y$, and $z$, the critical value is simply the circumradius of this triangle. Every mixed triangle is either of the form $v_1v_2w$ or $vw_1w_2$, where $v_1v_2$ is

an edge of $\mathrm{Del}_k$, and $w_1w_2$ and edge of $\mathrm{Del}_{k+1}$. In the first case, the three Voronoi regions meet as soon as $v_1$ and $v_2$ meet, so the critical value of the pure edge $v_1v_2$ (determined below) is the critical value of the triangle. The second case is analogous.

It remains to compute the critical values of vertices, pure edges, and mixed edges. All three cases are handled by the same principle which we briefly sketch here and describe in the following paragraph in detail. Recall that our goal is to compute $\min_{p\in I} \delta_k(p)$ where $I$ is the intersection of the involved Voronoi regions, and $\delta_k$ is the distance to the $k$-th nearest neighbor. Following standard notation (e.g. [76]), we call a simplex *attached* if $\delta_k$ is attained at the boundary of $I$. In all three cases, we have a geometric attachment test to determine whether the simplex is attached or not. To give an example, the attachment test for a vertex $\{a_1, \dots, a_k\}$ is whether the minimum enclosing circle of $\{a_1, \dots, a_k\}$ contains no other site of $A$. For unattached simplices, the critical value follows immediately (in the example above, it is the radius of the minimum enclosing circle). For attached simplices, we have to traverse the boundary of $I$ and pick the minimal critical value among those features as the critical value of the simplex. By handling the pure edges before the pure vertices and the pure simplices before the mixed edges, we can assume that the critical values of the boundary features have already been assigned.

Details on critical value computation. We start with the case of a pure edge of $\mathrm{Del}_k$ between two vertices $v_1 = \{a_1, \dots, a_{k-1}, x\}$ and $v_2 = \{a_1, \dots, a_{k-1}, y\}$. Along the Voronoi edge, $x$ and $y$ are the (equidistant) $k$-th nearest neighbors, and hence, $\delta_k$ restricted to the Voronoi edge equals the distance to $x$. However, the distance to $x$ along the bisector of $x$ and $y$ is a unimodal function, with a minimum at the midpoint $m$ of $x$ and $y$. This implies the following two cases: if $m$ is on the Voronoi edge, $\delta_k$ is minimized on $m$ for the Voronoi edge, and the critical value is half the distance of $x$ and $y$ (the unattached case). Otherwise, $\delta_k$ is minimized at a boundary vertex of the Voronoi edge, which is a Voronoi vertex that is dual to one of the triangles incident to the Delaunay edge $v_1v_2$. Consequently, the critical value of the edge in this case is the smaller of the two critical values of its incident triangles, which have been determined before.

To decide whether the edge is attached, we have to check whether the midpoint $m$ is in the Voronoi edge or not. For that, we consider the circle with $xy$ as diameter and check whether $\{a_1, \dots, a_{k-1}\}$ are contained. If so, we ensure that all further sites except $\{a_1, \dots, a_{k-1}, x, y\}$ are outside of the circle. Instead of testing all sites (which would result in an $O(n)$-algorithm), it suffices to check up to two sites, namely those additional sites that are involved in the Voronoi vertices that are the endpoints of the Voronoi edge. We omit further details.

Now, consider a vertex $v$ of $\mathrm{Del}_k$. Let $v = \{a_1, \dots, a_k\}$ and define $\delta_k^{(v)}(p) := \max_{i=1,\dots,k} \|p - a_i\|$. Then $\delta_k = \delta_k^{(v)}$ within the Voronoi region dual to $v$. However, extended to $\mathbb{R}^2$, $\delta_k^{(v)}$ is unimodal, with a minimum at the center of the *minimum enclosing circle* of $a_1, \dots, a_k$ (this is the first point covered by the $k$ balls around the $a_i$ when the radius increases). This suggests the following algorithm. We compute the minimum enclosing circle of $a_1, \dots, a_k$ with center $c$ and radius $r$. If the $k$ nearest neighbors of $c$ are $a_1, \dots, a_k$, the critical value of $v$ is $r$. Otherwise, $c$ is outside of the Voronoi region of $v$, and $\delta_k$ is minimized at the boundary of the Voronoi region (i.e, the vertex is attached). In that case, we traverse the incident edges of $v$ (corresponding dually to the boundary segments of the Voronoi region) and take the minimal critical value as critical value of the vertex.

To determine whether the $k$ nearest neighbors of $c$ are $a_1, \dots, a_k$, we ensure that all sites except $a_1, \dots, a_k$ are outside of the minimum enclosing circle. Instead of checking all sites, it is enough to consider *neighboring sites* of $v$. These are all sites $x$ such that there is an edge $vw$ in $\mathrm{Del}_k$ with $w = \{a_1, \dots, a_{i-1}, x, a_{i+1}, \dots, a_k\}$. The number of these sites is bounded by the degree of $v$ in $\mathrm{Del}_k$.

It remains to compute the critical value of mixed edges $vw$ with $v = \{a_1, \dots, a_k\}$ and $w = \{a_1, \dots, a_k, x\}$. We have to find the minimal $\delta_k$ with the intersection of the two regions. Let $c$ be the center of the minimum enclosing ball of $\{a_1, \dots, a_k, x\}$. If $c$ is in the intersection of the two Voronoi regions, the radius if the minimum enclosing ball is the critical value. Otherwise, the minimum is attained at the boundary of the intersection. We call a boundary segment of the region $\{a_1, \dots, a_k\}$ an *x-segment* if it is part of a bisector of $x$ and some $a_i$. Likewise, a boundary segment of the region $\{a_1, \dots, a_k, x\}$ is

an *x-segment* if it is part of a bisector of $x$ and some other site $y$. Then, the $x$-segments of both regions are the boundary of the intersection of the two Voronoi regions. The critical value is hence the minimal critical value over all $x$-segments.

Identifying the dual Delaunay edges of $x$-segments is a simple combinatorial check over all neighbors of the Delaunay vertices $\{a_1, \ldots, a_k\}$ and $\{a_1, \ldots, a_k, x\}$. To check whether $c$ (the meb center) is in the intersection, we check whether $x$ is on the boundary of the meb (if not, then $c$ is not in the Voronoi region of $\{a_1, \ldots, a_k\}$), and we ensure that all other sites are outside of the ball. Similar to before, it is enough to only check the neighboring sites of $w$ for this step.

Complexity. The size of $\mathrm{Del}_k$ for $n$ points is upper bounded by $O(kn)$ [68]. It follows that the number of pure simplices is at most

$$\sum_{k=1}^{K} O(kn) = O(K^2 n).$$

This is also the bound on the size of the whole bifiltration because every mixed simplex can be charged to one pure vertex or pure edge such that each pure simplex is only charged a constant number of times.

The computation of the simplices is dominated by the computation of the Delaunay complexes for all $k$, which can be done in $O(K^2 n \log n)$. We also need to determine the critical values of each simplex. Using local attachment tests, the amortized time for computing a critical value is $O(k)$ for a simplex of level $k$. Hence, we arrive at a total complexity of $O(K^3 n)$ for computing all critical values. The space complexity of the algorithm is bounded by the size of the output structure. We summarize

**Theorem 8.** *The bifiltration* S-Cov *for levels up to $K$ has size $O(K^2 n)$ and can be computed in $O(K^2 n(K + \log n))$ time and $O(K^2 n)$ space.*

Delaunay-Cech filtrations. The main technical difficulty in the algorithm is the computation of the critical values, in particular, in the attachment tests for pure and mixed simplices. We claim that these complications are unnecessary: for a simplex $\sigma = [v_0, \dots, v_d]$ of S-Cov, let $\bigcup \sigma := \bigcup_{i=0,\dots,d} v_i$, where $v_i$ is interpreted as a subset of sites. Let $r_\sigma$ be the radius of the minimum enclosing circle of $\bigcup \sigma$. Note that $r_\sigma$ is the smallest radius for which all $\mathrm{Cov}_r(v_i)$ will intersect. We define a different bifiltration, called the *Delaunay-Cech bifiltration*, which consists of the same simplices as S-Cov, but using $r_\sigma$ as critical value.

**Conjecture 1.** *The Delaunay-Cech bifiltration and the multicover bifiltration induce isomorphic bipersistence modules.*

Indeed, for $K = 1$, the Delaunay-Cech bifiltration is the Delaunay-Cech filtration as studied in [12]. The results of that work imply that the filtration yields the same persistence module as the alpha filtration (which equals S-Cov for $K = 1$). Moreover, in all instances that we tested, the two bifiltrations yield the same persistence module (to be precise, we compared the persistence diagrams obtained for a fixed parameter $k$, for various choices of $k$). We consider this as sufficient evidence to conjecture the result, at least for planar point sets.

## 4.7 Experiments

We implemented the algorithm from Section 4.6 in C++, using the Cgal library (version 4.14)[1]. In particular, we used the `2D triangulation` package [174] to compute $k$-th order Delaunay triangulations and used the packages `Exact_predicates_inexact_constructions_kernel` [30] and `Min_circle_2` [91] for our geometric primitives.

We present some preliminary experiments on point sets in $[0,1] \times [0,1]$ chosen uniformly at random with double-precision coordinates. They were performed on a workstation with 6 CPU cores with 3.5 GHz per core and

[1] CGAL, Computational Geometry Algorithms Library, https://www.cgal.org

| $N$ | output size | $\frac{\text{output}}{N}$ | time (sec) | $\frac{\text{time}}{N \log N} \cdot 10^6$ | time (Del-Cech) |
|---|---|---|---|---|---|
| 5000 | 1.02M | 203.276 | 1.62541 | 38.2 | 1.45021 |
| 10000 | 2.04M | 203.594 | 3.43589 | 37.3 | 2.93504 |
| 20000 | 4.08M | 203.785 | 7.44641 | 37.6 | 6.15255 |
| 40000 | 8.16M | 203.886 | 15.8817 | 37.5 | 12.6515 |
| 80000 | 16.31M | 203.936 | 32.8864 | 36.4 | 25.6397 |
| 160000 | 32.64M | 203.969 | 67.3067 | 35.1 | 53.4575 |
| 320000 | 65.27M | 203.983 | 134.697 | 33.2 | 107.696 |

Table 4.1: Results on uniformly sampled point sets with $N$ points, using $K = 4$. All results are averaged over 5 runs with independently generated data sets.

| $K$ | output size | $\frac{\text{output}}{1000 \cdot K^2}$ | time (sec) | $\frac{\text{time}}{K^3}$ | time (Del-Cech) |
|---|---|---|---|---|---|
| 2 | 0.84M | 209.862 | 1.38905 | 0.174 | 1.02612 |
| 4 | 4.08M | 254.731 | 6.99719 | 0.109 | 5.47801 |
| 8 | 17.7M | 276.986 | 36.9301 | 0.072 | 28.8319 |
| 16 | 73.7M | 287.789 | 184.538 | 0.045 | 147.507 |
| 32 | 299.6M | 292.593 | 885.786 | 0.027 | 845.883 |

Table 4.2: Results on uniformly sampled point sets with 20000 points. All results are averaged over 5 runs with independently generated data sets.

64 GB of RAM, running Ubuntu 16.04.5. Note that our algorithm runs on a single core.

Fixing $K$ to 4 and increasing the number of points, we obtain the results in Table 4.1. We observe that the output scales linearly with the input size, as predicted by the complexity bound. We also see that the running time is slightly super-linear, but is dominated by $N \log N$, again in accordance to the complexity bound. We also show the running time for computing the Delaunay-Cech bifiltration. We observe a modest speed-up for this variant.

Around 20% of the running time is spent for the computation of the Delaunay triangulations. The remaining 80% are split more or less evenly between pure and mixed simplices (with the majority of time spent on computing the critical values). These numbers are stable over all input sizes. We also remark that when adding the unnecessary mixed edges and triangles caused

| $K$ | output size | $\frac{\text{output}}{1000 \cdot K^2}$ | time (sec) |
|---|---|---|---|
| 2 | 20663 | 5.16575 | 0.0600431 |
| 4 | 99490 | 6.21812 | 0.226487 |
| 8 | 425276 | 6.64494 | 0.642191 |
| 16 | 1704988 | 6.66011 | 3.05044 |
| 32 | 6511904 | 6.35928 | 15.1532 |
| 64 | 23564161 | 5.75297 | 79.402 |
| 128 | 77291600 | 4.7175 | 391.232 |
| 256 | 204930178 | 3.12699 | 1644.14 |

Table 4.3: Results on uniformly sampled point sets with 500 points.

by intersections in a single point, the size of the complex increases by a factor of 2, independent of $N$ and $K$.

In Table 4.2, we fix $N$ to 20000 and vary $K$. Already for $K = 32$, almost the entire 64 GB of RAM were in use. We observe that the size of the bifiltration seems to scale super-quadratically with respect to $K$, apparently contradicting the complexity bound. By further experiments with a smaller $N$ (see Table 4.3), we observed that the ratio is decreasing again for larger values of $K$, meaning that the table does not reflect the asymptotic behavior. We also observe that the running time is better than the worst-case prediction of $O(K^3)$. Again, the Delaunay-Cech filtration yields a small speed-up.

In these experiments, we have observed that the relative time for Delaunay triangulations gradually decreases for increasing $k$, and the computations of critical values becomes more dominant in the running time. We speculate, however, that this effect might be an artifact of our implementation which is not optimized towards large values of $k$.

All numbers displayed are averages over 5 random instances. We remark that the deviation from the average is very small in general ($< 1\%$ for complex size and $< 10\%$ in running time).

## 4.8 Conclusion and future work

We have given an efficient simplicial model for the multicover bifiltration. Our prototypical implementation shows that, with our algorithm, multicover bifiltrations can be computed for problem instances that are clearly out-of-reach with previous approaches.

We see our current progress as a first step within a greater study of multicovers. On the theoretical side, we are aware of the fact that Lemma 4 can be lifted to the level of homotopy equivalences and even deformation retracts of simplicial complexes. Hence, the restricted covers Vor-Cov of the multicover bifiltration actually yield a strong jointly well covered filtration along the density parameter. For clarity of exposition we decided to stick to the level of homology, however.
We are curious to see whether the geometric construction of the zigzag by Edelsbrunner and Osang [86] is a deformation retract of $\widetilde{\mathrm{Del}}$ and if the straightening technique can also be applied to their construction.
In the more general framework, it would be interesting to find out if there are interesting jointly well covered (multi-)filtrations that are not strong jointly well covered (multi-)filtrations.
Finally, we plan to investigate the prospects of proving our conjecture on higher-order Delaunay-Cech complexes (Conjecture 1).

Furthermore, we plan to connect our implementation with existing software for multiparameter persistence. The next step will be the computation of a minimal presentation for the bipersistence module using the algorithm from [132]. This will open the door to compute the indecomposables of the module, for which polynomial time algorithms exist [71, 112]. We are curious to investigate which indecomposables typically arise, for instance, for multicovers of randomly generated point sets. Further possibility are the visualization of the persistence module with RIVET [130], or distance computations between point clouds using the persistence module as a proxy, using the matching distance [18, 117, 118].

We also plan several extensions and improvements of our implementation: we intent to make our code more space-efficient and better suited for large values of $K$. Also, we plan to extend it to 3 dimensions. Note that the

algorithm becomes more involved because even for generic point sets, there are $\binom{4}{2} = 6$ second-order regions meeting in a Voronoi vertex. We speculate that our trick of avoiding certain mixed simplices will be of importance also in $\mathbb{R}^3$.

We end by addressing an apparent drawback of our straightening approach: the resulting simplicial complex might be too large to be useful in practice. Indeed, our experiments show a significant increase in size when $K$ increases. We propose two approaches to overcome this issue: first of all, instead of generating the bifiltration for each value between 1 and $K$, it may suffice to increase $k$ by more than 1 in each step. Of course, the incremental nature of computing the $k$-th order Delaunay triangulation requires to consider all intermediate $k$'s, but we avoid storing their simplices. Alternatively, we observe that for construction the simplices of the bifiltration on level $k+1$, we only have to keep the simplices on level $k$ in memory. This means that we can provide the bifiltration as an output stream without storing it completely in memory. Clearly, to benefit from this concept, subsequent algorithmic steps (e.g., computing a minimal presentation or indecomposables) have to be implemented as *streaming algorithms*. We plan to investigate the potential of this approach. Alternatively, it would be interesting to find efficient algorithms to compute persistence diagrams of essentially one-way zigzags, and to compute multiparameter persistence modules obtained by one-way zigzags in at least one direction.

# 5 Paper 2: The Representation Theorem of Persistence Revisited and Generalized

This is joint work with Michael Kerber. The journal version is [61]. We slightly rearrange it and give an updated outlook.

Abstract. The Representation Theorem by Zomorodian and Carlsson has been the starting point of the study of persistent homology under the lens of representation theory. In this work, we give a more accurate statement of the original theorem and provide a complete and self-contained proof. Furthermore, we generalize the statement from the case of linear sequences of $R$-modules to $R$-modules indexed over more general monoids. This generalization subsumes the Representation Theorem of multiparameter persistence as a special case.

## 5.1 Introduction

For understanding persistence in algebraic terms, the main objects are *persistence modules*. In the simplest case, such a persistence module consists of a sequence of $R$-modules indexed over $\mathbb{N}$ and module homomorphisms connecting consecutive modules, as in the following diagram:

$$M_0 \xrightarrow{\varphi_0} M_1 \xrightarrow{\varphi_1} \dots \xrightarrow{\varphi_{i-1}} M_i \xrightarrow{\varphi_i} M_{i+1} \xrightarrow{\varphi_{i+1}} \dots$$

A persistence module as above is of *finitely generated type* if each $M_i$ is finitely generated and there is an $m \in \mathbb{N}$ such that $\varphi_i$ is an isomorphism for all $i \geq m$. Under this condition, Zomorodian and Carlsson [176] observed that a persistence module can be expressed as single module over the polynomial ring $R[t]$:

**ZC-Representation Theorem.** *[Theorem 3.1 in [176]] Let $R$ be a commutative ring with unity. The category of persistence modules of finitely generated type[1] over $R$ is equivalent to the category of finitely generated graded modules over $R[t]$.*

The importance of this equivalence stems from the case most important for applications, namely if $R$ is a field. In this case, graded $R[t]$-modules, and hence also persistence modules of finitely generated type, permit a decomposition

$$\left(\bigoplus_{i=1}^{n} \Sigma^{\alpha_i} R\,[t]\right) \oplus \left(\bigoplus_{j=1}^{m} \Sigma^{\beta_j} R\,[t] \,/\, (t^{n_j})\right)$$

where $\Sigma^{\cdot}$ denotes a shift in the grading. The integers $\alpha_i, \beta_j, n_j$ give rise to the aforementioned barcode of the persistence module; see [176] for details. Subsequent work studied the property of more general persistence modules, for instance, for modules indexed over any subset of $\mathbb{R}$ (and not necessarily

[1] In [176], the term "finite type" is used instead, but we renamed it here as we will define another finiteness condition later.

of finite type) [53, 62] and for the case that the $M_i$ and $\varphi_i$ are replaced with any objects and morphisms in a target category [34, 33].

Given the importance of the ZC-Representation Theorem, it is remarkable that a comprehensive proof seems not to be present in the literature. In [176], the authors assign an $R[t]$-module to a persistence module of finite type and simply state:

> The proof is the Artin-Rees theory in commutative algebra (Eisenbud, 1995).

In Zomorodian's textbook [175], the same statement is accompanied with this proof (where $\alpha$ is the assignment mentioned above):

> It is clear that $\alpha$ is functorial. We only need to construct a functor $\beta$ that carries finitely generated non-negatively graded $k[t]$-modules [sic] to persistence modules of finite[ly generated] type. But this is readily done by sending the graded module $M = \oplus_{i=0}^{\infty} M_i$ to the persistence module $\{M_i, \varphi_i\}_{i \in \mathbb{N}}$ where $\varphi_i : M^i \to M^{i+1}$ is multiplication by t. It is clear that $\alpha\beta$ and $\beta\alpha$ are canonically isomorphic to the corresponding identity functors on both sides. This proof is the Artin-Rees theory in commutative algebra (Eisenbud, 1995).

While that proof strategy works for the most important case of fields, it fails for "sufficiently" bad choices of $R$, as the following example shows:

Let $R = \mathbb{Z}[x_1, x_2, \ldots]$ and consider the graded $R[t]$ module $M := \oplus_{i \in \mathbb{N}} M_i$ with $M_i = R/ < x_1, \ldots, x_i >$ where multiplication by $t$ corresponds to the map $M_i \to M_{i+1}$ that assigns $p \bmod x_i$ to a polynomial $p$. $M$ is generated by $\{1\}$. However, the persistence module $\beta(M)$ as in Zomorodian's proof is not of finitely generated type, because no inclusion $M_i \to M_{i+1}$ is an isomorphism.

This counterexample raises the question: what are the requirements on the ring $R$ to make the claimed correspondence valid? In the light of the cited Artin-Rees theory, it appears natural to require $R$ to be a Noetherian ring (that is, every ascending chain of ideals becomes stationary), because the theory is formulated for such rings only; see [89, 102]. Indeed, as carefully

exposed in the master's thesis of the first author [59], the above proof strategy works under the additional assumption of $R$ being Noetherian. We sketch the proof in Section 5.3.

Contributions. As our first result, we prove a generalized version of the ZC-Representation Theorem. In short, we show that the original statement becomes valid without additional assumptions on $R$ if "finitely generated type" is replaced with "finitely presented type" (that is, in particular, every $M_i$ must be finitely presented). Furthermore, we remove the requirement of $R$ being commutative and arrive at the following result.

**Theorem.** *Let $R$ be a ring with unity. The category of persistence modules of finitely presented type over $R$ is isomorphic to the category of finitely presented graded modules over $R[t]$.*

The example from above does not violate the statement of this theorem because the module $M$ is not finitely presented. Also, the statement implies the ZC-Representation Theorem for commutative Noetherian rings, because if $R$ is commutative with unity and Noetherian, finitely generated modules are finitely presented.

Our proof follows the same path as sketched by Zomorodian, using the functors $\alpha$ and $\beta$ to define a (straight-forward) correspondence between persistence modules and graded $R[t]$-modules. The technical difficulty lies in showing that these functors are well-defined if restricted to subclasses of finitely presented type. It is worth to remark that our proof is elementary and self-contained and does not require Artin-Rees theory at any point. We think that the ZC-Representation Theorem is of such outstanding importance in the theory of persistent homology that it deserves a complete proof in the literature.

As our second result, we give a Representation Theorem for a more general class of persistence modules. We work over an arbitrary ring $R$ with unity and generalize the indexing set of persistence modules to a big class of monoids. We denote monoids by $(G, \star)$. We consider a subclass which we call "good" monoids in this work (see Section 5.4 for the definition

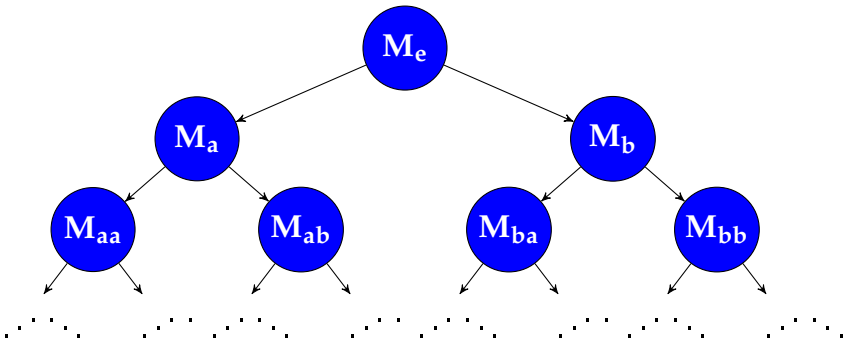


Figure 5.1: Graphical illustration of a generalized persistence module. The underlying monoid is the set of words over $\{a, b\}$. For each monoid element, the persistence module contains an $R$-module, and for each arrow, the module contains a homomorphism (which is not specified in the figure).

and a discussion of related concepts). Among them is the case $\mathbb{N}^k$ corresponding to multiparameter persistence modules, but also other monoids such as $(\mathbb{Q}_{\geq 0}, +)$, $(\mathbb{Q} \cap (0, 1], \cdot)$ and the non-commutative word monoid as illustrated in Figure 5.1. It is not difficult to show that such generalized persistence modules can be isomorphically described as a single module over the monoid ring $R[G]$.

Our second main result is that finitely presented graded modules over $R[G]$ correspond again to generalized persistence modules with a finiteness condition. Specifically, finiteness means that there exists a finite set $S$ of indices (i.e., elements in the monoid) such that for each monoid element $g$ with associated $R$-module $R_g$, there exists an $s \in S$ such that each map $R_s \to R_{\tilde{g}}$ is an isomorphism, whenever $\tilde{g}$ lies between $s$ and $g$.

For $G = \mathbb{N}^k$, we prove that this condition is equivalent to the property that all sequences in our persistence module are of finite type (as a persistence module over $\mathbb{N}$), see Figure 5.2, but this equivalence fails for general (good) monoids. Particularly, our second main result implies the first one, because for $G = \mathbb{N}$, the monoid ring $R[\mathbb{N}]$ is precisely the polynomial ring $R[t]$.

Outline. Although our first main result is a special case of the second one, we decided to give a complete treatment of the classical case of linear

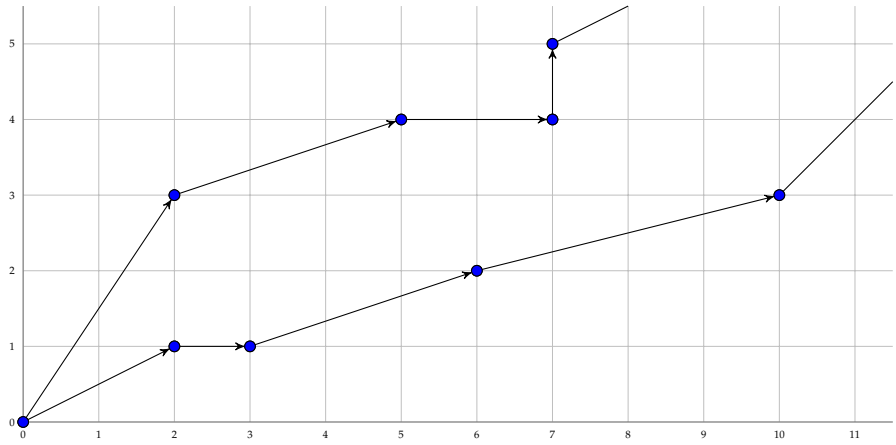


Figure 5.2: Graphical illustration of two sequences in a generalized persistence module over the monoid $\mathbb{N}^2$. The corresponding $R$-modules and homomorphisms are not specified in the figure.

sequences first. We prove the Representation Theorem in Section 5.2. The additional concepts required for the monoidal case are introduced in Section 5.4. The Generalized Representation Theorem is proved in Section 5.5. We give a conclusion in Section 5.6.

## 5.2 The ZC-Representation Theorem

Persistence modules and $R[t]$-modules. *Persistence modules* are the major object of interest in the theory of persistent homology. We motivate it with the following typical example: Given a nested sequence of topological spaces indexed over the integers

$$X_0 \hookrightarrow X_1 \hookrightarrow X_2 \hookrightarrow X_3 \hookrightarrow X_4 \cdots,$$

then the inclusions maps $X_i \to X_j$ induce group homomorphisms $\varphi_{i,j} : H_*(X_i) \to H_*(X_j)$. By functoriality of homology, $\varphi_{i,i}$ is the identity and $\varphi_{i,j}$ is the composition of $\varphi_{k,k+1}$ for $i \leq k \leq j-1$. The following definition captures these algebraic properties:

**Definition 10.** Let $R$ be a ring with unity. A *discrete algebraic persistence module* ($DAPM$) is a tuple $\mathcal{M} = \left((M_i)_{i\in\mathbb{N}}, (\varphi_{i,j})_{i\leq j\in\mathbb{N}}\right)$, such that $M_i$ is an $R$-module, $\varphi_{i,j} : M_i \to M_j$ is a module morphism, $\varphi_{i,i} = 1_{M_i}$ and $\varphi_{i,k} = \varphi_{j,k} \circ \varphi_{i,j}$ for all $i \leq k \leq j$.

A $DAPM$ is completely specified by the modules and the morphisms between consecutive modules, so it is usually just written as

$$\mathcal{M} : \; M_0 \xrightarrow{\varphi_0} M_1 \xrightarrow{\varphi_1} \ldots \xrightarrow{\varphi_{i-1}} M_i \xrightarrow{\varphi_i} M_{i+1} \xrightarrow{\varphi_{i+1}} \ldots \tag{5.1}$$

where $\varphi_i := \varphi_{i,i+1}$.

*DAPMs* over $R$ are closely related to graded $R[t]$-modules: indeed, given a $DAPM$ $\mathcal{M}$ as in (5.1), we can associate to it a graded $R[t]$-module by setting

$$\alpha(\mathcal{M}) := \bigoplus_{i\in\mathbb{N}} M_i \tag{5.2}$$

where multiplication by $t$ is defined by $t \cdot m_i := \varphi_i(m_i) \in M_{i+1}$ for $m_i \in M_i$. Vice versa, an $R[t]$-module $\oplus_{i\in\mathbb{N}} M_i$ defines a $DAPM$ by

$$\beta\left(\bigoplus_{i\in\mathbb{N}} M_i\right) := M_0 \xrightarrow{\varphi_0} M_1 \xrightarrow{\varphi_1} M_2 \to \ldots \tag{5.3}$$

where the morphisms are just multiplication with $t$, that is $\varphi_i(m_i) := t \cdot m_i$.

**Definition 11.** For two $DAPMs$ $\left((M_i)_{i\in\mathbb{N}}, (\varphi_{i,j})_{i\leq j\in\mathbb{N}}\right)$, $\left((N_i)_{i\in\mathbb{N}}, (\psi_{i,j})_{i\leq j\in\mathbb{N}}\right)$, a family $\xi_* = (\xi_i : M_i \to N_i)_{i\in\mathbb{N}}$ of module morphisms is called *discrete algebraic persistence module morphism* if $\psi_{i,j} \circ \xi_i = \xi_j \circ \varphi_{i,j}$. Equivalently, the following diagram commutes:

$$\begin{array}{ccccccccc}
M_0 & \xrightarrow{\varphi_0} & \ldots & \xrightarrow{\varphi_{i-1}} & M_i & \xrightarrow{\varphi_{i,}} & M_{i+1} & \xrightarrow{\varphi_{i+1}} & \ldots \\
\downarrow{\scriptstyle \xi_0} & & & & \downarrow{\scriptstyle \xi_i} & & \downarrow{\scriptstyle \xi_{i+1}} & & \\
N_0 & \xrightarrow{\psi_0} & \ldots & \xrightarrow{\psi_{i-1}} & N_i & \xrightarrow{\psi_i} & N_{i+1} & \xrightarrow{\psi_{i+1}} & \ldots
\end{array}$$

With such morphisms, the class of all $DAPMs$ over $R$ becomes a category, which we call R-**Persmod**.

**Lemma 7.** *The maps $\alpha$ and $\beta$ from (5.2) and (5.3) extend to functors between R-**Persmod** and R[t]-**Gr-Mod** which form an isomorphic pair of functors. In particular, the two categories are isomorphic.*

*Proof.* Given a $DAPM$ morphism

$$\begin{array}{ccccccccccc} M_0 & \xrightarrow{\varphi_0} & \dots & \xrightarrow{\varphi_{i-1}} & M_i & \xrightarrow{\varphi_i,} & M_{i+1} & \xrightarrow{\varphi_{i+1}} & \dots \\ \downarrow{\scriptstyle \xi_0} & & & & \downarrow{\scriptstyle \xi_i} & & \downarrow{\scriptstyle \xi_{i+1}} & & \\ N_0 & \xrightarrow{\psi_0} & \dots & \xrightarrow{\psi_{i-1}} & N_i & \xrightarrow{\psi_i} & N_{i+1} & \xrightarrow{\psi_{i+1}} & \dots \end{array}$$

between two $DAPMs$ $\mathcal{M}$ and $\mathcal{N}$, we define

$$\alpha(\xi_*) : \bigoplus_{i\in\mathbb{N}} M_i \to \bigoplus_{i\in\mathbb{N}} N_i, (m_i)_{i\in\mathbb{N}} \mapsto (\xi_i(m_i))_{i\in\mathbb{N}}.$$

Let us check that $\alpha$ is a well-defined functor. Recall that for $\xi_* = (\xi_i)_{i\in\mathbb{N}}$, a $DAPM$ morphism between $\mathcal{M}$ and $\mathcal{N}$, we define $\alpha(\xi_*)$ as the map assigning to $(m_i)_{i\in\mathbb{N}} \in \oplus M_i$ the value $(\xi_i(m_i))_{i\in\mathbb{N}}$. Let us define $f := \alpha(\xi_*)$ for shorter notation. Indeed, $f$ is a graded module morphism: it is a group homomorphism, as each $\xi_i$ is, it clearly satisfies $f(M_i) \subset N_i$, and it holds that for $m = (m_0, m_1, \dots)$ we get

$$\begin{aligned} f(tm) &= f(0, tm_0, tm_1, \dots) = (0, \xi_1(tm_0), \xi_2(tm_1), \dots) \\ &= (0, t\xi_0(m_0), t\xi_1(m_1), \dots) = t(\xi_i(m_i))_{i\in\mathbb{N}} = tf(m), \end{aligned}$$

where the third equality comes from the property of $DAPM$ morphisms.

For the functorial properties, it is clear that $\alpha$ maps the identity $DAPM$ morphism to the identity of the corresponding graded modules. If $\xi_*$, $\xi'_*$ are $DAPM$ morphisms and $m$ as before, we calculate

$$\begin{aligned} (\alpha(\xi'_* \circ \xi_*))(m) &= (\xi'_i(\xi_i(m_i)))_{i\in\mathbb{N}} \\ &= \alpha(\xi'_*)(\xi_i(m_i))_{i\in\mathbb{N}} \\ &= (\alpha(\xi'_*) \circ \alpha(\xi_*))(m). \end{aligned}$$

Vice versa, a morphism

$$\eta : \bigoplus_{i\in\mathbb{N}} M_i \to \bigoplus_{i\in\mathbb{N}} N_i$$

in R[t]-**Gr-Mod** induces a homomorphism $\eta_i : M_i \to N_i$ for each $i \in \mathbb{N}$, and these induced maps are compatible with multiplication with $t$. Hence, the diagram

$$\begin{array}{ccccccccc} M_0 & \xrightarrow{t} & \dots & \xrightarrow{t} & M_i & \xrightarrow{t} & M_{i+1} & \xrightarrow{t} & \dots \\ \downarrow{\scriptstyle \eta_0} & & & & \downarrow{\scriptstyle \eta_i} & & \downarrow{\scriptstyle \eta_{i+1}} & & \\ N_0 & \xrightarrow{t} & \dots & \xrightarrow{t} & N_i & \xrightarrow{t} & N_{i+1} & \xrightarrow{t} & \dots \end{array}$$

commutes and so, setting $\beta(\eta) := (\eta_0, \eta_1, \dots)$ yields a $DAPM$ morphism between $\beta(\oplus_{i\in\mathbb{N}} M_i)$ and $\beta(\oplus_{i\in\mathbb{N}} N_i)$.

More precisely, fix two graded $R[t]$-modules $\oplus M_i$ and $\oplus N_i$ and let $\mathcal{M} := \beta(\oplus M_i)$ and $\mathcal{N} := \beta(\oplus N_i)$. A graded morphism $\eta : \oplus M_i \to \oplus N_i$ implies a sequence of maps $(\xi_i)_{i\in\mathbb{N}} := \beta(\eta)$ where $\xi_i$ is just the restriction of $\eta$ to $M_i$. It follows that $\beta$ gives group homomorphisms $\xi_i : M_i \to N_i$ which are also $R$-module morphisms because for $r \in R$, $m_i \in M_i$ we get $\xi_i(rm_i) = \eta(rm_i) = r\eta(m_i) = r\xi_i(m_i)$. Since the connecting maps in $\mathcal{M}$ and $\mathcal{N}$ are induced by multiplication with $t$, we have that for $m_i \in M_i$,

$$\xi_{i+1}(tm_i) = \eta(tm_i) = t\eta(m_i) = t\xi_i(m_i),$$

proving that $\beta(\eta)$ is indeed a $DAPM$ morphism.

For functoriality, it is again clear that $\beta$ maps the identity to the identity morphism. For two graded $R[t]$-module morphisms $\eta, \eta'$ and any sequence $(m_i)_{i\in\mathbb{N}}$ with $m_i \in M_i$ for all $i \in \mathbb{N}$, we get

$$\begin{aligned} (\beta(\eta' \circ \eta))(m_i)_{i\in\mathbb{N}} &= (\eta'(\eta(m_i))_{i\in\mathbb{N}} \\ &= \beta(\eta')(\eta(m_i))_{i\in\mathbb{N}} \\ &= (\beta(\eta') \circ \beta(\eta))(m_i)_{i\in\mathbb{N}}. \end{aligned}$$

Finally, the construction immediately implies that $\alpha \circ \beta$ equals the identity functor on R[t]-**Gr-Mod** and $\beta \circ \alpha$ equals the identity functor on R-**Persmod**. □

FINITENESS CONDITIONS. In the context of computation and classification, it is natural to impose some finiteness condition on persistence modules, yielding a full subcategory of R-**Persmod**. Restricting the functor $\alpha$ from Lemma 7 to this subcategory yields a corresponding subcategory of R[t]-**Gr-Mod**. But does the correspondence established above also carry over the finiteness condition in an appropriate way? This is the question we study in this subsection.

**Definition 12.** A *DAPM* $\mathcal{M} = \left((M_i)_{i\in\mathbb{N}}, (\varphi_{i,j})_{i\leq j\in\mathbb{N}}\right)$ is *of finite type* if there is a $D \in \mathbb{N}$ such that for all $D \leq i \leq j$ the map $\varphi_{i,j}$ is an isomorphism. $\mathcal{M}$ is called *of finitely presented (generated) type* if it is of finite type and $M_i$ is finitely presented (generated) as an $R$-module for all $i \in \mathbb{N}$.

We will show next that *DAPMs* of finitely presented type over $R$ are isomorphic to finitely presented graded $R[t]$-modules using the functors $\alpha$ and $\beta$ above.

**Lemma 8.** *If a DAPM* $\mathcal{M} = \left((M_i)_{i\in\mathbb{N}}, (\varphi_{i,j})_{i\leq j\in\mathbb{N}}\right)$ *is of finitely presented type,* $\alpha(\mathcal{M})$ *is finitely presented.*

*Proof.* Let $D \in \mathbb{N}$ be such that for all $D \leq i \leq j$, $\varphi_{i,j} : M_i \to M_j$ is an isomorphism. Let $\mathfrak{G}_i$ be a generating set for $M_i$. We claim that $\bigcup_{i=1}^{D} \mathfrak{G}_i$ is a generating set for $\alpha(\mathcal{M})$. To see that, it suffices to show that every homogeneous element in $\alpha(\mathcal{M}) = \oplus M_i$ is generated by the union of the $G_i$. So, fix $k \in \mathbb{N}$ and $m_k$ homogeneous of degree $k$. If $k \leq D$, then $m_k$ is generated by the elements of $\mathfrak{G}_k$ by construction. If $k > D$, we show that $m_k$ is generated by $\mathfrak{G}_D$. For that, let $m_D := \varphi_{D,k}^{-1}(m_k)$ which exists because $\varphi_{D,k}$ is isomorphism. $m_D$ is generated by $\mathfrak{G}_D$, hence $m_k$ is generated by $\varphi_{D,k}(\mathfrak{G}_D)$. By construction of $\alpha$, $\varphi_{D,k}(\mathfrak{G}_D) = t^{k-D}\mathfrak{G}_D$ and since $t^{k-D}$ is a ring element in $R[t]$, $m_k$ is generated by $\mathfrak{G}_D$. This shows that $\alpha(\mathcal{M})$ is finitely generated.

It remains to show that $\alpha(\mathcal{M})$ is also finitely presented. Let $\mu_i : R^{n_i} \to M_i$ be the generating surjective map that corresponds to $\mathfrak{G}_i$. Writing $n = \sum_{i=1}^{D} n_i$, there is a map $\mu : R[t]^n \to \alpha(\mathcal{M})$ that corresponds to the the generating set $\bigcup_{i=1}^{D} \mathfrak{G}_i$. If $\mathfrak{g}_i$ is a generator, we will use the notation $\mathfrak{e}_i$ to denote the corresponding generator of $R[t]^n$.

We now define a finite set of elements of $\ker \mu$. First of all, let $\mathfrak{Z}_i$ be the generating set of $\ker \mu_i$ for $0 \leq i \leq D$. Clearly, all elements of $\mathfrak{Z}_i$ are also in $\ker \mu$. Moreover, for any $0 \leq i < j \leq D$, and any generator $\mathfrak{g}_i$ in $\mathfrak{G}_i$ with $\varphi_{i,j}(\mathfrak{g}_i) \neq 0$, we can write

$$\varphi_{i,j}(\mathfrak{g}_i) = \sum_{v=0}^{n_j} \lambda_v \mathfrak{g}_j^{(v)}$$

where $\lambda_v \in R$ and $\mathfrak{G}_j = \{\mathfrak{g}_j^{(0)}, \ldots, \mathfrak{g}_j^{(n_j)}\}$. In that case, the corresponding element

$$t^{j-i}\mathfrak{e}_i - \sum_{v=0}^{n_j} \lambda_v \mathfrak{e}_j^{(v)}$$

is in $\ker \mu$. We let $\mathfrak{Z}_{i,j}$ denote the (finite) set obtained by picking one element as above for each $\mathfrak{g}_i$ with $\varphi_{i,j}(\mathfrak{g}_i) \neq 0$. We claim that $\mathfrak{Z} := \bigcup_{i=0}^{D} \mathfrak{Z}_i \cup \bigcup_{0 \leq i < j \leq D} \mathfrak{Z}_{i,j}$ generates $\ker \mu$:

Fix an element in $x \in \ker \mu$, which is of the form

$$x = \sum_{\ell} \lambda_\ell \mathfrak{e}_\ell$$

with $\lambda_\ell \in R[t]$ and $\mathfrak{e}_\ell$ a generator of $R[t]^n$. We can assume that $x$ is homogeneous of some degree $k$. We first consider the case that $k \leq D$ and all $\lambda_\ell$ are of degree 0. Then, all $\mathfrak{e}_\ell$ that appear in $x$ are of the same degree, and hence, their images under $\mu$ are generators of $M_k$. It follows that $x$ is generated by the set $\mathfrak{Z}_k$.

Next, we consider the case that $k \leq D$, and some $\lambda_\ell$ is of positive degree. Because $x$ is homogeneous, $\lambda_\ell$ is then of the form $r_\ell t^{d_\ell}$ for some $r_\ell \in R$ and $d_\ell > 0$. Since the degree of $\mathfrak{e}_\ell$ is $k - d_\ell$, there is an element $\mathfrak{z}_\ell$ in $\mathfrak{Z}_{k-d_\ell,k}$ of the form $\mathfrak{z}_\ell = t^{d_\ell}\mathfrak{e}_\ell - \sum_{v=0}^{n_\ell} \tilde{\lambda}_v \mathfrak{e}_k^{(v)}$ with all $\mathfrak{e}_k^{(v)}$ of degree $k$ and each $\tilde{\lambda}_v \in R$. Then in $x - r_\ell \mathfrak{z}_\ell$ the coefficient of $\mathfrak{e}_\ell$ in $x$ is 0, and we only introduce summands with coefficients of degree 0 in $t$.

Iterating this construction for each summand with coefficient of positive degree, we get an element $x' = x - \sum_w r_w \mathfrak{z}_w$ with $r_w \in R$ and $\mathfrak{z}_w$ elements of $\mathfrak{Z}$, and $x'$ only having coefficient of degree 0 in $t$. This yields to $x = x' + \sum_w r_w \mathfrak{z}_w$. Using the first part, it follows that $x$ is generated by $\mathfrak{Z}$.

Finally, we consider the case that $k > D$. In that case, each $\lambda_\ell$ is of degree at least $k - D$, because the maximal degree of $\mathfrak{e}_\ell$ is $D$. So, $x = t^{k-D}x'$ with $x'$ homogeneous of degree $D$. Since $0 = \mu(x) = t^{k-D}\mu(x')$, $x' \in \ker \mu$ as well. By the second part, $x'$ is hence generated by $\mathfrak{Z}$, and so is $x$. □

For the next two lemmas, we fix a finitely presented graded $R[t]$-module $\mathbf{M} := \oplus_{i\in\mathbb{N}} M_i$ with a map

$$R[t]^n \xrightarrow{\mu} \mathbf{M}$$

such that $\ker \mu$ is finitely generated. Moreover, we let $\mathfrak{G} := \{\mathfrak{g}^{(1)}, \ldots, \mathfrak{g}^{(n)}\}$ denote generators of $\mathbf{M}$ and $\mathfrak{Z} := \{\mathfrak{z}^{(1)}, \ldots, \mathfrak{z}^{(m)}\}$ denote a generating set of $\ker \mu$. We assume that each $\mathfrak{g}^{(i)}$ and each $\mathfrak{z}^{(j)}$ is homogeneous (with respect to the grading of the corresponding module), and we let $\deg(\mathfrak{g}^{(i)})$, $\deg(\mathfrak{z}^{(j)})$ denote the degrees. We further assume that $\mathfrak{G}$ and $\mathfrak{Z}$ are sorted by degrees in non-decreasing order.

**Lemma 9.** *Each $M_i$ is finitely presented as an $R$-module.*

*Proof.* We argue first that $M_i$ is finitely generated. Set $d_j := \deg(\mathfrak{g}^{(j)})$ for $1 \leq j \leq n$. Let $n_i$ denote the number of elements in $\mathfrak{G}$ with degree at most $i$. Define the map $\mu_i : R^{n_i} \to M_i$, by mapping the $j$th generator $\mathfrak{e}_i^{(j)}$ of $R^{n_i}$ to the element $t^{i-d_j}\mathfrak{g}^{(j)}$. It is then straight-forward to see that the map $\mu_i$ is surjective, proving that $M_i$ is finitely generated.

We show that $\ker \mu_i$ is finitely generated as well. Let $\mathfrak{e}^{(1)}, \ldots, \mathfrak{e}^{(n)}$ be the generators of $R[t]^n$ mapping to $\mathfrak{g}^{(1)}, \ldots, \mathfrak{g}^{(n)}$ under $\mu$. Let $m_i$ denote the number of elements in $\mathfrak{Z}$ such that $d'_j := \deg(\mathfrak{z}^{(j)}) \leq i$. For every $\mathfrak{z}^{(j)}$ with $1 \leq j \leq m_i$, consider $t^{i-d'_j}\mathfrak{z}^{(j)}$, which can be written as

$$t^{i-d'_j}\mathfrak{z}^{(j)} = \sum_{k=1}^{n_i} r_k t^{i-d_k}\mathfrak{e}^{(k)}$$

with $r_k \in R$. Now, define

$$\mathfrak{z}_i^{(j)} := \sum_{k=1}^{n_i} r_k \mathfrak{e}_i^{(k)}$$

and define $\mathfrak{Z}_i := \{\mathfrak{z}_i^{(j)} \mid 1 \leq i \leq m_i\}$. We claim that $\mathfrak{Z}_i$ generates $\ker \mu_i$. First of all, it is clear that $\mu_i(\mathfrak{z}_i^{(j)}) = \mu(\mathfrak{z}^{(j)}) = 0$. Now fix $x \in \ker \mu_i$ arbitrarily. Then, $x$ is a linear combination of elements in $\{\mathfrak{e}_i^{(1)}, \dots, \mathfrak{e}_i^{(n_i)}\}$ with coefficients in $R$. Replacing $\mathfrak{e}_i^{(j)}$ with $t^{i-d_j}\mathfrak{e}^{(j)}$, we obtain $x' \in R[t]^n$ homogeneous of degree $i$. By assumption, we can write $x'$ as linear combination of elements in $\mathfrak{Z}$, that is,

$$x' = \sum_{k=1}^{m_i} r'_k t^{i-d'_k} \mathfrak{z}^{(k)}$$

with $r'_k \in R$. Then, it holds that

$$x = \sum_{k=1}^{m_i} r'_k \mathfrak{z}_i^{(k)},$$

which follows simply by comparing coefficients: let $j \in \{1, \dots, n_i\}$ and let $c_j \in R$ be the coefficient of $\mathfrak{e}_i^{(j)}$ in $x$. Let $c'_j$ be the coefficient of $\mathfrak{e}_i^{(j)}$ in the sum $\sum_{k=1}^{m_i} r'_k \mathfrak{z}_i^{(k)}$, expanding each $\mathfrak{z}_i^{(k)}$ by its linear combination as above. Then by construction, $c_j$ is the coefficient of $t^{i-d_j}\mathfrak{e}^{(j)}$ in $x'$, and $c'_j$ is the coefficient of $t^{i-d_j}\mathfrak{e}^{(j)}$ in the sum $\sum_{k=1}^{m_i} r'_k t^{i-d'_k}\mathfrak{z}^{(k)}$. Since this sum equals $x'$, it follows that $c_j = c'_j$. Since $x$ was chosen arbitrary from $\ker \mu_i$, it follows $\mathfrak{Z}_i$ generates the kernel. □

**Lemma 10.** *$\beta(\mathbf{M})$ is of finite type. In particular, it is of finitely presented type with Lemma 9.*

*Proof.* Fix

$$D := max\{\deg(\mathfrak{g}^{(j)}), \deg(\mathfrak{z}^{(k)}) \mid 1 \leq j \leq n, 1 \leq k \leq m\}.$$

It suffices to show that multiplication by $t$ induces an isomorphism $M_i \to M_{i+1}$ for every $i \geq D$. Let $y \in M_{i+1}$. Then, $y = \sum_{j=1}^{n} \lambda_j \mathfrak{g}^{(j)}$ with $\lambda_j \in R[t]$ of degree at least 1. Hence, $y = ty'$ with $y' \in M_i$, showing that multiplication with $t$ gives a surjective map.

For injectivity, let $y \in M_i$ such that $ty = 0$. Let $x \in R[t]^n$ be such that $\mu(x) = y$. Then $\mu(tx) = ty = 0$. Hence, $tx$ can be written as

$$tx = \sum_{j=0}^{m} \tilde{\lambda}_j \mathfrak{z}^{(j)}$$

where each non-trivial $\lambda_j$ is a polynomial of degree at least one, because each $\mathfrak{z}^{(j)}$ is of degree at most $D$ and $tx$ is of degree at least $D+1$. Therefore, there is also a decomposition

$$tx = \sum_{j=0}^{m} t\lambda_j \mathfrak{z}^{(j)} = t \sum_{j=0}^{m} \lambda_j \mathfrak{z}^{(j)}.$$

Since $R[t]^n$ is free, this implies that $x$ equals the sum on the right hand side, implying that $x \in \ker \mu$, so $y = 0$. □

The Representation Theorem. The preceding lemmas of this section immediately reply the following version of the Representation Theorem.

**Theorem 9.** *Let $R$ be a ring with unity. The category of finitely presented graded $R[t]$-modules is isomorphic to the category of discrete algebraic persistence modules of finitely presented type.*

*Proof.* The two categories are subcategories of R[t]-**Gr-Mod** and R-**Persmod**, respectively. Since $\alpha$ and $\beta$, restricted to these subcategories, map a $DAPM$ of finitely presented type to a finitely presented graded $R[t]$-module (Lemma 8) and vice versa (Lemma 9 and Lemma 10), these categories are isomorphic. □

What happens if we replace "finitely presented" with the weaker condition "finitely generated" throughout? The proof of Lemma 8 shows that if $\mathcal{M}$ is of finitely generated type, $\alpha(\mathcal{M})$ is finitely generated. Vice versa, if a graded $R[t]$-module $\mathbf{M} = \oplus_{i \in \mathbb{N}} M_i$ is finitely generated, each $M_i$ is finitely generated, too. However, it does not follow in general that $\beta(\mathbf{M})$ is of finite type, as the example from the introduction shows. This problem disappears with additional requirements on the ring:

**Corollary 1.** *If $R$ is commutative and Noetherian, the category of finitely generated graded $R[t]$-modules is isomorphic to the category of discrete algebraic persistence modules of finitely generated type.*

*Proof.* By Lemma 1, the Corollary is just Theorem 9 restated. □

## 5.3 Proving the ZC-Representation Theorem using Artin-Rees theory

We showed how to prove the Representation Theorem elementarily. Since Artin-Rees theory is quoted in [175, 176] to provide a proof for Theorem 9 (over commutative Noetherian rings with unity), we take a closer look at the connections between Artin-Rees theory and such a proof. To do this, we consider the following notion of filtrations of modules:

**Definition 13.** Let $A$ be a commutative Noetherian ring with unity. Let $I \subseteq A$ be an ideal, $M$ an $A$-module. An *$I$-filtration of $M$* is a collection $(M_n)_{n\in\mathbb{N}}$ such that $M = M_0 \supseteq M_1 \supseteq M_2 \supseteq \dots$ and $IM_n \subseteq M_{n+1}$ for all $n \in \mathbb{N}$. An $I$-filtration is called *$I$-stable* if there is an $n_0 \in \mathbb{N}$ such that $IM_n = M_{n+1}$ for all $n \geq n_0$.

Now, consider an ideal $I \subseteq A$ and an $I$-filtration $(M_n)_{n\in\mathbb{N}}$ of a finitely generated $A$-module $M$. Let $\overline{A} := \bigoplus_{i\in\mathbb{N}} I^i$, $\overline{M} := \bigoplus_{i\in\mathbb{N}} M_i$. We obtain a criterion for $(M_n)_{n\in\mathbb{N}}$ to be $I$-stable:

**Lemma 11** (Criterion for stability)**.** *Let $A$ be a commutative Noetherian ring with unity, $I \subseteq A$ an ideal. Let $M$ be a finitely generated $A$-module, $(M_n)_{n\in\mathbb{N}}$ an $I$-filtration of $M$. Then the following are equivalent:*

1. *$\overline{M}$ is a finitely generated $\overline{A}$-module.*
2. *$(M_n)_{n\in\mathbb{N}}$ is $I$-stable.*

This criterion helps to prove the famous Artin-Rees Lemma. It states that given a stable filtration of a finitely generated module $M$ and a submodule $N$ of $M$, then intersecting each member of the filtration with $N$ again yields a stable filtration. The Artin-Rees Lemma can for instance be used to prove Krull's Intersection Theorem [89] and to study modules over local rings [102]. For a proof of the above criterion, the Artin-Rees Lemma and the connection between the two lemmas, we refer to [102].

Let us see how this helps to prove the ZC-Representation Theorem for a commutative Noetherian ring $R$ with unity. Setting $A = R[t]$ and $I$ as the ideal generated by $t$, we obtain $\overline{A} = R[t]$. By Lemma 1, $R[t]$ is Noetherian and finite presentation and finite generation coincide not only for $R$-modules, but also for $R[t]$-modules.

Let $\mathcal{M}$ be a $DAPM$ over $R$ of finitely generated type. Consider the filtration $(\widetilde{M}_n)_{n\in\mathbb{N}}$ defined by $\widetilde{M}_0 = \oplus_{i\in\mathbb{N}} M_i$ and $\widetilde{M}_n = (t^n)\widetilde{M}_0$ for $n > 0$. By finite type assumption, there exists an $n_o \in \mathbb{N}$ such that $(t)\widetilde{M}_n = \widetilde{M}_{n+1}$ for all $n \geq n_0$. To use the above criterion, we have to ensure that $\oplus_{i\in\mathbb{N}} M_i$ is a finitely generated $R[t]$-module. We do not see how this could follow from Artin-Rees theory since finite generation is an assumption in most of the statements. A proof for the finite generation of $\oplus_{i\in\mathbb{N}} M_i$ is the first part of our proof of Lemma 8.

Conversely, using the above criterion, finite generation of the $R[t]$-module $\oplus_{i\in\mathbb{N}} M_i$ directly implies $(t)$-stability of the filtration $(\widetilde{M}_n)_{n\in\mathbb{N}}$. Hence the corresponding $DAPM$ $\beta(\oplus_{i\in\mathbb{N}} M_i)$ is of finite type. It is left to prove that each $M_i$ is finitely generated as an $R$-module. This can easily be seen by the first five lines of our proof of Lemma 9.

Artin-Rees theory is defined over commutative Noetherian rings with unity and filtrations of subsets of modules. Therefore it does not yield a proof for more general rings or, at least not immediately, for more general indexing monoids than $\mathbb{N}$. We turn to prove the Representation Theorem over more general indexing monoids in the following sections.

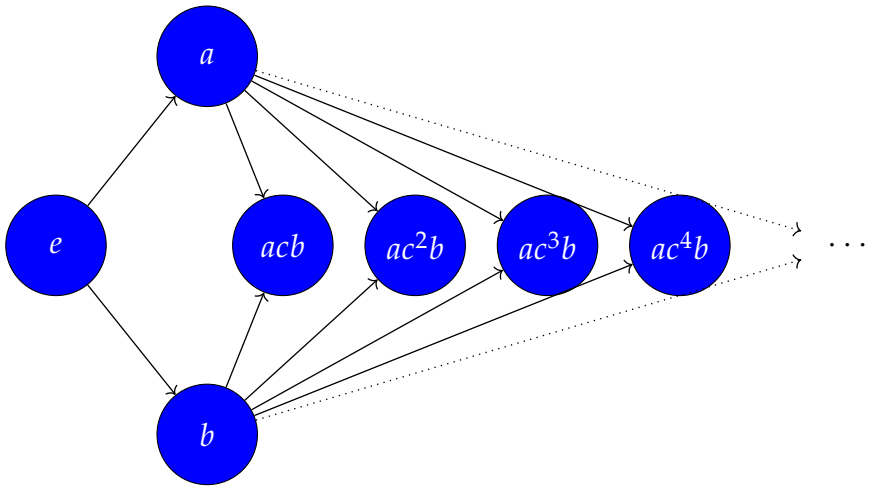


Figure 5.3: Graphical illustration of a monoid that is not good. The monoid is the non-commutative monoid generated by three elements $a, b, c$ modulo the congruence generated by $ac^n b \approx bc^n a$ for all $n \in \mathbb{N}_{>0}$. The plcm of $\{a, b\}$ are the elements of the countable set $\{ac^n b\}_{n \in \mathbb{N}_{>0}}$.

## 5.4 Good monoids

The category of $G$-graded $R[G]$-modules R[$G$]-**Gr-Mod** exist without further assumptions on monoids. However, in order to generalize the Representation Theorem to monoids, we will require additional properties on monoids.

We call $g_2$ a *(left-)multiple* of $g_1$ and write $g_1 \preceq g_2$ if there exists an $h \in G$ such that $h \star g_1 = g_2$. A *proper multiple* of $g_1$ is a multiple $g_2$ with $g_1 \neq g_2$, written as $g_1 \prec g_2$. For a subset $\tilde{G} \subseteq G$ an element $h$ is called *common multiple* of $\tilde{G}$ if $g \preceq h$ for all $g \in \tilde{G}$. We call a common multiple $h$ of $\tilde{G}$ *partially least*, if there is no multiple $h'$ of $\tilde{G}$ such that $h' \prec h$. We write *plcm* for partially least common multiples. We say that the monoid $G$ is *weak plcm* if for any finite subset $H \subseteq G$ there are at most finitely many distinct partially least common multiples of $H$.[2]

[2]It is called "weak" plcm to point out that the plcm does not have to exist or to be unique

A monoid is *anti-symmetric* if $g_1 \preceq g_2$ and $g_2 \preceq g_1$ imply that $g_1 = g_2$. This is equivalent to the condition that $\preceq$ turns $G$ into a poset. In an anti-symmetric monoid, no element (except $e$) can have an inverse element.

**Definition 14.** We call a monoid *good* if it is cancellative, anti-symmetric and weak plcm.

Some easy commutative examples for good monoids with uniquely existing plcms are $(\mathbb{N}^k, +)$, $\left(\mathbb{Q}^k_{\geq 0}, +\right)$, $\left(\mathbb{R}^k_{\geq 0}, +\right)$, $((0,1], \cdot)$, $(\mathbb{Q} \cap (0,1], \cdot)$ and $([1,\infty), \cdot)$. A fundamental class of good monoids are free monoids, which can be expressed as finite sequences of elements of a set. In non-commutative free monoids, a subset admits common left multiples if and only if it contains a maximal element. If this exists, it is also the unique plcm. Constructing cancellative anti-symmetric monoids that are not weak plcm does not come naturally. Consider the non-commutative free monoid generated by $a, b, c$. Introduce the congruence generated by $ac^n b \approx bc^n a$ for all $n \in \mathbb{N}_{>0}$ (see Figure 5.3). Then there are infinitely many plcm for $\{a, b\}$ in the quotient monoid, since every equivalence class with representative $ac^n b$ is partially least for $\{a, b\}$. In particular, good monoids are not closed under homomorphisms.

A convenient way to visualize a monoid is a directed multigraph where each vertex corresponds to an element of $G$. For a vertex corresponding to $g \in G$, there is an outgoing edge for each $h \in G$ going to the vertex $h \star g$. We ignore the self loops induced by the neutral element of $G$ on each vertex. In this interpretation, $g_1 \preceq g_2$ if and only if there is an edge from the vertex labeled $g_1$ to the vertex labeled $g_2$ in the graph. Right-cancellativity means that there is at most one edge between any pair of vertices, that is, the multigraph is a graph. Left-cancellativity means that edges obtained by multiplication by $h$ from pairwise distinct vertices $g_1, ..., g_n$ can not lead to the same vertex $g$. Anti-symmetry simply implies that the graph is acyclic (modulo self-loops). Weak plcm means that each finite subset of vertices has a finite set of minimal common successors. As a consequence, a good monoid is either trivial or infinite, because if $G$ has at least two elements, there are at least two outgoing edges per vertex, and one of them cannot be a self-loop because of right-cancellativity. Because of acyclicity, we can thus

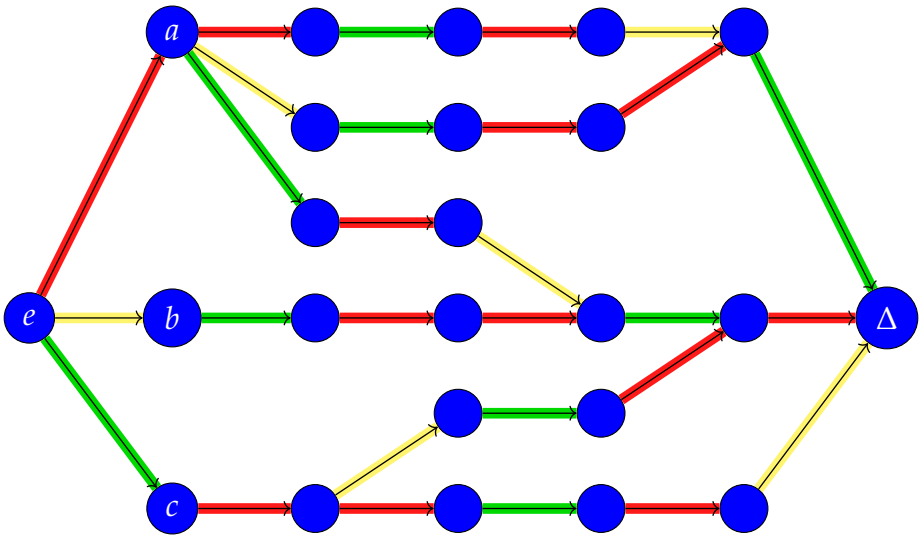


Figure 5.4: A Hasse diagram illustrating a finite part of a good monoid. It is the Garside monoid obtained by the free non-commutative monoid $< a, b, c >$ modulo the congruence generated by $baca \approx a^2cb$, $ca^2cb \approx acbac$ and $acbac \approx cbaca$. The redly, yellowly, and greenly highlighted arrows represent left-multiplication with the elements $a$, $b$ and $c$, respectively. A Garside element of a monoid is an element whose left and right divisors coincide, are finite and generate the monoid. $\Delta$ is the minimal Garside element. For more details on this example and how such examples can be considered as Garside monoids or divisibility monoids we refer to [147].

form an infinite sequence of elements. For concrete pictures, it is usually convenient to draw only a subset of vertices and edges.

Related concepts. The cancellation property is a classical assumption [56] and is sometimes even part of the definition of a monoid [97]. The property of a monoid being weak plcm is less standard. It gives rise to a connection to the vivid branch of factorization theory [10, 97]. Least common multiples are defined in a related way, namely that a (left- )lcm of a set of elements of a monoid is a right-divisor of all other common multiples. If a monoid is cancellative and anti-symmetric, then any set of lcms consists of at most one element. Therefore, monoids with these assumptions or with uniquely existing lcms are sometimes called lcm monoids [64]. Note that the existence of a plcm does not imply the existence of an lcm. Conversely, if an

lcm exists and is unique, it is also the unique plcm. Therefore, divisibility monoids [122] Garside monoids [65] and Gaussian monoids [66] are examples for subclasses of good monoids. These subclasses are involved in trace theory [75] and braid theory [64, 65, 66], respectively. See Figure 5.4 for a concrete example of a Garside monoid. Anti-symmetric monoids are sometimes also called centerless, conical, positive, zerosumfree [170], reduced [97] or monoids with trivial unit group [56]. The preorder induced by left-factorization is related to one of Green's preorders [103]. Given an anti-symmetric monoid $G$, the aforementioned preorder is a partial order and gives rise to a right-partially ordered monoid $(G, \star, \preceq)$, since clearly $g_1 \preceq g_2$ implies $h \star g_1 \preceq h \star g_2$ for all $h \in G$. If $G$ is commutative, then $(G, \star, \preceq)$ is a partially ordered monoid.

## 5.5 The Representation Theorem over monoids

Generalized persistence modules and $R[G]$-modules. We will now extend the Representation Theorem from linear sequences of the form

$$M_0 \xrightarrow{\varphi_0} M_1 \xrightarrow{\varphi_1} M_2 \xrightarrow{\varphi_2} \dots$$

to representations of a monoid $(G, \star, \preceq)$, right-partially ordered by left factorization. For simplicity, we will assume throughout this section that $(G, \star)$ is a good monoid – see the conclusion for a discussion of how the conditions of $G$ could be further relaxed. We define persistence modules over $G$:

**Definition 15.** Let $R$ be a ring with unity. A *generalized algebraic persistence module (GAPM)* is a tuple $\mathcal{M}_G = \left( \left(M_g\right)_{g \in G}, \left(\varphi_{g_1,g_2}\right)_{g_1 \preceq g_2 \in G} \right)$ such that $M_g$ is an $R$-module, $\varphi_{g_1,g_2} : M_{g_1} \to M_{g_2}$ is a module morphism, $\varphi_{g,g} = 1_{M_g}$ and $\varphi_{g_1,g_3} = \varphi_{g_2,g_3} \circ \varphi_{g_1,g_2}$ for all $g \in G$, $g_1 \preceq g_2 \preceq g_3 \in G$.

Much more succinctly, we could equivalently define a $GAPM$ as a functor from the poset category $G$ to $R$-**Mod**. It is clear that a $GAPM$ over the

monoid $\mathbb{N}$ is just a $DAPM$. Of interest is also the case $G = \left(\mathbb{N}^k, +\right)$, which has been investigated for example in [43].

As in the case of $G = \mathbb{N}$, arbitrary $GAPM$ are closely related to $R[G]$-modules. Given a $GAPM$ $\mathcal{M}_G$, we can assign a graded $R[G]$-module to it by setting

$$\alpha\left(\mathcal{M}_G\right) := \bigoplus_{g \in G} M_g \tag{5.4}$$

where multiplication by an element $h \in G$ is defined by $h \cdot m_g := \varphi_{g,h\star g}(m_g) \in M_{h\star g}$ for all $g \in G$ and all $m_g \in M_g$.
Vice versa, an $R[G]$-module $\oplus_{g\in G} M_g$ defines a $GAPM$ by

$$\beta\left(\bigoplus_{g \in G} M_g\right) := \left(\left(M_g\right)_{g\in G}, \left(\varphi_{g_1,g_2}\right)_{g_1 \preceq g_2 \in G}\right) \tag{5.5}$$

where the morphisms are again defined conversely. More precisely, for all $g_1 \preceq g_2 \in G$ and all $m_{g_1} \in M_{g_1}$, we define $\varphi_{g_1,g_2}(m_{g_1}) := h \cdot m_{g_1}$ with $h \star g_1 = g_2$. Note that $h$ is uniquely defined because $G$ is assumed to be right-cancellative.

**Definition 16.** A family of module morphisms $\xi_G = \left(\xi_g : M_g \to N_g\right)_{g\in G}$ between two $GAPM$ $\left(\left(M_g\right)_{g\in G}, \left(\varphi_{g_1,g_2}\right)_{g_1 \preceq g_2 \in G}\right)$, $\left(\left(N_g\right)_{g\in G}, \left(\psi_{g_1,g_2}\right)_{g_1 \preceq g_2 \in G}\right)$ over the same ring $R$ with unity is called *generalized algebraic persistence module morphism* if

$$\psi_{g_1,g_2} \circ \xi_{g_1} = \xi_{g_2} \circ \varphi_{g_1,g_2}$$

for all $g_1 \preceq g_2 \in G$. Equivalently, all diagrams of the following form commute:

$$\begin{array}{ccc} M_{g_1} & \xrightarrow{\varphi_{g_1,g_2}} & M_{g_2} \\ \downarrow{\scriptstyle \xi_{g_1}} & & \downarrow{\scriptstyle \xi_{g_2}} \\ N_{g_1} & \xrightarrow{\psi_{g_1,g_2}} & N_{g_2} \end{array}$$

With such morphisms, the class of all $GAPMs$ over $R$ becomes a category, which we call R-**Persmod**$^G$.

**Lemma 12.** *The maps $\alpha$ and $\beta$ from (5.4) and (5.5) extend to functors between R-**Persmod**$^G$ and R[G]-**Gr-Mod** which form an isomorphic pair of functors. In particular, the two categories are isomorphic.*

*Proof.* For a $GAPM$ morphism $(\xi_g : M_g \to N_g)_{g\in G}$ between two $GAPMs$ $\mathcal{M}_G$ and $\mathcal{N}_G$, we define

$$\alpha(\xi_G) : \bigoplus_{g\in G} M_g \to \bigoplus_{g\in G} N_g, (m_g)_{g\in G} \mapsto (\xi_g(m_g))_{g\in G}.$$

Recall that for $\xi_G = (\xi_g)_{g\in G}$, a $GAPM$ morphism between $\mathcal{M}_G$ and $\mathcal{N}_G$, we define $\alpha(\xi_G)$ as the map assigning to $(m_g) \in \oplus M_g$ the value $(\xi_g(m_g))$. Let us define $f := \alpha(\xi_G)$ for shorter notation. Again, $f$ is a graded module morphism: it is a group homomorphism, as each $\xi_g$ is, it clearly satisfies $f(M_g) \subset N_g$, and it holds that for $m = (m_g)_{g\in G}$ and $h \in G$ we get

$$\begin{aligned}
f(hm) &= f\left(\left(\begin{cases} hm_{\widetilde{g}}; & \exists \widetilde{g} \in G : h \star \widetilde{g} = g \\ 0; & \text{otherwise} \end{cases}\right)_{g\in G}\right) \\
&= \left(\left(\begin{cases} \xi_{h\star\widetilde{g}}(hm_{\widetilde{g}}); & \exists \widetilde{g} \in G : h \star \widetilde{g} = g \\ 0; & \text{otherwise} \end{cases}\right)_{g\in G}\right) \\
&= \left(\left(\begin{cases} h\xi_{\widetilde{g}}(m_{\widetilde{g}}); & \exists \widetilde{g} \in G : h \star \widetilde{g} = g \\ 0; & \text{otherwise} \end{cases}\right)_{g\in G}\right) \\
&= \left(\left(\begin{cases} h\xi_{\widetilde{g}}(m_{\widetilde{g}}); & \exists \widetilde{g} \in G : h \star \widetilde{g} = g \\ 0; & \text{otherwise} \end{cases}\right)_{g\in G}\right) \\
&= h\left(\xi_g(m_g)\right)_{g\in G} \\
&= hf(m),
\end{aligned}$$

where the third equality comes from the property of $GAPM$ morphisms.

For the functorial properties, it is clear that $\alpha$ maps the identity $GAPM$ morphism to the identity of the corresponding graded module. If $\xi_G$, $\xi'_G$ are

$GAPM$ morphisms and $m$ as before, we calculate

$$\begin{aligned}(\alpha(\xi'_* \circ \xi_*))(m) &= \left(\xi'_g(\xi_g(m_g))\right)_{g\in G} \\ &= \alpha(\xi'_*)\left(\xi_g(m_g)\right)_{g\in G} \\ &= (\alpha(\xi'_*) \circ \alpha(\xi_*))(m).\end{aligned}$$

Vice versa, a morphism

$$\eta : \bigoplus_{g\in G} M_g \to \bigoplus_{g\in G} N_g$$

in R[$G$]-**Gr-Mod** induces a homomorphism $\eta_g : M_g \to N_g$ for each $g \in G$, and these induced maps are compatible with multiplication of each $h \in G$. Hence, the diagram

$$\begin{array}{ccc} M_g & \xrightarrow{h} & M_{h\star g} \\ \downarrow{\scriptstyle \xi_g} & & \downarrow{\scriptstyle \xi_{h\star g}} \\ N_g & \xrightarrow{h} & N_{h\star g} \end{array}$$

commutes and so, setting $\beta(\eta) := (\eta_g)_{g\in G}$ yields a $GAPM$ morphism between $\beta(\oplus_{g\in G} M_g)$ and $\beta(\oplus_{g\in G} N_g)$.

For functoriality, it is clear that $\beta$ maps the identity between graded modules to the identity $GAPM$ morphism. For two graded $R[G]$-module morphisms $\eta, \eta'$ and any $(m_g)_{g\in G}$ with $m_g \in M_g$ for all $g \in G$, we get

$$\begin{aligned}(\beta(\eta' \circ \eta))\,(m_g)_{g\in G} &= (\eta'(\eta(m_g))_{g\in G} \\ &= \beta(\eta')\,(\eta(m_g))_{g\in G} \\ &= (\beta(\eta') \circ \beta(\eta))\,(m_g)_{g\in G}\,.\end{aligned}$$

Finally, the construction immediately implies that $\alpha \circ \beta$ equals the identity functor on R[$G$]-**Gr-Mod** and $\beta \circ \alpha$ equals the identity functor on R-**Persmod**$^G$, hence $(\alpha, \beta)$ is an isomorphic pair of functors. □

FINITENESS CONDITIONS. As in the case of linear sequences, we are interested in the subcategory of R-**Persmod**$^G$ that is isomorphic to the category of finitely presented $R[G]$-modules. In order to describe the desired subcategory constructively, we introduce the notions of frames:

**Definition 17.** Let $\mathcal{M}_G = \left((M_g)_{g\in G}, (\varphi_{g_1,g_2})_{g_1\preceq g_2\in G}\right)$ be a *GAPM*. For $g \in G$, $h \in G$ is a *frame* of $g$ (wrt. $\mathcal{M}_G$) if $h \preceq g$ and for all $h \preceq \tilde{g} \preceq g$, the map $\varphi_{h,\tilde{g}}$ is an isomorphism. We say that $H \subseteq G$ is a *framing set* of $\mathcal{M}_G$ if every $g \in G$ has a frame in $H$. $\mathcal{M}_G$ is of *finite type* if there exists a finite framing set for $G$. It is called of *finitely presented (generated) type* if it is of finite type and each $M_g$ is finitely presented (generated) as an $R$-module.

From this definition, it follows that $e$ is an element in each framing set because of anti-symmetry. Moreover, trivially, each $\mathcal{M}_G$ has a framing set, namely $G$ itself. Another useful property is that if $g \in G$ and $h$ is a frame of $g$, then for every $\tilde{g}$ with $h \preceq \tilde{g} \preceq g$, $\varphi_{\tilde{g},g}$ is an isomorphism as well, just because $\varphi_{\tilde{g},g} \circ \varphi_{h,\tilde{g}} = \varphi_{h,g}$.

We discuss a related concept that is equivalent in some cases. Let $\mathcal{M}_G = \left((M_g)_{g\in G}, (\varphi_{g_1,g_2})_{g_1\preceq g_2\in G}\right)$ be a *GAPM*. We define $(g_i)_{i\in\mathbb{N}}$ to be a sequence in $G$ if $g_i \in G$ and $g_i \preceq g_{i+1}$ for all $i \in \mathbb{N}$. A sequence $(g_i)_{i\in\mathbb{N}}$ in $G$ induces a sequence $(M_{g_i})_{i\in\mathbb{N}}$ in $\mathcal{M}_G$ with connecting morphisms $\varphi_{g_i,g_{i+1}} : M_{g_i} \to M_{g_{i+1}}$. We say that the latter sequence becomes *stationary* if there exists a $D \in \mathbb{N}$ such that $\varphi_{g_i,g_{i+1}}$ is an isomorphism for all $i \geq D$. Note that (stationary) sequences in a GAPM are (finite type) DAPMs.

**Lemma 13.** *For a GAPM* $\mathcal{M}_G = \left((M_g)_{g\in G}, (\varphi_{g_1,g_2})_{g_1\preceq g_2\in G}\right)$ *of finite type, every sequence in* $\mathcal{M}_G$ *becomes stationary.*

*Proof.* Consider a sequence $(g_i)_{i\in\mathbb{N}}$ in $G$. Let $H = \{h_1, \ldots, h_k\}$ be a finite set that frames $\mathcal{M}_G$. Now, for every $g_i$, if $h_j \preceq g_i$, also $h_j \preceq g_\ell$ for $i \leq \ell$. Hence, setting $H_i := \{h \in H \mid h \preceq g_i\}$, we get that $H_0 \subseteq H_1 \subseteq \ldots$, and since $H$ is finite, there is a $D \in \mathbb{N}$ such that $H_D = H_{D+1} = \ldots$.

Now, fix some $i \geq D$. Pick a frame $h \in H$ of $g_{i+1}$. By construction, $h \in H_D$ and hence, $h \preceq g_i$ as well. Hence, $h \preceq g_i \preceq g_{i+1}$, which implies that $\varphi_{g_i,g_{i+1}}$ is an isomorphism. □

The converse of the statement is not true in general: Consider the monoid $(\mathbb{Q}_{\geq 0}, +)$. The monoid is good, since the (unique) plcm of a finite subset is the maximal element in the set. We construct a $GAPM$ $\mathcal{M}_G$ by setting $M_0 := R$ and $M_q := 0$ for all $q > 0$ and let all maps be the zero maps. It is then obvious that every sequence becomes stationary. However, no finite subset can frame $\mathcal{M}_G$ because for every choice of finite subsets $\{0, q_1, ..., q_D\}$ with $q_i > 0$ there are elements $q > 0$ such that $q < q_i$ for all $i \in \{1, ..., D\}$.

In the previous example, we also observe that the corresponding $R[\mathbb{Q}_{\geq 0}]$-module is finitely generated. In some cases, however, both conditions are indeed equivalent:

**Lemma 14.** *If $G = \mathbb{N}^k$, a $GAPM$ is of finite type if and only if every sequence becomes stationary.*

*Proof.* Fix $\mathcal{M}_{\mathbb{N}^k} = \left( \left(M_g\right)_{g \in \mathbb{N}^k}, \left(\varphi_{g_1, g_2}\right)_{g_1 \preceq g_2 \in \mathbb{N}^k} \right)$. Let $H \subset \mathbb{N}^k$ be a (not necessarily finite) set framing $\mathcal{M}_{\mathbb{N}^k}$. We call $H$ *reduced* if there is no pair $h_1 \neq h_2 \in H$, such that $h_1$ is a frame of $h_2$. If $H$ is not reduced, and $h_1 \preceq h_2$ is a pair as above, it is not difficult to show that $H \setminus \{h_2\}$ is a framing set for $\mathcal{M}_{\mathbb{N}^k}$ as well. Moreover, for $G = \mathbb{N}^k$, every decreasing sequence of elements with respect to $\prec$ has a minimal element. That implies that there exists a reduced framing set for $\mathcal{M}_{\mathbb{N}^k}$.

By the previous lemma, we know that if $\mathcal{M}_{\mathbb{N}^k}$ is of finite type, every sequence becomes stationary. For the converse, if $\mathcal{M}_{\mathbb{N}^k}$ is not of finite type, we choose a reduced framing set $H \subseteq \mathbb{N}^k$, which is necessarily infinite. We will now construct a non-stationary sequence iteratively, adding two elements to the sequence in each step. Set $g_0 := e \in \mathbb{N}^k$ and $H_1 := H \setminus \{g_0\}$; during the construction, $H_i$ will always be an infinite subset of $H$. For any such set $H_i$, by Dickson's Lemma ([152], Theorem 5.1), there exists a finite subset $A_i \subset H_i$ such that for every $h \in H_i$, there exists an $a \in A_i$ with $a \preceq h$. Define $M_i(a) := \{h \in H_i \mid a \prec h\}$ for $a \in A_i$. Since $H_i$ is infinite, there exists at least one $g_{2i} \in A_i$ such that $M_i(g_{2i})$ is infinite. Since $g_{2i-2}$ is not a frame of $g_{2i}$ (because they are both in $H$), there exists some $g_{2i-1} \in \mathbb{N}^k$ such that $g_{2i-2} \prec g_{2i-1} \preceq g_{2i}$ and $\varphi_{g_{2i-2}, g_{2i-1}}$ is not an isomorphism. We set $H_{i+1} := M_i(g_{2i})$ and proceed with the next iteration. In this way, we obtain a sequence $(g_i)_{i \in \mathbb{N}}$ with $g_i \preceq g_{i+1}$ that does not become stationary. □

We remark that the equivalence is not true in general as the aforementioned counterexample over $(\mathbb{Q}_{\geq 0}, +)$ shows. In this case, a reduced framing set does not exist. Dually, the monoid $(\mathbb{N}^{\mathbb{N}}, +)$ of all sequences of natural numbers yields an example for which the equivalence is not true either, but it is always possible to obtain reduced framing sets for GAPMs indexed over $(\mathbb{N}^{\mathbb{N}}, +)$.

Let us now see that *GAPMs* of finitely presented type over $R$ are isomorphic to finitely presented graded $R[G]$-modules using the functors $\alpha$ and $\beta$. The next three lemmas generalize the corresponding statements in Section 5.2, with similar proof ideas.

**Lemma 15.** *If a GAPM* $\mathcal{M}_G = \left( \left(M_g\right)_{g \in G}, \left(\varphi_{g_1, g_2}\right)_{g_1 \preceq g_2 \in G} \right)$ *is of finitely presented type,* $\alpha\left(\mathcal{M}_G\right)$ *is finitely presented.*

*Proof.* Fix $H = \{h_1, \ldots, h_D\}$ as finite set framing $\mathcal{M}_G$. Write $\mathfrak{G}_i$ for a finite generating set of $M_{h_i}$ and $n_i := |\mathfrak{G}_i|$. Let $g \in G$ and $h_i$ be a frame of $g$. In particular, there exists some $f \in G$ such that $f \star h_i = g$, meaning that in $\alpha\left(\mathcal{M}_G\right)$, the map $f : M_{h_i} \to M_g$ is an isomorphism. Hence, the elements of $f\mathfrak{G}_i$ generate $M_g$. This shows that $\bigcup_{i=1}^{D} \mathfrak{G}_i$ generates $\alpha\left(\mathcal{M}_G\right)$.

For the second part, let $\mu_i : R^{n_i} \to M_{h_i}$ be the generating surjective map that corresponds to $\mathfrak{G}_i$ where $i \in \{1, ..., D\}$. Writing $n = \sum_{i=1}^{D} n_i$, there is a map $\mu : R[G]^n \to \alpha(\mathcal{M})$ that corresponds to the the generating set $\bigcup_{i=1}^{D} \mathfrak{G}_i$. If $\mathfrak{g}_i$ is a generator, we will use the notation $\mathfrak{e}_i$ to denote the corresponding generator of $R[G]^n$.

We now define a finite set of elements of $\ker \mu$. First of all, let $\mathfrak{Z}_i$ be the generating set of $\ker \mu_i$ for $0 \leq i \leq D$. Clearly, all elements of $\mathfrak{Z}_i$ are also in $\ker \mu$. Moreover, for $h_i \preceq h_j$ and any generator $\mathfrak{g}_i$ in $\mathfrak{G}_i$ with $\varphi_{h_i, h_j}(\mathfrak{g}_i) \neq 0$, we can write

$$\varphi_{h_i, h_j}(\mathfrak{g}_i) = \sum_{v=1}^{n_j} \lambda_v \mathfrak{g}_j^{(v)}$$

where $\lambda_v \in R$ and $\mathfrak{G}_j = \{\mathfrak{g}_j^{(1)}, \dots, \mathfrak{g}_j^{(n_j)}\}$. In that case, the corresponding element

$$f_{i,j}\mathfrak{e}_i - \sum_{v=1}^{n_j} \lambda_v \mathfrak{e}_j^{(v)}$$

is in $\ker \mu$ where $f_{i,j}$ is the unique element such that $f_{i,j} \star h_i = h_j$.

We let $\mathfrak{Z}_{i,j}$ denote the finite set obtained by picking one element as above for each $\mathfrak{g}_i$ with $\varphi_{h_i,h_j}(\mathfrak{g}_i) \neq 0$. We claim that $\mathfrak{Z} := \bigcup_{i=0}^{D} \mathfrak{Z}_i \cup \bigcup_{h_i \preceq h_j} \mathfrak{Z}_{i,j}$ generates $\ker \mu$:

Fix an element in $x \in \ker \mu$, which is of the form

$$x = \sum_{\ell} \lambda_\ell \mathfrak{e}_\ell$$

with $\lambda_\ell \in R[G]$ and $\mathfrak{e}_\ell$ a generator of $R[G]^n$. We can assume that $x$ is homogeneous of some degree $g$. First we consider the case that $g = h_j \in H$ and all $\lambda_\ell$ are of degree $e$. Then, all $\mathfrak{e}_\ell$ that appear in $x$ are of the same degree, and hence, their images under $\mu$ are generators of $M_{h_j}$. It follows that $x$ is generated by the set $\mathfrak{Z}_j$.

Next, we consider the case that $g = h_j \in H$ and some $\lambda_\ell$ is of non-trivial degree. Because $x$ is homogeneous, $\lambda_\ell$ is then of the form $r_\ell f_{\ell,j}$ for some $r_\ell \in R$ and non-trivial $f_{\ell,j} \in G$. Since the degree of $\mathfrak{e}_\ell$ is a $h_\ell$ with $f_{\ell,j} \star h_\ell = h_j$, there is an element $\mathfrak{z}_\ell$ in $\mathfrak{Z}_{\ell,j}$ of the form $\mathfrak{z}_\ell = f_{\ell,j}\mathfrak{e}_\ell - \sum_{v=1}^{n_\ell} \tilde{\lambda}_v \mathfrak{e}_j^{(v)}$ with all $\mathfrak{e}_j^{(v)}$ of degree $h_j$ and each $\tilde{\lambda}_v \in R$. Then, by turning from $x$ to $x - r_\ell \mathfrak{z}_\ell$, we turn the coefficient of $\mathfrak{e}_\ell$ into 0 and we only introduce summands with coefficients of degree $e$ in any non-trivial $g \in G$. Iterating this construction for each summand with coefficient of positive degree, we get an element $x' = x - \sum_w r_w \mathfrak{z}_w$ with $r_w \in R$ and $\mathfrak{z}_w$ elements of $\mathfrak{Z}$, and $x'$ only having coefficients of degree $e$ in any non-trivial $g \in G$. By the first part, $x'$ is generated by $\mathfrak{Z}$, hence so is $x$.

Finally, let $g \notin H$. Then, there exists some $h_i \in H$ and some $f \in G$ such that $f \star h_i = g$ and multiplication with $f$ yields an isomorphism $M_{h_i} \to M_g$. Hence, we have that $x = fx'$ with $x'$ homogeneous of degree $h_i$. Since $0 = \mu(x) = f\mu(x')$, it follows that $x' \in \ker \mu$. By the above cases, $x'$ is generated by $\mathfrak{Z}$, and hence, so is $x$. □

For the next two lemmas, we fix a finitely presented graded $R[G]$-module $\mathbf{M} := \oplus_{g \in G} M_g$ with a map

$$R[G]^n \xrightarrow{\mu} \mathbf{M}$$

such that $\ker \mu$ is finitely generated. Moreover, we let $\mathfrak{G} := \{\mathfrak{g}^{(1)}, \ldots, \mathfrak{g}^{(n)}\}$ denote generators of $\mathbf{M}$ and $\mathfrak{Z} := \{\mathfrak{z}^{(1)}, \ldots, \mathfrak{z}^{(m)}\}$ denote a generating set of $\ker \mu$. We assume that each $\mathfrak{g}^{(i)}$ and each $\mathfrak{z}^{(j)}$ is homogeneous (with respect to the grading of the corresponding module), and we let $\deg(\mathfrak{g}^{(i)})$, $\deg(\mathfrak{z}^{(j)})$ denote the degrees.

**Lemma 16.** *Each $M_g$ is finitely presented as an $R$-module.*

*Proof.* We argue first that $M_g$ is finitely generated. Let $n_g$ denote the number of elements $\mathfrak{g}^{(j)}$ in $\mathfrak{G}$ such that $\deg(\mathfrak{g}^{(j)}) \preceq g$. Let $h_j \in G$ such that $h_j \star \deg(\mathfrak{g}^{(j)}) = g$. Define the map $\mu_g : R^{n_g} \to M_g$, by mapping the $j$th generator $\mathfrak{e}_g^{(j)}$ of $R^{n_g}$ to the element $h_j \mathfrak{g}^{(j)}$. Then the map $\mu_g$ is surjective, proving that $M_i$ is finitely generated.

We show that $\ker \mu_g$ is finitely generated as well. Let $\mathfrak{e}^{(1)}, \ldots, \mathfrak{e}^{(n)}$ be the generators of $R[G]^n$ mapping to $\mathfrak{g}^{(1)}, \ldots, \mathfrak{g}^{(n)}$ under $\mu$. Let $m_g$ denote the number of elements in $\mathfrak{Z}$ such that $\deg(\mathfrak{z}^{(j)}) \preceq g$. Let $h'_j \in G$ such that $h'_j \star \deg(\mathfrak{z}^{(j)}) = g$. For every $\mathfrak{z}^{(j)}$ with $1 \leq j \leq m_g$, consider $h'_j \mathfrak{z}^{(j)}$, which can be written as

$$h'_j \mathfrak{z}^{(j)} = \sum_{k=1}^{n_g} r_k h_k \mathfrak{e}^{(k)}$$

with $r^{(k)} \in R$. Now, define

$$\mathfrak{z}_g^{(j)} := \sum_{k=1}^{n_g} r_k \mathfrak{e}_g^{(k)}$$

and $\mathfrak{Z}_g := \{\mathfrak{z}_g^{(j)} \mid 1 \leq i \leq m_g\}$. We claim that $\mathfrak{Z}_g$ generates $\ker \mu_g$. First of all, we get $\mu_g(\mathfrak{z}_g^{(j)}) = \mu(\mathfrak{z}^{(j)}) = 0$. Now fix $x \in \ker \mu_g$ arbitrarily. Then, $x$ is a linear combination of elements in $\{\mathfrak{e}_g^{(1)}, \ldots, \mathfrak{e}_g^{(n_g)}\}$ with coefficients in $R$.

Replacing $\mathfrak{e}_g^{(j)}$ with $h_j\mathfrak{e}^{(j)}$, we obtain $x' \in R[G]^n$ homogeneous of degree $g$. By assumption, we can write $x'$ as linear combination of elements in $\mathfrak{Z}$, that is,

$$x' = \sum_{k=1}^{m_g} r'_k h'_k \mathfrak{z}^{(k)}$$

with $r'_k \in R$. Then, it holds that

$$x = \sum_{k=1}^{m_g} r'_k \mathfrak{z}_g^{(k)},$$

which follows by comparing coefficients: let $j \in \{1, \dots, n_g\}$ and let $c_j \in R$ be the coefficient of $\mathfrak{e}_g^{(j)}$ in $x$. Let $c'_j$ be the coefficient of $\mathfrak{e}_g^{(j)}$ in the sum $\sum_{k=1}^{m_g} r'_k \mathfrak{z}_g^{(k)}$, expanding each $\mathfrak{z}_g^{(k)}$ by its linear combination as above. By construction, $c_j$ is the coefficient of $h_k\mathfrak{e}^{(j)}$ in $x'$, and $c'_j$ is the coefficient of $h_k\mathfrak{e}^{(j)}$ in the sum $\sum_{k=1}^{m_i} r'_k h'_k \mathfrak{z}^{(k)}$. Since this sum equals $x'$, it follows that $c_j = c'_j$. Since $x$ was chosen arbitrarily from $\ker \mu_g$, it follows that $\mathfrak{Z}_g$ generates the kernel. □

**Lemma 17.** *$\beta(\mathbf{M})$ is of finite type. In particular, it is of finitely presented type with Lemma 16.*

*Proof.* Define

$$D := \left\{ \deg(\mathfrak{g}^{(j)}) \mid 1 \le j \le n \right\} \cup \left\{ \deg(\mathfrak{z}^{(k)}) 1 \le k \le m \right\}.$$

For every subset $D'$ of $D$, let $plcm(D')$ denote the set of partially least common multiples of $D'$. Then, set

$$H := \bigcup_{D' \subseteq D} plcm(D').$$

Note that $e \in H$ (using $D' = \emptyset$) and $D \subset H$ (when $D'$ ranges over the singleton sets). Also, $H$ is finite because $D$ is finite and $G$ is weak plcm.

We claim that $H$ frames $\beta(\mathbf{M})$. Let $g \in G$ be arbitrary. We have to find an element $h \in H$ such that $h \preceq g$ and for all $h \preceq \tilde{g} \preceq g$ with $\tilde{f} \star h = \tilde{g}$, multiplication with $\tilde{f}$ is an isomorphism $M_h \to M_{\tilde{g}}$.

If $g \in H$, that claim is trivial using $h := g$ and $\tilde{f} := e$. So, let us assume that $g \notin H$. Let $D'(g) := \{\ell \in D \mid \ell \preceq g\}$. Then, $g$ is a common multiple of $D'(g)$. However, it is not a partially least common multiple because in that case, it would belong to $H$. Hence, there exists a plcm $h$ of $D'(g)$ such that $h \preceq g$. Note also that $D'(g) = D'(h)$ in this case. Let $h \preceq \tilde{g} \preceq g$ and $\tilde{f}$ be such that $\tilde{f} \star h = \tilde{g}$.

We first show that multiplication by $\tilde{f}$ is surjective. For that, fix some $x \in M_{\tilde{g}}$. Then $x$ is generated by a linear combination of the generators $\mathfrak{g}^{(j)}$, and among those, only those in $D'(\tilde{g}) = D'(g)$ can have non-zero coefficients. Hence, $x$ takes the form

$$x = \sum_{j \in \{1,\dots,n\}, \deg(\mathfrak{g}^{(j)}) \in D'(g)} f_j r_j \mathfrak{g}^{(j)}$$

with $r_j \in R$ and $f_j \in G$ such that $f_j \star \deg(\mathfrak{g}^{(j)}) = \tilde{g}$. Let $f'_j$ be such that $f'_j \star \deg(\mathfrak{g}^{(j)}) = h$. Then, using $\tilde{f}$ from above,

$$\tilde{f} \star f'_j \star \deg(\mathfrak{g}^{(j)}) = \tilde{g} = f_j \star \deg(\mathfrak{g}^{(j)}),$$

which implies that $\tilde{f} \star f'_j = f_j$ because $G$ is right-cancellative. Hence we can write

$$\begin{aligned} x &= \sum_{j \in \{1,\dots,n\}, \deg(\mathfrak{g}^{(j)}) \in D'(g)} (\tilde{f} \star f'_j) r_j \mathfrak{g}^{(j)} \\ &= \tilde{f} \sum_{j \in \{1,\dots,n\}, \deg(\mathfrak{g}^{(j)}) \in D'(g)} f'_j r_j \mathfrak{g}^{(j)}, \end{aligned}$$

which shows that $x$ has a preimage in $M_h$.

For the injectivity of multiplication with $\tilde{f}$, let $y \in M_h$ such that $\tilde{f}y = 0$. Let $x \in R[G]^n$ such that $\mu(x) = y$. Then $\mu(\tilde{f}x) = \tilde{f}y = 0$ and hence, $\tilde{f}x$ is generated by the $\mathfrak{z}^{(k)}$. Similar as in the first part of the proof, only such $\mathfrak{z}^{(k)}$ can appear whose degree lies in $D'(g)$. Hence, writing

$$\tilde{f}x = \sum_{k \in \{1,\dots,m\}, \deg(\mathfrak{z}^{(k)}) \in D'(g)} f_k r_k \mathfrak{z}^{(k)},$$

we know that $f_k \star \deg(\mathfrak{z}^{(k)}) = \tilde{g}$. The same way as in the first part of the proof, we get that $f_k = \tilde{f} \star f'_k$ with some $f'_k \in G$. It follows that

$$\tilde{f}x = \tilde{f} \sum_{k\in\{1,\dots,m\},\deg(\mathfrak{z}^{(k)})\in D'(g)} f'_k r_k \mathfrak{z}^{(k)}.$$

Since $G$ is left-cancellative, $R[G]$ is left-cancellative with respect to multiplication by any monoid element. This property carries over to the free module $R[G]^n$ and it follows that

$$x = \sum_{k\in\{1,\dots,m\},\deg(\mathfrak{z}^{(k)})\in D'(g)} f'_k r_k \mathfrak{z}^{(k)}.$$

Thus $x$ can be written as linear combination of the $\mathfrak{z}^{(k)}$, proving that $y = \mu(x) = 0$. □

The Generalized Representation Theorem. The preceding lemmas imply the Generalized Representation Theorem:

**Theorem 10.** *Let $R$ be a ring with unity. The category of finitely presented graded $R[G]$-modules is isomorphic to the category of generalized algebraic persistence modules over $R$ of finitely presented type.*

*Proof.* The categories are subcategories of R[$G$]-**Gr-Mod** and R-**Persmod**$^G$, respectively. Since $\alpha$ and $\beta$, restricted to these subcategories, map a $GAPM$ of finitely presented type to a finitely presented graded $R[G]$-module (Lemma 15) and vice versa (Lemma 16 and Lemma 17), these categories are isomorphic. □

Clearly, this statement contains Theorem 9 using $G := \mathbb{N}$.

As in Theorem 9, replacing "finitely presented" with "finitely generated" invalidates the claim. Passing to a Noetherian ring $R$, however, does not immediately revalidate it, because $R[G]$ is not Noetherian in general. Still, the following statement follows easily:

**Corollary 2.** *If $R$ and $R[G]$ are Noetherian rings with unity, the category of finitely generated graded $R[G]$-modules is isomorphic to the category of discrete algebraic persistence modules of finitely generated type.*

We remark that Hilbert's Basis Theorem can be applied iteratively (see [163], 15.1). Using $R\left[\mathbb{N}^k\right] \cong R\left[t_1, ..., t_k\right] \cong R\left[t_1, ..., t_{k-1}\right]\left[t_k\right]$, we obtain

**Corollary 3.** *Let $R$ be a commutative Noetherian ring with unity, $k \in \mathbb{N}$. The category of finitely generated graded $R\left[\mathbb{N}^k\right]$-modules is isomorphic to the category of algebraic persistence modules over $\mathbb{N}^k$ of finitely generated type.*

## 5.6 Conclusion and future work

The Representation Theorem for persistence modules is one of the landmark results in the theory of persistent homology. In this paper, we formulated a more precise statement of this classical theorem over arbitrary rings with unity where we replaced finite generation with finite presentation. We provided a proof which only relies on elementary module theory. Furthermore, we generalized the Representation Theorem from naturally indexed modules to modules indexed over a more general class of monoids. The key difficulty was to find the right finiteness condition for persistence modules in this case to certify the equivalence with finitely presented modules graded over the monoid. Since the underlying ring does not have to be commutative, the Representation Theorem should rather be considered as a statement on general persistence, including the case of persistent homology.

Alternatively, in categorical language, persistence modules over $\mathbb{N}$ are functors $\mathbb{N} \to R$-**Mod** where $\mathbb{N}$ is interpreted as the totally ordered set $(\mathbb{N}, \leq)$. For the Representation Theorem we used that $\mathbb{N}$ is a monoid and endowed the functor $\mathbb{N} \to R$-**Mod** with an algebraic structure $R[t]$. We showed that the generalization of this situation is replacing $\mathbb{N}$ with a poset $(G, \preceq)$ that is induced by left-factorization in a good monoid $(G, \star)$. Moreover, we defined the subcategory of finite-type-functors $G \to R$-**Mod** precisely. The concept of frames enables us to locate the persistent features in the monoid.

An obvious question is how the finiteness condition changes when the requirements on the monoid are further relaxed. The anti-symmetry of the monoid is not a severe assumption because elements $g_1, g_2$ with $g_1 \preceq g_2$ and $g_2 \preceq g_1$ induce isomorphic connecting maps in the corresponding $GAPM$ and therefore can be treated as one component of the monoid. Also, we can relax the right-cancellative condition such that between any two elements $g_1, g_2 \in G$, there are at most finitely many $h$ such that $h \star g_1 = g_2$. We restricted to good monoids for clarity of exposition. If applications occur that require filtrations with some complicated ordering structure, we suggest to consider a good monoid as underlying index set.

A next step is to find classification results, parameterizations and discrete invariants for finitely presented monoid-graded modules. It might be useful to consider a subclass of good monoids, e.g., finitely generated good monoids or monoids with a manageable factorization theory. The theory of persistence modules is well-studied in the case of $\mathbb{N}^k$ and might be transferred to more general monoids, as much as the situation of discrete invariants. Since there is no natural notion of barcodes in the case of $\mathbb{N}^k$, there is also no hope of finding barcodes for more general monoids. But it might be possible to generalize a discrete invariant from $\mathbb{N}^k$, for instance the discrete rank invariant, and generalize algorithms to $G$-indexed persistence.

Another next step is to understand persistence over finite posets or directed acyclic graphs as $GAPM$-persistence. To do this, efficient order embeddings into a suitable good monoid have to be constructed. Using the order dimension $\dim_P$ of a poset $P$, this can be done into $\mathbb{R}^{\dim_P}$. Such an embedding, however, can induce a large number of unnecessary least common multiples, and the dimension might be quite large. Therefore, the representation theory of the underlying monoid might be much more complicated than the representation theory of $P$. Our approach gives a larger variety of good monoids with potentially better properties. For an example of such a construction, see Figure 5.4. It would be interesting to understand if a poset induces a good monoid that has no unnecessary least common multiples and has a low number of generators.

# 6 Paper 3: A Kernel for Multiparameter Persistence

This is joint work with Ulderico Fugacci, Michael Kerber, Claudia Landi, and Bei Wang. The journal version of this paper is [60]. We slightly rephrase the original paper and give some further details.

Abstract. Topological data analysis and its main method, persistent homology, provide a toolkit for computing topological information of high-dimensional and noisy data sets. Kernels for one-parameter persistent homology have been established to connect persistent homology with machine learning techniques with applicability on shape analysis, recognition and classification. We contribute a kernel construction for multiparameter persistence by integrating a one-parameter kernel weighted along straight lines. We prove that our kernel is stable and efficiently computable, which establishes a theoretical connection between topological data analysis and machine learning for multivariate data analysis.

## 6.1 Introduction

TDA extracts a rich set of topological features from high-dimensional and noisy data sets that complement geometric and statistical features, which offers a different perspective for machine learning. The question is, *how can we establish and enrich the theoretical connections between TDA and machine learning*?

Interfacing persistence diagrams directly with machine learning poses technical difficulties, because persistence diagrams contain point sets in the plane that do not have the structure of an inner product, which allows length and angle to be measured. In other words, such diagrams lack a Hilbert space structure for kernel-based learning methods such as kernel SVMs or PCAs [150]. Recent work proposes several variants of *feature maps* [34, 121, 123, 150] that transform persistence diagrams into $L^2$-functions over $\mathbb{R}^2$. This idea immediately enables the application of topological features for kernel-based machine learning methods as establishing a kernel function implicitly defines a Hilbert space structure [150].

A serious limit of standard persistent homology and its initial interfacing with machine learning [34, 110, 121, 123, 150] is the restriction to only a single scale parameter, thereby confining its applicability to the univariate setting. However, in many real-world applications, such as data acquisition and geometric modeling, we often encounter richer information described by multivariate data sets [42, 43, 51]. Consider, for example, climate simulations where multiple physical parameters such as temperature and pressure are computed simultaneously; and we are interested in understanding the interplay between these parameters. Consider another example in multivariate shape analysis, various families of functions carry information about the geometry of 3D shape objects, such as mesh density, eccentricity [156] or Heat Kernel Signature [159]; and we are interested in creating multivariate signatures of shapes from such functions. Unlike the univariate setting, very few topological tools exist for the study of multivariate data [80, 83, 156], let alone the integration of multivariate topological features with machine learning.

The active area of *multiparameter persistent homology* [43] studies the extension of persistence to two or more (independent) scale parameters. A complete

discrete invariant such as the persistence diagram does not exist for more than one parameter [43]. To gain partial information, it is common to study *slices*, that is, one-dimensional affine subspaces where all parameters are connected by a linear equation. In this paper, we establish, for the first time, a theoretical connection between topological features and machine learning algorithms via the kernel approach for multiparameter persistent homology. Such a theoretical underpinning is necessary for applications in multivariate data analysis.

Contributions. We propose the first kernel construction for multiparameter persistent homology. Our kernel is *generic*, *stable* and can be *approximated in polynomial time*. For simplicity, we formulate all our results for the case of two parameters, although they extend to more than two parameters.

Our input is a data set that is filtered according to two scale parameters and has a finite description size; a *simplicial bifiltration*, which we will refer to as bifiltration for simplicity. Our main contribution is the definition of a feature map that assigns to a bifiltration $\mathcal{X}$ a function $\Phi_{\mathcal{X}} : \Delta^{(2)} \to \mathbb{R}$, where $\Delta^{(2)}$ is a subset of $\mathbb{R}^4$. Moreover, $\Phi^2_{\mathcal{X}}$ is integrable over $\Delta^{(2)}$, effectively including the space of bifiltrations into the Hilbert space $L^2(\Delta^{(2)})$. Therefore, based on the standard scalar product in $L^2(\Delta^{(2)})$, a 2-parameter kernel is defined such that for two given bifiltrations $\mathcal{X}$ and $\mathcal{Y}$ we have

$$\langle \mathcal{X}, \mathcal{Y} \rangle_{\Phi} := \int_{\Delta^{(2)}} \Phi_{\mathcal{X}} \Phi_{\mathcal{Y}} d\mu. \tag{6.1}$$

We construct our feature map by interpreting a point of $\Delta^{(2)}$ as a pair of (distinct) points in $\mathbb{R}^2$ that define a unique slice. Along this slice, the data simplifies to a monofiltration, and we can choose among a large class of feature maps and kernel constructions of standard, one-parameter persistence. To make the feature map well-defined, we restrict our attention to a finite rectangle $R$.

Our inclusion into a Hilbert space induces a distance between bifiltrations as

$$d_{\Phi}(\mathcal{X}, \mathcal{Y}) := \sqrt{\int (\Phi_{\mathcal{X}} - \Phi_{\mathcal{Y}})^2 d\mu}. \tag{6.2}$$

We prove a stability bound, relating this distance measure to the matching distance and the interleaving distance (see the paragraph on related work below). We also show that this stability bound is tight up to constant factors (see Section 6.4).

Finally, we prove that our kernel construction admits an efficient approximation scheme. Fixing an absolute error bound $\epsilon$, we give a polynomial time algorithm in $1/\epsilon$ and the size of the bifiltrations $\mathcal{X}$ and $\mathcal{Y}$ to compute a value $r$ such that $r \leq \langle \mathcal{X}, \mathcal{Y} \rangle_\Phi \leq r + \epsilon$. On a high level, the algorithm subdivides the domain into boxes of smaller and smaller width and evaluates the integral of (6.1) by lower and upper sums within each subdomain, terminating the process when the desired accuracy has been achieved. The technical difficulty lies in the accurate and certifiable approximation of the variation of the feature map when moving the argument within a subdomain.

Related work. Our approach heavily relies on the construction of stable and efficiently computable feature maps for monofiltrations. This line of research was started by Reininghaus et al. [150], whose approach we sketch in Section 6.2. Alternative kernel constructions appeared in [45, 121]. Kernel constructions fit into the general framework of including the space of persistence diagrams in a larger space with more favorable properties. Other examples of this idea are persistent landscapes [34] and persistent images [2], which can be interpreted as kernel constructions as well. Kernels and related variants defined on monofiltrations have been used to discriminate and classify shapes and surfaces [110, 150]. An alternative approach comes from the definition of suitable (polynomial) functions on persistence diagrams to arrive at a fixed-dimensional vector in $\mathbb{R}^d$ on which machine learning tasks can be performed; see [4, 5, 72, 113].

As previously mentioned, a persistence diagram for multiparameter persistence does not exist [43]. However, bifiltrations still admit meaningful distance measures, which lead to the notion of closeness of two bifiltrations. The most prominent such distance is the *interleaving distance* [131], which, however, has recently been proved to be NP-complete to compute and approximate [22]. Computationally attractive alternatives are (multiparameter) bottleneck distance [69] and the *matching distance* [18, 117], which compares the persistence diagrams along all slices (appropriately weighted) and picks

the worst discrepancy as the distance of the bifiltrations. This distance can be approximated up to a precision $\epsilon$ using an appropriate subsample of the lines [18], and also computed exactly in polynomial time [117]. Our approach extends these works in the sense that not just a distance, but an inner product on bifiltrations, is defined with our inclusion into a Hilbert space. In a similar spirit, the software library RIVET [130, 131] provides a visualization tool to explore bifiltrations by scanning through the slices.

## 6.2 Feature maps for persistence

A class of feature maps for persistence. In this paper, we look at the class of all feature maps that assign to a simplicial monofiltration $\mathcal{X}$ a function in $L^2(\Delta^{(1)})$. Recall that $\Delta^{(1)} := \{(x_1, x_2) \in \mathbb{R}^2 \mid x_1 < x_2\}$. For such a feature map $\phi_{\mathcal{X}}$, we define the following properties:

- *Absolutely boundedness.* There exists a constant $v_1 > 0$ such that, for any monofiltration $\mathcal{X}$ of size $n$ and any $x \in \Delta^{(1)}$, $0 \leq \phi_{\mathcal{X}}(x) \leq v_1 \cdot n$.
- *Lipschitzianity.* There exists a constant $v_2 > 0$ such that, for any monofiltration $\mathcal{X}$ of size $n$ and any $x, x' \in \Delta^{(1)}$, $|\phi_{\mathcal{X}}(x) - \phi_{\mathcal{X}}(x')| \leq v_2 \cdot n \cdot \|x - x'\|_2$.
- *Internal stability.* There exists a constant $v_3 > 0$ such that, for any pair of monofiltrations $\mathcal{X}, \mathcal{Y}$ of size $n$ and any $x \in \Delta^{(1)}$, $|\phi_{\mathcal{X}}(x) - \phi_{\mathcal{Y}}(x)| \leq v_3 \cdot n \cdot d_B(\mathcal{X}, \mathcal{Y})$.
- *Efficiency.* For any $x \in \Delta^{(1)}$, $\phi_{\mathcal{X}}(x)$ can be computed in polynomial time in the size of $\mathcal{X}$, that is, in $O(n^k)$ for some $k \geq 0$.

An example. We focus on one example: the *persistence scale-space kernel* [150]. In the corresponding feature map, all peaks are of the same height. To make the construction robust against perturbations, the function has to be equal to 0 across the diagonal. This is achieved by adding negative Gaussian peaks at the reflections of the off-diagonal points along the diagonal. Writing $\bar{z}$ for the reflection of a point $z$, we obtain the formula

$$\phi_{\mathcal{X}}(x) := \frac{1}{4\pi t} \sum_{z \in D(\mathcal{X})} e^{\frac{\|x-z\|_2^2}{4t}} - e^{\frac{\|x-\bar{z}\|_2^2}{4t}}, \tag{6.3}$$

where $t$ is the width of the Gaussian, which is a free parameter of the construction.

A linearized version of the above kernel would still be an element of our class of feature maps. By linearized, we mean that the Gaussian peaks are replaced by linear peaks.

## 6.3 Feature maps for multiparameter persistence

Let $\phi$ be a feature map (such as the scale-space kernel) that assigns to a monofiltration a function in $L^2(\Delta^{(1)})$. Starting from $\phi$, we construct a feature map $\Phi$ on the set of all bifiltrations $\Omega$ that has values in a Hilbert space.

The feature map $\Phi$ assigns to a bifiltration $\mathcal{X}$ a function $\Phi_{\mathcal{X}} : \Delta^{(2)} \to \mathbb{R}$. We set

$$\Delta^{(2)} := \left\{ (p, q) \mid p \in \mathbb{R}^2, q \in \mathbb{R}^2, p < q \right\}$$

as the set of all pairs of points where the first point is smaller than the second one. $\Delta^{(2)}$ can be interpreted naturally as a subset of $\mathbb{R}^4$, but we will usually consider elements of $\Delta^{(2)}$ as pairs of points in $\mathbb{R}^2$.

Fixing $(p, q) \in \Delta^{(2)}$, let $\ell$ denote the unique slice through these two points. Along this slice, the bifiltration gives rise to a monofiltration $\mathcal{X}_\ell$, and consequently a function $\phi_{\mathcal{X}_\ell} : \Delta^{(1)} \to \mathbb{R}$ using the considered feature map for monofiltrations. Moreover, using the parameterization of the slice $\ell$ as $b + \lambda \cdot a$, there exist real values $\lambda_p, \lambda_q$ such that $b + \lambda_p a = p$ and $b + \lambda_q a = q$. Since $p < q$ and $\lambda_p < \lambda_q$, hence $(\lambda_p, \lambda_q) \in \Delta^{(1)}$. We define $\Phi_{\mathcal{X}}(p, q)$ to be the weighted function value of $\phi_{\mathcal{X}_\ell}$ at $(\lambda_p, \lambda_q)$ (see also Figure 6.1), that is,

$$\Phi_{\mathcal{X}}(p, q) := w(p, q) \cdot \phi_{\mathcal{X}_\ell}(\lambda_p, \lambda_q), \tag{6.4}$$

where $w(p, q)$ is a weight function $w : \Delta^{(2)} \to \mathbb{R}$ defined below.

The weight function $w$ has two components. First, let $R$ be a bounded axis-aligned rectangle in $\mathbb{R}^2$; its bottom-left corner coincides with the origin of the

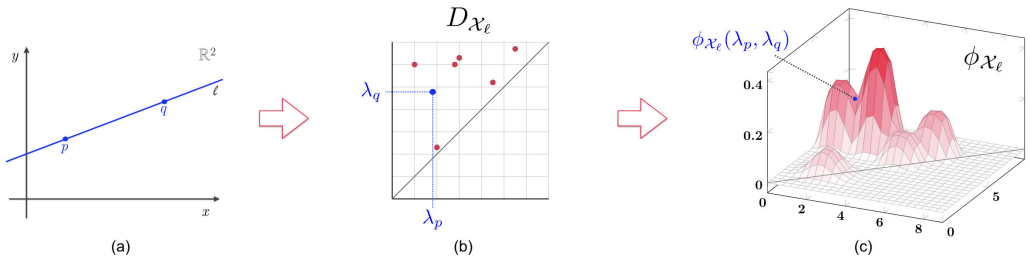


Figure 6.1: An illustration of the construction of a feature map for multiparameter persistence. (a) Given a bifiltration $\mathcal{X}$ and a point $(p, q) \in \Delta^{(2)}$, the line $\ell$ passing through them is depicted and the parameter $\lambda_p$ and $\lambda_q$ computed. (b) The point $(\lambda_p, \lambda_q)$ is embedded in the persistence diagram of the monofiltration $\mathcal{X}_\ell$ obtained as the slice of $\mathcal{X}$ along $\ell$. (c) The point $(\lambda_p, \lambda_q)$ is assigned the value $\phi_{\mathcal{X}_\ell}(\lambda_p, \lambda_q)$ via the feature map $\phi$.

coordinate axes. We define $w$ such that its weight is 0 if $p$ or $q$ is outside of $R$. Second, for pairs of points within $R \times R$, we assign a weight depending on the slope of the induced slices. Formally, let $\ell$ be parameterized as $b + \lambda \cdot a$ as above, and recall that $a$ is a unit vector with non-negative coordinates. Write $a = (a_1, a_2)$ and set $\hat{\ell} := \min\{a_1, a_2\}$. Then, we define

$$w(p, q) := \chi_R(p) \cdot \chi_R(q) \cdot \hat{\ell},$$

where $\chi_R$ is the characteristic function of $R$, mapping a point $x$ to 1 if $x \in R$ and 0 otherwise.

The factor $\hat{\ell}$ ensures that slices that are close to being horizontal or vertical attain less importance in the feature map. The same weight is assigned to slices in the matching distance [18]. $\hat{\ell}$ is not important for obtaining an $L^2$-function, but its meaning will become clear in the stability results of Section 6.4. We also remark that the largest weight is attained for the diagonal slice with a value of $1/\sqrt{2}$. Consequently, $w$ is a non-negative function upper bounded by $1/\sqrt{2}$.

To summarize, our map $\Phi$ depends on the choice of an axis-aligned rectangle $R$ and a choice of feature map for monofiltrations, which itself might have associated parameters. For instance, using the scale-space feature map requires the choice of the width $t$ (see (6.3)). It is only left to argue that the image of the feature map $\Phi$ is indeed an $L^2$-function.

**Theorem 11.** *If $\phi$ is absolutely bounded, then $\Phi_{\mathcal{X}}$ is in $L^2(\Delta^{(2)})$.*

*Proof.* Let $\mathcal{X}$ be a bifiltration of size $n$. As mentioned earlier, each slice $\mathcal{X}_\ell$ is of a size at most $n$. By absolute boundedness and the fact that the weight function is upper bounded by $\frac{1}{\sqrt{2}}$, it follows that $|\Phi_{\mathcal{X}}(p,q)| \leq \frac{v_1 n}{\sqrt{2}}$ for all $(p,q)$. Since the support of $\Phi_{\mathcal{X}}$ is compact ($R \times R$), the integral of $\Phi^2_{\mathcal{X}}$ over $\Delta^{(2)}$ is finite, being absolutely bounded and compactly supported. □

Generalizations. The construction of our feature map can be generalized in several directions: a more general class of weight functions is possible, the number of parameters is arbitrary, and a definition on the level of multiparameter persistence modules instead of simplicial multifiltrations is possible.

We argued why we think that our definition of the *weight function* $w$ is the most reasonable thing to do. In principle, however, one can define the weight function to be an arbitrary square-integrable function on $\Delta^{(2)}$, possibly even without restricting to a rectangle $R$. In this generality, we get

$$\begin{aligned} & \int_{\Delta^{(2)}} |\Phi_{\mathcal{X}}|^2 \, d\mu \\ = & \int_{\Delta^{(2)}} \left| w(p,q) \cdot \phi_{\mathcal{X}_\ell}(\lambda_p, \lambda_q) \right|^2 d\mu \\ \leq & \ (v_1 n)^2 \int_{\Delta^{(2)}} |w(p,q)|^2 \, d\mu < \infty, \end{aligned}$$

writing $\mu$ for the Lebesgue measure. This yields a version of Theorem 11 and thus the well-definedness of the generalized version of the feature map. Therefore, one may choose different weight functions in experimental cases. For instance, one could put a weight on the distance to $0 \in \mathbb{R}^2$.

Importantly, the construction readily generalizes to an *arbitrary number of parameters*. Generalizing $\Delta^{(2)}$ to $\Delta^{(k)}$, the feature map is defined completely analogously. Note that the standard weight $w$ is upper bounded by $1/\sqrt{k}$ instead of $1/\sqrt{2}$ as for $k = 2$.

Our feature map can also be defined on the level of *multiparameter persistence modules* instead of simplicial multifiltrations. We only have to ensure that the number of points in the persistence diagram of each slice is globally bounded, say, by $m$. This holds in particular if the multiparameter persistence module is finitely presented. In the class of feature maps in Section 6.2, we have to replace the size $n$ of a monofiltration with our global bound $m$, and the Bottleneck distance between filtrations with the Bottleneck distance between persistence modules. Consequently, we can also define the feature map on general multifiltrations that induce such multiparameter persistence modules.

## 6.4 Stability

An important and desirable property for a kernel for multiparameter persistence is its stability. In general, stability means that small perturbations in the input data imply small perturbations in the output data. In our setting, small changes between multifiltrations (with respect to matching distance) should not induce large changes in their corresponding feature maps (with respect to $L^2$ distance).

Adopted to our notation, the matching distance is defined as

$$d_{match}(\mathcal{X}, \mathcal{Y}) = \sup_{\ell \in \mathcal{L}} \left( \hat{\ell} \cdot d_B(\mathcal{X}_\ell, \mathcal{Y}_\ell) \right),$$

where $\mathcal{L}$ is the set of non-vertical lines with positive slope [19].

**Theorem 12.** *Let $\mathcal{X}$ and $\mathcal{Y}$ be two bifiltrations. If $\phi$ is absolutely bounded and internally stable, we have*

$$\|\Phi_{\mathcal{X}} - \Phi_{\mathcal{Y}}\|_{L^2} \leq C \cdot n \cdot \text{area}(R) \cdot d_{match}(\mathcal{X}, \mathcal{Y}),$$

*for some constant $C$.*

*Proof.* Absolute boundedness ensures that the left-hand side is well-defined by Theorem 11. Now we use the definition of $\|\cdot\|_{L^2}$ and the internal stability of $\phi$ to obtain

$$\begin{aligned}
&\|\Phi_{\mathcal{X}} - \Phi_{\mathcal{Y}}\|_{L^2}^2 \\
= &\int_{\Delta^{(2)}} \left| w(p,q)\cdot \phi_{\mathcal{X}_\ell}(\lambda_p,\lambda_q) - w(p,q)\cdot \phi_{\mathcal{Y}_\ell}(\lambda_p,\lambda_q)\right|^2 d\mu \\
\leq &\int_{\Delta^{(2)}} (w(p,q)\cdot v_3 \cdot n \cdot d_B(\mathcal{X}_\ell,\mathcal{Y}_\ell))^2\, d\mu \\
= &(v_3\cdot n)^2 \int_{\Delta^{(2)}} (w(p,q)\cdot d_B(\mathcal{X}_\ell,\mathcal{Y}_\ell))^2 d\mu.
\end{aligned}$$

Since $w(p,q)$ is zero outside $R\times R$, the integral does not change when restricted to $\Delta^{(2)}\cap(R\times R)$. Within this set, $w(p,q)$ simplifies to $\hat{\ell}$, with $\ell$ the line through $p$ and $q$. Hence, we can further bound

$$\begin{aligned}
= &(v_3\cdot n)^2 \int_{\Delta^{(2)}\cap(R\times R)} (\hat{\ell}\cdot d_B(\mathcal{X}_\ell,\mathcal{Y}_\ell))^2 d\mu \\
\leq &(v_3\cdot n)^2 \int_{\Delta^{(2)}\cap(R\times R)} \underbrace{\sup_{\ell\in\hat{\ell}} \left(\hat{\ell}\cdot d_B(\mathcal{X}_\ell,\mathcal{Y}_\ell)\right)}_{=d_{match}(\mathcal{X},\mathcal{Y})}{}^2 d\mu \\
= &(v_3\cdot n\cdot d_{match}(\mathcal{X},\mathcal{Y}))^2 \int_{\Delta^{(2)}\cap(R\times R)} 1 d\mu.
\end{aligned}$$

The claimed inequality follows by noting that the final integral is equal to $\frac{1}{4}\text{area}(R)^2$. □

As a corollary, we get the the same stability statement with respect to interleaving distance instead of matching distance [125]. Furthermore, we obtain a stability bound for sublevel set bifiltrations of functions $X\to\mathbb{R}^2$ [19]:

**Corollary 4.** *Let $F,G: X\to\mathbb{R}^2$ be two functions that give rise to sublevel set bifiltrations $\mathcal{X}$ and $\mathcal{Y}$, respectively. If $\phi$ is absolutely bounded and internally stable, we have*

$$\|\Phi_{\mathcal{X}} - \Phi_{\mathcal{Y}}\|_{L^2} \leq C\cdot n\cdot \text{area}(R)\cdot \|F-G\|_\infty,$$

*for some constant $C$.*

We remark that the appearance of $n$ in the stability bound is not desirable as the bound worsens when the complex size increases (unlike, for instance, the bottleneck stability bound in (3.2), which is independent of $n$). The factor of $n$ comes from the internal stability property of $\phi$, so we have to strengthen this condition on $\phi$. However, we show that such an improvement is impossible for a large class of "reasonable" feature maps.

For two bifiltrations $\mathcal{X}, \mathcal{Y}$ we define $\mathcal{X} \oplus \mathcal{Y}$ by setting $(\mathcal{X} \oplus \mathcal{Y})(p) := \mathcal{X}(p) \sqcup \mathcal{Y}(p)$ for all $p \in \mathbb{R}^2$. A feature map $\Phi$ is *additive* if $\Phi_{\mathcal{X} \oplus \mathcal{Y}} = \Phi(\mathcal{X}) + \Phi(\mathcal{Y})$ for all bifiltrations $\mathcal{X}, \mathcal{Y}$. $\Phi$ is called *non-trivial* if there is a bifiltration $\mathcal{X}$ such that $\|\Phi\|_{L^2} \neq 0$. Additivity and non-triviality for feature maps $\phi$ on monofiltrations is defined in the analogous way. Note that, for instance, the scale space feature map is additive. Moreover, because $(\mathcal{X} \oplus \mathcal{Y})_\ell = \mathcal{X}_\ell \oplus \mathcal{Y}_\ell$ for every slice $\ell$, a feature map $\Phi$ is additive if the underlying $\phi$ is additive.

For monofiltrations, no additive, non-trivial feature map $\phi$ can satisfy

$$\|\phi_{\mathcal{X}} - \phi_{\mathcal{Y}}\| \leq C \cdot n^\delta \cdot d_B(\mathcal{X}, \mathcal{Y})$$

with $\mathcal{X}, \mathcal{Y}$ monofiltrations and $\delta \in [0, 1)$; the proof of this statement is implicit in [150]. With similar ideas, we show that the same result holds in the multiparameter case.

**Theorem 13.** *If $\Phi$ is additive and there exists $C > 0$ and $\delta \in [0, 1)$ such that*

$$\|\Phi_{\mathcal{X}} - \Phi_{\mathcal{Y}}\|_{L^2} \leq C \cdot n^\delta \cdot d_{match}(\mathcal{X}, \mathcal{Y})$$

*for all bifiltrations $\mathcal{X}$ and $\mathcal{Y}$, then $\Phi$ is trivial.*

*Proof.* Assume to the contrary that there exists a bifiltration $\mathcal{X}$ such that $\|\Phi_{\mathcal{X}}\|_{L^2} > 0$. Then, writing $\mathcal{O}$ for the empty bifiltration, by additivity we get $\|\Phi_{\sqcup_{i=1}^n \mathcal{X}} - \Phi_{\mathcal{O}}\|_{L^2} = n\|\Phi_{\mathcal{X}} - \Phi_{\mathcal{O}}\|_{L^2} > 0$. On the other hand, $d_{match}(\mathcal{X}, \mathcal{O}) = d_{match}(\sqcup_{i=1}^n \mathcal{X}, \mathcal{O}) =$. Hence, with $C$ and $\delta$ as in the statement of the theorem,

$$\begin{aligned} \frac{\|\Phi_{\sqcup_{i=1}^n \mathcal{X}} - \Phi_{\mathcal{O}}\|_{L^2}}{C \cdot n^\delta \cdot d_{match}(\sqcup_{i=1}^n \mathcal{X}, \mathcal{O})} &= \frac{n\|\Phi_{\mathcal{X}} - \Phi_{\mathcal{O}}\|_{L^2}}{C \cdot n^\delta \cdot d_{match}(\mathcal{X}, \mathcal{O})} \\ &= n^{1-\delta} \frac{\|\Phi_{\mathcal{X}} - \Phi_{\mathcal{O}}\|_{L^2}}{C \cdot d_{match}(\mathcal{X}, \mathcal{O})} \xrightarrow{n \to \infty} \infty, \end{aligned}$$

a contradiction. □

GENERALIZATIONS. Let us remark that the given stability results can analogously be obtained for the generalizations mentioned before, i.e., different weights, a larger number of parameters, and on the level of multiparameter persistence modules.

In the proof of Theorem 12, the importance of $\hat{\ell}$ in the definition of the weight function became present. This factor is necessary to bound with respect to the matching distance. In fact, the stability results hold true for another version of a square-integrable weight function multiplied with the factor $\hat{\ell}$. Formally, if $w(p,q) = u(p,q) \cdot \hat{\ell}$ and $u$ is square-integrable, it is easy to see that

$$\begin{aligned} & \|\Phi_{\mathcal{X}} - \Phi_{\mathcal{Y}}\|_{L^2}^2 \\ \leq \; & (v_3 \cdot n \cdot d_{match}(\mathcal{X}, \mathcal{Y}))^2 \int\limits_{\Delta^{(2)}} u(p,q) d\mu \end{aligned}$$

holds true. Hence, the square-integral of $u$ replaces area$(R)$ in the inequality of the result of Theorem 12 and Corollary 4.

Let us also briefly discuss how to get a version of Theorem 12 for more than two parameters. For simplicial $k$-filtrations $\mathcal{X}, \mathcal{Y}$ of size at most $n$, using the notation $w(p,q) = u(p,q) \cdot \hat{\ell}$, we analogously obtain

$$\begin{aligned} & \|\Phi_{\mathcal{X}} - \Phi_{\mathcal{Y}}\|_{L^2}^2 \\ \leq \; & (v_3 \cdot n \cdot d_{match}(\mathcal{X}, \mathcal{Y}))^2 \int\limits_{\Delta^{(k)}} u(p,q) d\mu. \end{aligned}$$

Hence, we get the analogous versions of all stability results for $k$ parameters.

Finally, note that Theorem 12 and Theorem 13 can also be obtained on the algebraic level. As for Theorem 13, we need the direct sum of multiparameter persistence modules and we let $\mathcal{O}$ denote the multiparameter persistence module consisting of 0-vector spaces everywhere.

## 6.5 Approximability

We provide an approximation algorithm to compute the kernel of two bifiltrations $\mathcal{X}$ and $\mathcal{Y}$ up to any absolute error $\epsilon > 0$. Recall that our feature map $\Phi$ depends on the choice of a bounding box $R$. In this section, we assume $R$ to be the unit square $[0,1] \times [0,1]$ for simplicity. We prove the following theorem that shows our kernel construction admits an efficient approximation scheme that is polynomial in $1/\epsilon$ and the size of the bifiltrations.

**Theorem 14.** *Assume $\phi$ is absolutely bounded, Lipschitz, internally stable and efficiently computable. Given two bifiltrations $\mathcal{X}$ and $\mathcal{Y}$ of size $n$ and $\epsilon > 0$, we can compute a number $r$ such that $r \leq \langle \mathcal{X}, \mathcal{Y} \rangle_\Phi \leq r + \epsilon$ in polynomial time in $n$ and $1/\epsilon$.*

The proof of Theorem 14 will be illustrated in the following paragraphs. For easier reading, we postpone most of the technical details to Section 6.6.

Algorithm. Given two bifiltrations $\mathcal{X}$ and $\mathcal{Y}$ of size $n$ and $\epsilon > 0$, our goal is to efficiently approximate $\langle \mathcal{X}, \mathcal{Y} \rangle_\Phi$ by some number $r$. On the highest level, we compute a sequence of approximation intervals (with decreasing lengths) $J_1, J_2, J_3, \ldots$, each containing the desired kernel value $\langle \mathcal{X}, \mathcal{Y} \rangle_\Phi$. The computation terminates as soon as we find some $J_i$ of width at most $\epsilon$, in which case we return the left endpoint as an approximation to $r$.

For $s \in \mathbb{N}$ ($\mathbb{N}$ being the set of natural numbers), we compute $J_s$ as follows. We split $R$ into $2^s \times 2^s$ congruent squares (each of side length $2^{-s}$) which we refer to as *boxes*. See Figure 6.2(a) for an example when $s = 3$. We call a pair of such boxes a *box pair*. The integral from (6.1) can then be split into a sum of integrals over all $2^{4s}$ box pairs. That is,

$$\langle \mathcal{X}, \mathcal{Y} \rangle_\Phi = \int_{\Delta^{(2)}} \Phi_{\mathcal{X}} \Phi_{\mathcal{Y}} d\mu = \sum_{(B_1, B_2)} \int_{\Delta^{(2)} \cap (B_1 \times B_2)} \Phi_{\mathcal{X}} \Phi_{\mathcal{Y}} d\mu.$$

For each box pair, we compute an approximation interval for the integral, and sum them up using interval arithmetic to obtain $J_s$.

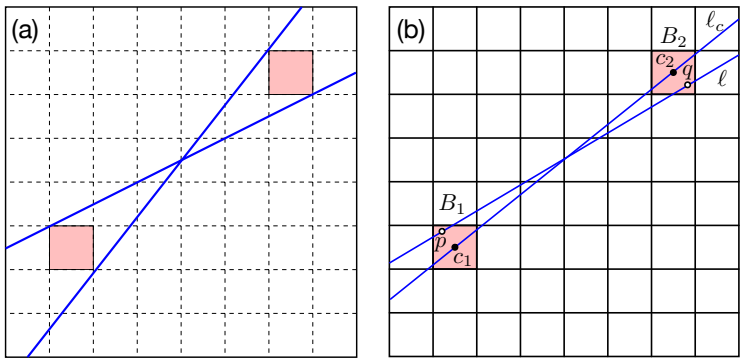


Figure 6.2: (a) The two given slices realize the largest and smallest possible slope among all slices traversing the pink box pair. It can be easily seen that the difference of the unit vector of the center line to one of the unit vectors of these two lines realizes $A$ for the given box pair. (b) Computing variations for the center slice and a traversing slice of a box pair.

We first give some (almost trivial) bounds for $\langle \mathcal{X}, \mathcal{Y} \rangle_\Phi$. Let $(B_1, B_2)$ be a box pair with centers located at $c_1$ and $c_2$, respectively. By construction, $\mathrm{vol}(B_1 \times B_2) = 2^{-4s}$. By the absolute boundedness of $\phi$, we have

$$\int_{\Delta^{(2)} \cap (B_1 \times B_2)} \Phi_{\mathcal{X}} \Phi_{\mathcal{Y}} d\mu \leq \int_{(B_1 \times B_2)} \left( \frac{1}{\sqrt{2}} v_1 n \cdot \frac{1}{\sqrt{2}} v_1 n \right) d\mu \tag{6.5}$$

$$= \frac{v_1^2 n^2}{2} \mathrm{vol}(B_1 \times B_2) = \frac{v_1^2 n^2}{2^{4s+1}}, \tag{6.6}$$

where $1/\sqrt{2}$ is the maximal weight. Let $U := \frac{v_1^2 n^2}{2^{4s+1}}$. If $c_1 \leq c_2$, then we can choose $[0, U]$ as approximation interval. Otherwise, if $c_1 \not\leq c_2$, then $\Delta^{(2)} \cap (B_1 \times B_2) = \emptyset$; we simply choose $[0, 0]$ as approximation interval.

We can derive a second lower and upper bound for $\langle \mathcal{X}, \mathcal{Y} \rangle_\Phi$ as follows. We evaluate $\Phi_{\mathcal{X}}$ and $\Phi_{\mathcal{Y}}$ at the pair of centers $(c_1, c_2)$, which is possible due to the efficiency hypothesis of $\phi$. Let $v_{\mathcal{X}} = \Phi_{\mathcal{X}}(c_1, c_2)$ and $v_{\mathcal{Y}} = \Phi_{\mathcal{Y}}(c_1, c_2)$. Then, we compute *variations* $\delta_{\mathcal{X}}, \delta_{\mathcal{Y}} \geq 0$ relative to the box pair, with the property that, for any pair $(p, q) \in B_1 \times B_2$, $\Phi_{\mathcal{X}}(p, q) \in [v_{\mathcal{X}} - \delta_{\mathcal{X}}, v_{\mathcal{X}} + \delta_{\mathcal{X}}]$, and $\Phi_{\mathcal{Y}}(p, q) \in [v_{\mathcal{Y}} - \delta_{\mathcal{Y}}, v_{\mathcal{Y}} + \delta_{\mathcal{Y}}]$. In other words, variations describe how far the value of $\Phi_{\mathcal{X}}$ (or $\Phi_{\mathcal{Y}}$) deviates from its value at $(c_1, c_2)$ within $B_1 \times B_2$. Combined with the derivations starting in (6.5), we have for any

pair $(p, q) \in B_1 \times B_2$,

$$\begin{aligned} &\max\{0, (v_{\mathcal{X}} - \delta_{\mathcal{X}})(v_{\mathcal{Y}} - \delta_{\mathcal{Y}})\} && (6.7)\\ \leq &\Phi_{\mathcal{X}}(p,q)\Phi_{\mathcal{Y}}(p,q) && (6.8)\\ \leq &\min\left\{\frac{v_1^2 n^2}{2}, (v_{\mathcal{X}} + \delta_{\mathcal{X}})(v_{\mathcal{Y}} + \delta_{\mathcal{Y}})\right\}. && (6.9) \end{aligned}$$

By multiplying the bounds obtained in (6.7) by the volume of $\Delta^{(2)} \cap (B_1 \times B_2)$, we get a lower and an upper bound for the integral of $\Phi_{\mathcal{X}}\Phi_{\mathcal{Y}}$ over a box pair $(B_1, B_2)$. By summing over all possible box pairs, the obtained lower and upper bounds are the endpoints of $J_s$.

VARIATIONS. We are left with computing the variations relative to a box pair. For simplicity, we set $\delta := \delta_{\mathcal{X}}$ and explain the procedure only for $\mathcal{X}$; the treatment of $\mathcal{Y}$ is similar.

We say that a slice $\ell$ *traverses* $(B_1, B_2)$ if it intersects both boxes in at least one point. One such slice is the *center slice* $\ell_c$, which is the slice through $c_1$ and $c_2$. See Figure 6.2(b) for an illustration. We set $D$ to be the maximal bottleneck distance of the center slice and every other slice traversing the box pair (to be more precise, of the persistence diagrams along the corresponding slices). We set $W$ as the maximal difference between the weight of the center slice and any other slice traversing the box pair, where the weight $w$ is defined as in Section 6.3. Write $\lambda_{c_1}$ for the parameter value of $c_1$ along the center slice. For every slice $\ell$ traversing the box pair and any point $p \in \ell \cap B_1$, we have a value $\lambda_p$, yielding the parameter value of $p$ along $\ell$. We define $L_1$ as the maximal difference of $\lambda_p$ and $\lambda_{c_1}$ among all choices of $p$ and $\ell$. We define $L_2$ in the same way for $B_2$ and set $L := \max\{L_1, L_2\}$. With these notations, we obtain Lemma 18 below.

**Lemma 18.** *For all* $(p, q) \in B_1 \times B_2$,

$$|\Phi_{\mathcal{X}}(p,q) - \Phi_{\mathcal{X}}(c_1,c_2)| \leq \frac{v_3 n}{\sqrt{2}} D + v_1 n W + v_2 n L.$$

*Proof.* Plugging in (6.4) and using triangle inequality, we obtain

$$\begin{aligned}
&|\Phi_{\mathcal{X}}(p,q) - \Phi_{\mathcal{X}}(c_1,c_2)| \\
=&\left|\hat{\ell}\phi_{\mathcal{X}_\ell}(\lambda_p,\lambda_q) - \hat{\ell}_c\phi_{\mathcal{X}_{\ell_c}}(\lambda_{c_1},\lambda_{c_2})\right| \\
\leq&\hat{\ell}\left|\phi_{\mathcal{X}_\ell}(\lambda_p,\lambda_q) - \phi_{\mathcal{X}_{\ell_c}}(\lambda_p,\lambda_q)\right| + \phi_{\mathcal{X}_{\ell_c}}(\lambda_p,\lambda_q)\left|\hat{\ell} - \hat{\ell}_c\right| \\
&+ \hat{\ell}_c\left|\phi_{\mathcal{X}_{\ell_c}}(\lambda_p,\lambda_q) - \phi_{\mathcal{X}_{\ell_c}}(\lambda_{c_1},\lambda_{c_2})\right|
\end{aligned}$$

and bound the three parts separately. The first summand is upper bounded by $\frac{v_3 nD}{\sqrt{2}}$ because of internal stability of the feature map $\phi$ and because $\hat{\ell} \leq \frac{1}{\sqrt{2}}$ for any slice $\ell$. The second summand is upper bounded by $v_1 nW$ by the absolute boundedness of $\phi$. The third summand is bounded by $v_2 nL$, because $\|(\lambda_p,\lambda_q) - (\lambda_{c_1},\lambda_{c_2})\|_2 \leq \sqrt{2}\|(\lambda_p,\lambda_q) - (\lambda_{c_1},\lambda_{c_2})\|_\infty \leq L$ and by $\phi$ being Lipschitz, $\left|\phi_{\mathcal{X}_{\ell_c}}(\lambda_p,\lambda_q) - \phi_{\mathcal{X}_{\ell_c}}(\lambda_{c_1},\lambda_{c_2})\right| \leq \sqrt{2}v_2 nL$, and $\hat{\ell} \leq \frac{1}{\sqrt{2}}$. The result follows. □

Next, we bound $D$ by simple geometric quantities. We use the following lemma, whose proof appeared in [125]:

**Lemma 19** ([125]). *Let $\ell$ and $\ell'$ be two slices with parameterizations $b + \lambda a$ and $b' + \lambda a'$, respectively. Then, the bottleneck distance of the two persistence diagrams along these slices is upper bounded by*

$$\frac{2\|a - a'\|_\infty + \|b - b'\|_\infty}{\hat{\ell}\hat{\ell}'}.$$

We define $A$ as the maximal infinity distance of the directional vector of the center slice $\ell_c$ and any other slice $\ell$ traversing the box pair. We define $B$ as the maximal infinity distance of the base point of $\ell_c$ and any other $\ell$. Finally, we set $M$ as the minimal weight among all slices traversing the box pair. Using Lemma 19, we see that

$$D \leq \frac{2A + B}{M\hat{\ell}_c},$$

and we set

$$\delta := \frac{v_3 n(2A+B)}{\sqrt{2}M\hat{\ell}_c} + v_1 nW + v_2 nL. \tag{6.10}$$

It follows from Lemma 18 and Lemma 19 that $\delta$ indeed satisfies the required variation property.

We remark that $\delta$ might well be equal to $\infty$, if the box pair admits a traversing slice that is horizontal or vertical, in which case the lower and upper bounds derived from the variation are vacuous. While (6.10) looks complicated, the values $v_1, v_2, v_3$ are constants coming from the considered feature map $\phi$, and all the remaining values can be computed in constant time using elementary geometric properties of a box pair. We only explain the computation of $A$ in Figure 6.2(a) and skip the details of the other values.

Analysis. At this point, we have not made any claim that the algorithm is guaranteed to terminate. However, its correctness follows at once because $J_s$ indeed contains the desired kernel value. Moreover, handling one box pair has a complexity that is polynomial in $n$, because the dominant step is to evaluate $\Phi_{\mathcal{X}}$ at the center $(c_1, c_2)$. Hence, if the algorithm terminates at iteration $s_0$, its complexity is

$$\sum_{s=1}^{s_0} O\left(2^{4s} poly(n)\right).$$

This is because in iteration $s$, $2^{4s}$ box pairs need to be considered. Clearly, the geometric series above is dominated by the last iteration, so the complexity of the method is $O(2^{4s_0} poly(n))$. The last (and technically most challenging) step is to argue that $s_0 = O(\log n + \log \frac{1}{\epsilon})$, which implies that the algorithm indeed terminates and its complexity is polynomial in $n$ and $1/\epsilon$.

To see that we can achieve any desired accuracy for the value of the kernel, i.e., that the interval width tends to 0, we observe that, if the two boxes $B_1$, $B_2$ are sufficiently far away and the resolution $s$ is sufficiently large, the magnitudes $A$, $B$, $W$, and $L$ in (6.10) are all small, because the parameterizations of two slices traversing the box pair are similar (see Lemmas 23, 24, 25, and 26 in Section 6.6). Moreover, if every slice traversing the box pair has a

sufficiently large weight (i.e., the slice is close to the diagonal), the value $M$ in (6.10) is sufficiently large. These two properties combined imply that the variation of such a box pair (which we refer to as the *good* type) tends to 0 as $s$ goes to $\infty$. Hence, the bound based on the variation tends to the correct value for good box pairs.

However, no matter how high the resolution, there are always *bad* box pairs for which either $B_1$, $B_2$ are close, or are far but close to horizontal and vertical, and hence yield a very large variation. For each of these box pairs, the bounds derived from the variation are vacuous, but we still have the trivial bounds $[0, U]$ based on the absolute boundedness of $\phi$. Moreover, the total volume of these bad box pairs goes to 0 when $s$ goes to $\infty$ (see Lemma 21 and Lemma 22 in Section 6.6). So, the contribution of these box pairs tends to 0. These two properties complete the proof of Theorem 14.

A more careful investigation of our proof shows that the complexity of our algorithm can be expressed as $O(n^{80+k}(1/\epsilon)^{40})$, where $k$ is the efficiency constant of the feature map as defined at the end of Section 6.2.[1]

## 6.6 Details on the Proof of Theorem 14

Overview. Recall that our approximation algorithm produces an approximation interval $J_s$ for $s \in \mathbb{N}$ by splitting the unit square into $2^s \times 2^s$ boxes. For notational convenience, we write $u := 2^{-s}$ for the side length of these boxes.

We would like to argue that the algorithm terminates after $O(\log n + \log \frac{1}{\epsilon})$ iterations, which means that after that many iterations, an interval of width $\epsilon$ has been produced. The following Lemma 20 gives an equivalent criterion in terms of $u$ and $n$.

**Lemma 20.** *Assume that there are constants $e_1, e_2 > 0$, such that* $\operatorname{width}(J_s) = O(n^{e_1} u^{e_2})$. *Then,* $\operatorname{width}(J_{s_0}) \leq \epsilon$ *for some* $s_0 = O\left(\log n + \log \frac{1}{\epsilon}\right)$.

[1] We made little effort to optimize the exponents in this bound.

*Proof.* Assume that $\text{width}(J_s) \leq cn^{e_1}u^{e_2}$ for constants $c$ and $s$ sufficiently large. Since $u = 2^{-s}$, a simple calculation shows that $cn^{e_1}u^{e_2} \leq \epsilon$ if and only if $s \geq \frac{\log c + e_1 \log n + \log \frac{1}{\epsilon}}{e_2}$. Hence, choosing

$$s := \left\lceil \frac{\log c + e_1 \log n + \log \frac{1}{\epsilon}}{e_2} \right\rceil = O\left(\log n + \log \frac{1}{\epsilon}\right)$$

ensures that $\text{width}(J_{s_0}) \leq \epsilon$. □

In the rest of this section, we will show that $\text{width}(J_s) = O(n^2u^{0.1})$.

Classifying box pairs. For the analysis, we partition the box pairs considered by the algorithm into 4 disjoint classes. We call a box pair $(B_1, B_2)$:

- *null* if $c_1 \not\leq c_2$,
- *close* if $c_1 \leq c_2$ such that $\|c_1 - c_2\|_2 < \sqrt{u}$,
- *non-diagonal* if $c_1 \leq c_2$ such that $\|c_1 - c_2\|_2 \geq \sqrt{u}$ and any line $\ell$ that traverses $(B_1, B_2)$ satisfies $\hat{\ell} < u^{\frac{1}{5}}$,
- *good* if it is of neither of the previous three types.

According to this notation, the integral from (6.1) can then be split as

$$\langle \mathcal{X}, \mathcal{Y} \rangle_\Phi = \langle \mathcal{X}, \mathcal{Y} \rangle_{null} + \langle \mathcal{X}, \mathcal{Y} \rangle_{close} + \langle \mathcal{X}, \mathcal{Y} \rangle_{non-diag} + \langle \mathcal{X}, \mathcal{Y} \rangle_{good},$$

where, $\langle \mathcal{X}, \mathcal{Y} \rangle_{null}$ is defined as $\sum_{(B_1,B_2)\, null} \int_{\Delta^{(2)} \cap (B_1 \times B_2)} \Phi_{\mathcal{X}} \Phi_{\mathcal{Y}} d\mu$, and analogously for the other ones. We let $J_{s,null}$, $J_{s,close}$, $J_{s,non-diag}$, $J_{s,good}$ denote the four approximation intervals obtained from our algorithm when summing up the contributions of the corresponding box pairs. Then clearly, $J_s$ is the sum of these four intervals. For simplicity, we will write $J_{null}$ instead of $J_{s,null}$ when $s$ is fixed, and likewise for the other three cases.

We observe first that the algorithm yields $J_{null} = [0, 0]$, so null box pairs can simply be ignored. Box pairs that are either close or non-diagonal are referred to as *bad* box pairs in Section 6.5. We proceed by showing that the width of $J_{close}$, $J_{non-diag}$, and $J_{good}$ are all bounded by $O(n^2u^{0.1})$.

BAD BOX PAIRS. We start with bounding the width of $J_{close}$. Let $\mathcal{B}_{\text{close}}$ be the union of all close box pairs. Note that our algorithm assigns to each box pair $(B_1, B_2)$ an interval that is a subset of $[0, U]$. Recall that $U = \frac{v_1^2 n^2}{2^{4s+1}}$. $U$ can be rewritten as $\frac{v_1^2 n^2}{2}\text{vol}(B_1 \times B_2)$, where $\text{vol}(B_1 \times B_2)$ is the 4-dimensional volume of the box pair $(B_1, B_2)$. It follows that

$$\text{width}(J_{close}) \leq \frac{v_1^2 n^2}{2}\text{vol}(\mathcal{B}_{\text{close}}). \tag{6.11}$$

**Lemma 21.** *For $u \leq \frac{1}{2}$, $\text{vol}(\mathcal{B}_{close}) \leq 4\pi u$.*

*Proof.* Fixed a point $p \in R$, for each point $q \in R$ such that $(p, q) \in \mathcal{B}_{\text{close}}$ and $p < q$, there exists a unique close box pair $(B_1, B_2)$ that contains $(p, q)$. By definition of close box pair, we have that:

$$\|p - q\|_2 \leq \|p - c_1\|_2 + \|c_1 - c_2\|_2 + \|c_2 - q\|_2 \leq \sqrt{u} + \sqrt{2}u.$$

Moreover, for $u \leq \frac{1}{2}$, $\sqrt{2}u \leq \sqrt{u}$, and so $\|p - q\|_2 \leq 2\sqrt{u}$. Equivalently, $q$ belongs to the 2-ball $B(p, 2\sqrt{u})$ centered at $p$ and of radius $2\sqrt{u}$. Then,

$$\begin{aligned}\text{vol}(\mathcal{B}_{\text{close}}) &= \int_{\mathcal{B}_{\text{close}}} 1 d\mu \leq \int_{p \in R} \int_{q \in B(p, 2\sqrt{u})} 1 d\mu \\ &\leq \int_{p \in R} 4\pi u d\mu = 4\pi u.\end{aligned}$$ □

Consequently, combined with (6.11), we have

$$\text{width}(J_{close}) \leq \frac{4\pi v_1^2 n^2}{2} u = O(n^2 u^{0.1}).$$

Note that $u < 1$ and hence, $u \leq u^{0.1}$.

For the width of $J_{non-diag}$, we use exactly the same reasoning, making use of the following Lemma 22. Let $\mathcal{B}_{\text{non-diag}}$ be the union of all non-diagonal box pairs.

**Lemma 22.** *For $u \leq 2^{-\frac{5}{2}}$, $\text{vol}(\mathcal{B}_{non\text{-}diag}) \leq \sqrt{2}u^{\frac{1}{5}}$.*

*Proof.* Fixed a point $p \in R$, for each point $q \in R$ such that $(p,q) \in \mathcal{B}_{\text{non-diag}}$ and $p < q$, there exists a unique non-diagonal box pair $(B_1, B_2)$ that contains $(p,q)$. We have that $q$ lies in:

- Triangle $T_1(p)$ of vertices $p = (p_1, p_2)$, $(1, p_2)$, and $(1, p_2 + (1-p_1)\frac{a_2}{a_1})$, if the line $\ell$ of maximum slope passing through $B_1 \times B_2$ is such that $\hat{\ell} = a_2$ where $a = (a_1, a_2)$ is the (positive) unit direction vector of $\ell$;
- Triangle $T_2(p)$ of vertices $p = (p_1, p_2)$, $(p_1, 1)$, and $(p_1 + (1-p_2)\frac{a_1}{a_2}, 1)$, if the line $\ell$ of minimum slope passing through $B_1 \times B_2$ is such that $\hat{\ell} = a_1$ where $a = (a_1, a_2)$ is the (positive) unit direction vector of $\ell$.

Let us bound the area of the two triangles. Since the calculations are analogous, let us focus on $T_1(p)$. By definition, the basis of $T_1(p)$ is smaller than 1 while its height is bounded by $\frac{a_2}{a_1}$. The maximum value for the height of $T_1(p)$ is achieved for $a_2 = u^{\frac{1}{5}}$. So, by exploiting the identity $a_1^2 + a_2^2 = 1$, we have

$$\left(\frac{a_2}{a_1}\right)^2 = \frac{u^{\frac{2}{5}}}{1 - u^{\frac{2}{5}}}.$$

Under the conditions $u \leq 2^{-\frac{5}{2}}$ and $\frac{1}{2}u^{-\frac{2}{5}} \geq 1$ we have

$$\frac{a_2}{a_1} \leq \sqrt{2}u^{\frac{1}{5}}.$$

Therefore, $\text{area}(T_1(p)) \leq \frac{\sqrt{2}}{2}u^{\frac{1}{5}}$. Similarly, $\text{area}(T_2(p)) \leq \frac{\sqrt{2}}{2}u^{\frac{1}{5}}$. Finally,

$$\begin{aligned}
\text{vol}(\mathcal{B}_{\text{non-diag}}) &= \int_{\mathcal{B}_{\text{non-diag}}} 1 d\mu \\
&\leq \int_{p \in R} \int_{q \in T_1(p) \cup T_2(p)} 1 d\mu \\
&\leq \int_{p \in R} \sqrt{2}u^{\frac{1}{5}} d\mu \leq \sqrt{2}u^{\frac{1}{5}}.
\end{aligned}$$

□

Good box pairs. For good box pairs, we use the fact that the variation of a box pair yields a subinterval of $[(v_{\mathcal{X}} - \delta_{\mathcal{X}})(v_{\mathcal{Y}} - \delta_{\mathcal{Y}})\text{vol}(B_1 \times B_2), (v_{\mathcal{X}} + \delta_x)(v_{\mathcal{Y}} + \delta_{\mathcal{Y}})\text{vol}(B_1 \times B_2)]$ as an approximation, so the width is bounded

by $2(v_{\mathcal{X}}\delta_{\mathcal{Y}} + v_{\mathcal{Y}}\delta_{\mathcal{X}})\text{vol}(B_1 \times B_2)$. Let $\mathcal{B}_{\text{good}}$ be the union of all good box pairs. Since the volumes of all good box pairs sum up to at most one, that is, $\text{vol}(\mathcal{B}_{\text{good}}) \leq 1$, it follows that the width of $J_{good}$ is bounded by $2(v_{\mathcal{X}}\delta_{\mathcal{Y}} + v_{\mathcal{Y}}\delta_{\mathcal{X}})$. By absolute boundedness, $v_{\mathcal{X}}$ and $v_{\mathcal{Y}}$ are in $O(n)$, and recall that by definition,

$$\delta_{\mathcal{X}} = \frac{v_3 n(2A+B)}{\sqrt{2}M\hat{\ell}_c} + v_1 nW + v_2 nL = O\left(n\left(\frac{A+B}{M^2} + W + L\right)\right)$$

based on the fact that $\hat{\ell} \geq M$. The same bound holds for $\delta_{\mathcal{Y}}$. Hence,

$$\text{width}(J_{good}) = O\left(n^2\left(\frac{A+B}{M^2} + W + L\right)\right).$$

It remains to show that $\frac{A+B}{M^2} + W + L = O(u^{0.1})$. Note that $M \geq u^{\frac{1}{5}}$ because the box pair is assumed to be good. We will show in the next lemmas that $A$, $B$, $W$, and $L$ are all in $O(\sqrt{u})$, proving that the term is indeed in $O(u^{0.1})$. This completes the proof of the complexity of the algorithm.

**Lemma 23.** *Let $(B_1, B_2)$ be a good box pair. Let $a$, $a'$ be the unit direction vectors of two lines that pass through the box pair. Then, $\|a - a'\|_\infty \leq 2\sqrt{u}$. In particular, $A = O(\sqrt{u})$.*

*Proof.* Since $(B_1, B_2)$ is a good box pair, the largest value for $\|a - a'\|_\infty$ is achieved when $\ell$ and $\ell'$ correspond to the lines passing through the box pair$(B_1, B_2)$ with minimum and maximum slope, respectively. By denoting as $c_1 = (c_{1,x}, c_{1,y})$, $c_2 = (c_{2,x}, c_{2,y})$ the centers of $B_1$, $B_2$, we define $\ell$ to be the line passing through the points $c_1 + (-\frac{u}{2}, \frac{u}{2})$, $c_2 + (\frac{u}{2}, -\frac{u}{2})$. Similarly, let us call $\ell'$ the line passing through the points $c_1 + (\frac{u}{2}, -\frac{u}{2})$, $c_2 + (-\frac{u}{2}, \frac{u}{2})$. So, the unit direction vector $a$ of $\ell$ can be expressed as

$$a = \frac{(c_2 + (\frac{u}{2}, -\frac{u}{2})) - (c_1 + (-\frac{u}{2}, \frac{u}{2}))}{\left\|(c_2 + (\frac{u}{2}, -\frac{u}{2})) - (c_1 + (-\frac{u}{2}, \frac{u}{2}))\right\|_2}.$$

Similarly, the unit direction vector $a'$ of $\ell'$ is described by

$$a' = \frac{(c_2 + (-\frac{u}{2}, \frac{u}{2})) - (c_1 + (\frac{u}{2}, -\frac{u}{2}))}{\left\|(c_2 + (-\frac{u}{2}, \frac{u}{2})) - (c_1 + (\frac{u}{2}, -\frac{u}{2}))\right\|_2}.$$

Then, by denoting as $\langle \cdot, \cdot \rangle$ the scalar product,

$$\begin{aligned}\|a - a'\|_\infty^2 \leq \|a - a'\|_2^2 &= \|a\|_2^2 + \|a'\|_2^2 - 2\langle a, a' \rangle = 2(1 - \langle a, a' \rangle) \\ &= 2\Big(1 - \langle \frac{c_2 - c_1 + (u, -u)}{\|c_2 - c_1 + (u, -u)\|_2}, \frac{c_2 - c_1 + (-u, u)}{\|c_2 - c_1 + (-u, u)\|_2} \rangle\Big) \\ &= 2\Big(1 - \frac{\|c_2 - c_1\|_2^2 - 2u^2}{\|c_2 - c_1 + (u, -u)\|_2 \, \|c_2 - c_1 + (-u, u)\|_2}\Big).\end{aligned}$$

By an elementary calculation, one can prove that

$$\begin{aligned}&\|c_2 - c_1 + (u, -u)\|_2 \, \|c_2 - c_1 + (-u, u)\|_2 \\ =&\sqrt{4u^2\big(u^2 + 2(c_{2,x} - c_{1,x})(c_{2,y} - c_{1,y})\big) + \|c_2 - c_1\|_2^4}.\end{aligned}$$

Then,

$$\begin{aligned}&\|a - a'\|_\infty^2 \\ \leq& 2\Big(1 - \frac{\|c_2 - c_1\|_2^2 - 2u^2}{\sqrt{4u^2\big(u^2 + 2(c_{2,x} - c_{1,x})(c_{2,y} - c_{1,y})\big) + \|c_2 - c_1\|_2^4}}\Big) \\ =& 2\Big(1 + \frac{2u^2 - \|c_2 - c_1\|_2^2}{\sqrt{4u^2\big(u^2 + 2(c_{2,x} - c_{1,x})(c_{2,y} - c_{1,y})\big) + \|c_2 - c_1\|_2^4}}\Big).\end{aligned}$$

Since $(B_1, B_2)$ is a good box pair, $\|c_2 - c_1\|_2 \geq \sqrt{u}$. So,

$$\|a - a'\|_\infty^2 \leq 2\Big(1 + \frac{2u - 1}{\sqrt{4\big(u^2 + 2(c_{2,x} - c_{1,x})(c_{2,y} - c_{1,y})\big) + 1}}\Big).$$

Since $\sqrt{4\big(u^2 + 2(c_{2,x} - c_{1,x})(c_{2,y} - c_{1,y})\big) + 1} \geq 1$, we have that

$$\|a - a'\|_\infty^2 \leq 2(1 + 2u - 1) = 4u.$$

Therefore,

$$\|a - a'\|_\infty \leq 2\sqrt{u}. \qquad \square$$

**Lemma 24.** *Let $(B_1, B_2)$ be a good box pair. Let $\ell = a\lambda + b$, $\ell' = a'\lambda + b'$ be two lines that pass through the box pair such that $a$, $a'$ are unit direction vectors and $b$, $b'$ are the intersection points with the diagonal of the second and the fourth quadrant. Then $\|b - b'\|_\infty \leq 4\sqrt{u}$. In particular, $B = O(\sqrt{u})$.*

*Proof.* Since $(B_1, B_2)$ is a good box pair, the largest value for $\|b - b'\|_\infty$ is achieved when $\ell$ and $\ell'$ correspond to the lines passing through the box pair$(B_1, B_2)$ with minimum and maximum slope, respectively. By denoting the centers of $B_1$ and $B_2$ by $c_1$ and $c_2$, we define $\ell$ to be the line passing through the points $c_1 + (-\frac{u}{2}, \frac{u}{2})$, $c_2 + (\frac{u}{2}, -\frac{u}{2})$. Similarly, let us call $\ell'$ the line passing through the points $c_1 + (\frac{u}{2}, -\frac{u}{2})$, $c_2 + (-\frac{u}{2}, \frac{u}{2})$. So, $\ell$ can be expressed as

$$(x, y) = \frac{c_2 + (\frac{u}{2}, -\frac{u}{2}) - c_1 - (-\frac{u}{2}, \frac{u}{2})}{\left\|c_2 + (\frac{u}{2}, -\frac{u}{2}) - c_1 - (-\frac{u}{2}, \frac{u}{2})\right\|_2} t + c_1 + (-\frac{u}{2}, \frac{u}{2}),$$

where $t$ is a parameter running on $\mathbb{R}$. By intersecting $\ell$ with the line $y = -x$, we get:

$$\begin{aligned} &\frac{c_{2,x} + \frac{u}{2} - c_{1,x} + \frac{u}{2}}{\left\|c_2 + (\frac{u}{2}, -\frac{u}{2}) - c_1 - (-\frac{u}{2}, \frac{u}{2})\right\|_2} t + c_{1,x} - \frac{u}{2} \\ =&\frac{-c_{2,y} + \frac{u}{2} + c_{1,y} + \frac{u}{2}}{\left\|c_2 + (\frac{u}{2}, -\frac{u}{2}) - c_1 - (-\frac{u}{2}, \frac{u}{2})\right\|_2} t - c_{1,y} - \frac{u}{2}, \end{aligned}$$

which can be written as

$$c_{1,x} + c_{1,y} = \frac{c_{1,x} + c_{1,y} - c_{2,x} - c_{2,y}}{\left\|c_2 + (\frac{u}{2}, -\frac{u}{2}) - c_1 - (-\frac{u}{2}, \frac{u}{2})\right\|_2} t,$$

letting us deduce that

$$t = \frac{(c_{1,x} + c_{1,y}) \left\|c_2 + (\frac{u}{2}, -\frac{u}{2}) - c_1 - (-\frac{u}{2}, \frac{u}{2})\right\|_2}{c_{1,x} + c_{1,y} - c_{2,x} - c_{2,y}}.$$

So, by replacing $t$ in the equation of $\ell$ we retrieve $b$:

$$\begin{aligned} b = & \frac{c_2 + (\frac{u}{2}, -\frac{u}{2}) - c_1 - (-\frac{u}{2}, \frac{u}{2})}{\left\|c_2 + (\frac{u}{2}, -\frac{u}{2}) - c_1 - (-\frac{u}{2}, \frac{u}{2})\right\|_2} \\ & \frac{(c_{1,x} + c_{1,y}) \left\|c_2 + (\frac{u}{2}, -\frac{u}{2}) - c_1 - (-\frac{u}{2}, \frac{u}{2})\right\|_2}{c_{1,x} + c_{1,y} - c_{2,x} - c_{2,y}} + c_1 + (-\frac{u}{2}, \frac{u}{2}) \\ = & \frac{(u, -u)(c_{1,x} + c_{1,y})}{c_{1,x} + c_{1,y} - c_{2,x} - c_{2,y}} + \frac{(c_2 - c_1)(c_{1,x} + c_{1,y})}{c_{1,x} + c_{1,y} - c_{2,x} - c_{2,y}} \\ & + c_1 + (-\frac{u}{2}, \frac{u}{2}). \end{aligned}$$

Similarly,

$$\begin{aligned} b' = & \frac{(-u, u)(c_{1,x} + c_{1,y})}{c_{1,x} + c_{1,y} - c_{2,x} - c_{2,y}} + \frac{(c_2 - c_1)(c_{1,x} + c_{1,y})}{c_{1,x} + c_{1,y} - c_{2,x} - c_{2,y}} \\ & + c_1 + (\frac{u}{2}, -\frac{u}{2}). \end{aligned}$$

So,

$$\begin{aligned} \left\|b - b'\right\|_\infty &= \left\| \left(2\frac{c_{1,x} + c_{1,y}}{c_{1,x} + c_{1,y} - c_{2,x} - c_{2,y}} - 1\right)(u, -u) \right\|_\infty \\ &= \left| \frac{c_{1,x} + c_{1,y} + c_{2,x} + c_{2,y}}{c_{2,x} + c_{2,y} - c_{1,x} - c_{1,y}} \right| \|(u, -u)\|_\infty \\ &\leq \frac{4r}{|c_{2,x} + c_{2,y} - c_{1,x} - c_{1,y}|} u. \end{aligned}$$

Since $(B_1, B_2)$ is a good box pair,

$$c_{2,x} + c_{2,y} - c_{1,x} - c_{1,y} = \|c_2 - c_1\|_1 \geq \|c_2 - c_1\|_2 \geq \sqrt{u}.$$

Finally,

$$\left\|b - b'\right\|_\infty \leq \frac{4}{\sqrt{u}} u = 4\sqrt{u}. \qquad \square$$

**Lemma 25.** *Let $(B_1, B_2)$ be a good box pair. Let $\hat{\ell}$, $\hat{\ell}'$ be the weights of two lines $\ell$ and $\ell'$ that pass through the box pair. Then $|\hat{\ell} - \hat{\ell}'| \leq 4\sqrt{u}$. In particular, $W = O(\sqrt{u})$.*

*Proof.* If $\hat{\ell} = a_1$ and $\hat{\ell}' = a'_1$, then, by applying Lemma 23,

$$|\hat{\ell} - \hat{\ell}'| = |a_1 - a'_1| \leq \left\|a - a'\right\|_\infty \leq 2\sqrt{u}.$$

On the other hand, if $\hat{\ell} = a_1$ and $\hat{\ell}' = a'_2$, then there exists a line $\ell''$ passing through the box pair $(B_1, B_2)$ such that $a'' = (\frac{\sqrt{2}}{2}, \frac{\sqrt{2}}{2})$. By applying twice Lemma 23,

$$\begin{aligned} |\hat{\ell} - \hat{\ell}'| = |a_1 - a'_2| &\leq |a_1 - \frac{\sqrt{2}}{2}| + |\frac{\sqrt{2}}{2} - a'_2| \\ &= |a_1 - a''_1| + |a''_2 - a'_2| \leq \left\|a - a''\right\|_\infty + \left\|a'' - a'\right\|_\infty \\ &\leq 4\sqrt{u}. \end{aligned}$$

The cases $\hat{\ell} = a_2$, $\hat{\ell}' = a'_2$ and $\hat{\ell} = a_2$, $\hat{\ell}' = a'_1$ can be treated analogously to the previous ones. □

**Lemma 26.** *Let $(p, q)$, $(p', q')$ be two points in a good box pair $(B_1, B_2)$ and let $\ell$, $\ell'$ be the lines passing through $p$, $q$ and $p'$, $q'$, respectively. In accordance with the usual parametrization, we have that $|\lambda_p - \lambda_{p'}| \leq \sqrt{2}u + 4\sqrt{u}$ and $|\lambda_q - \lambda_{q'}| \leq \sqrt{2}u + 4\sqrt{u}$. As a consequence, $L = O(\sqrt{u})$.*

*Proof.* Thanks to the definition of $\lambda_p$, the triangular inequality and Lemma 24, we have that:

$$\begin{aligned} \lambda_p = \|p - b\|_2 &\leq \left\|p - p'\right\|_2 + \left\|p' - b'\right\|_2 + \left\|b' - b\right\|_2 \\ &\leq \sqrt{2}u + \lambda_{p'} + 4\sqrt{u}. \end{aligned}$$

So, we have that $\lambda_p - \lambda_{p'} \leq \sqrt{2}u + 4\sqrt{u}$, and, similarly, $\lambda_{p'} - \lambda_p \leq \sqrt{2}u + 4\sqrt{u}$. Then,

$$|\lambda_p - \lambda_{p'}| \leq \sqrt{2}u + 4\sqrt{u}.$$

Analogously, it can be proven that

$$|\lambda_q - \lambda_{q'}| \leq \sqrt{2}u + 4\sqrt{u}.$$ □

## 6.7 Conclusion and future work

We restate our main results for the case of a simplicial multifiltration $\mathcal{X}$ with $k$ parameters: there is a feature map that associates to $\mathcal{X}$ a real-valued function $\Phi_{\mathcal{X}}$ whose domain is of dimension $2k$, and introduces a kernel between a pair of multifiltrations with a stable distance function. The stability bounds depend on the ($2k$-dimensional) volume of a chosen bounding box, or, more generally, on the integral of a square-integrable function. Moreover, assuming that $k$ is a constant, we claim that the kernel can be approximated in polynomial time to any constant (with the polynomial exponent depending on $k$). A proof of this statement for $k > 2$ requires to adapt the definitions and proofs of Sections 6.5 and 6.6. We omit the details and leave this to future work.

On another level, it would be interesting to investigate the properties of the so-called Reproducing Kernel Hilbert Space (RKHS) [17] of kernels for multiparameter persistence. A RKHS is the Hilbert space that is spanned by all one-variable evaluations $K(x, \cdot)$ of a kernel $K$. Any RKHS consists of continuous and linear functionals. By the Moore-Aronszajn Theorem [7], any feature map induces a unique RKHS. For certain feature maps of one parameter persistence some basic properties are known [121]. It would be interesting to see if desirable properties of RKHS of feature maps of ordinary persistence could be transferred to the multiparameter case.

The next step is an efficient implementation of our kernel approximation algorithm. We have implemented a prototype in C++, realizing a more adaptive version of the described algorithm. We have observed rather poor performance due to the sheer number of box pairs to be considered. Some improvements under consideration are to precompute all combinatorial persistence diagrams (cf. the barcode templates from [131]), to refine the search space adaptively using a quad-tree instead of doubling the resolution and to use techniques from numerical integration to handle real-world data sizes. We hope that an efficient implementation of our kernel will validate the assumption that including more than a single parameter will attach more information to the data set and improve the quality of machine learning algorithms using topological features.

# 7 Outlook

We outline some research tasks for future work on the pipeline of multiparameter persistence, in addition to what we mention in the papers.

There is the need of more feasible constructions of *multifiltrations*. That includes standard constructions but also new approaches, for instance studying data sampled from algebraic varieties under the lens of multiparameter persistence.

It is not clear which *invariants* are most suitable. We believe it is interesting to compare standard invariants, recent more complicated invariants, and potential future invariants in terms of theory, computation, implementation, and applications. An important task for future work is to create efficient algorithms to compute useful invariants for more than two parameters. It would also be very interesting to see if useful multifiltrations provably induce relatively simple persistence modules, i.e., in an interval decomposable or block decomposable form. In these cases, one should investigate whether simple invariants suffice.

As for *interpretations*, we believe that the connections to machine learning algorithms deserve further studies. Besides an efficient implementation of a multiparameter kernel, interfaces of multiparameter persistence with other machine learning methods would be useful. For instance, deep learning methods could be generalized to the multiparameter case. Asides from that, it would also be interesting to discover subclasses of multiparameter persistence modules in which the computation of the interleaving distance is not NP-hard.

We believe that many more *applications* of multiparameter persistence will be possible and will yield to breakthroughs in data science and related areas. This, requires more theoretical and computational results as well as more efficient implementations of the whole pipeline, however. A further extension of the open access software RIVET to an even more powerful toolbox would substantially increase the use of multiparameter persistence.

# List of Figures

# References


[1] Jiři Adámek, Horst Herrlich, and George E. Strecker. *Abstract and Concrete Categories – The Joy of Cats*. Dover Publications, 2009.

[2] Henry Adams, Tegan Emerson, Michael Kirby, Rachel Neville, Chris Peterson, Patrick Shipman, Sofya Chepushtanova, Eric Hanson, Francis Motta, and Lori Ziegelmeier. Persistence images: A stable vector representation of persistent homology. *Journal of Machine Learning Research*, 18(1):218–252, 2017.

[3] Henry Adams, Andrew Tausz, and Mikael Vejdemo-Johansson. javaplex: A research software package for persistent (co)homology. In Hoon Hong and Chee Yap, editors, *Mathematical Software – ICMS 2014*, pages 129–136. Springer Berlin Heidelberg, 2014. Software available at http://appliedtopology.github.io/javaplex/.

[4] Aaron Adcock, Erik Carlsson, and Gunnar Carlsson. The ring of algebraic functions on persistence bar codes. *Homology, Homotopy and Applications*, 18:381–402, 2016.

[5] Aaron Adcock, Daniel Rubin, and Gunnar Carlsson. Classification of hepatic lesions using the matching metric. *Computer vision and image understanding*, 121:36–42, 2014.

[6] Paul Alexandroff. Über den allgemeinen Dimensionsbegriff und seine Beziehungen zur elementaren geometrischen Anschauung. *Mathematische Annalen*, 98(1):617–635, 1928.

[7] Nachman Aronszajn. Theory of reproducing kernels. *Transactions of the American mathematical society*, 68(3):337–404, 1950.

[8] Franz Aurenhammer. Power diagrams: properties, algorithms and applications. *SIAM Journal on Computing*, 16(1):78–96, 1987.

[9] Franz Aurenhammer and Hiroshi Imai. Geometric relations among Voronoi diagrams. *Geometriae Dedicata*, 27(1):65–75, 1988.

[10] Nicholas R. Baeth and Daniel Smertnig. Factorization theory: From commutative to noncommutative settings. *Journal of Algebra*, 441:475 – 551, 2015.

[11] Ulrich Bauer. Ripser: efficient computation of Vietoris-Rips persistence barcodes. Software available at https://github.com/Ripser/ripser, 2019.

[12] Ulrich Bauer and Herbert Edelsbrunner. The Morse theory of Čech and Delaunay complexes. *Transactions of the AMS*, 369:3741–3762, 2017.

[13] Ulrich Bauer, Michael Kerber, and Jan Reininghaus. Distributed computation of persistent homology. In *2014 proceedings of the sixteenth workshop on algorithm engineering and experiments (ALENEX)*, pages 31–38. SIAM, 2014. Software available at https://code.google.com/p/dipha/.

[14] Ulrich Bauer, Michael Kerber, Jan Reininghaus, and Hubert Wagner. PHAT – persistent homology algorithms toolbox. *Journal of Symbolic Computation*, 78:76 – 90, 2017. Algorithms and Software for Computational Topology. Software available at https://code.google.com/p/phat/.

[15] Paul Bendich, James S. Marron, Ezra Miller, Alex Pieloch, and Sean Skwerer. Persistent homology analysis of brain artery trees. *The annals of applied statistics*, 10(1):198, 2016.

[16] Mattia G. Bergomi, Adriano Baratè, and Barbara Di Fabio. Towards a topological fingerprint of music. In Alexandra Bac and Jean-Luc Mari, editors, *Computational Topology in Image Context*, pages 88–100. Springer International Publishing, 2016.

[17] Alain Berlinet and Christine Thomas-Agnan. *Reproducing Kernel Hilbert Space in Probability and Statistics*. Springer, 2004.

[18] Silvia Biasotti, Andrea Cerri, Patrizio Frosini, and Daniela Giorgi. A new algorithm for computing the 2-dimensional matching distance between size functions. *Pattern Recognition Letters*, 32(14):1735–1746, 2011.

[19] Silvia Biasotti, Andrea Cerri, Patrizio Frosini, Daniela Giorgi, and Claudia Landi. Multidimensional size functions for shape comparison. *Journal of Mathematical Imaging and Vision*, 32(2):161, 2008.

[20] Silvia Biasotti, Bianca Falcidieno, and Michela Spagnuolo. Extended Reeb graphs for surface understanding and description. In *Proceedings of the 9th International Conference on Discrete Geometry for Computer Imagery*, pages 185–197, 2000.

[21] Håvard Bakke Bjerkevik and Magnus Bakke Botnan. Computational complexity of the interleaving distance. In *LIPIcs-Leibniz International Proceedings in Informatics*, volume 99. Schloss Dagstuhl-Leibniz-Zentrum fuer Informatik, 2018.

[22] Håvard Bakke Bjerkevik, Magnus Bakke Botnan, and Michael Kerber. Computing the interleaving distance is NP-hard. *Foundations of Computational Mathematics*, pages 1–35, 2019.

[23] Karol Borsuk. On the imbedding of systems of compacta in simplicial complexes. *Fundamenta Mathematicae*, 35(1):217–234, 1948.

[24] Magnus Botnan. Interval decomposition of infinite zigzag persistence modules. *Proceedings of the American Mathematical Society*, 145(8):3571–3577, 2017.

[25] Magnus Bakke Botnan and William Crawley-Boevey. Decomposition of persistence modules. *arXiv:1811.08946*, 2018.

[26] Magnus Bakke Botnan and Gard Spreemann. Approximating persistent homology in Euclidean space through collapses. *Applicable Algebra in Engineering, Communication and Computing*, 26(1-2):73–101, 2015.

[27] Glen E. Bredon. *Topology and Geometry*. Graduate texts in mathematics. Springer-Verlag, 1993.

[28] Paul Breiding, Sara Kališnik, Bernd Sturmfels, and Madeleine Weinstein. Learning algebraic varieties from samples. *Revista Matemática Complutense*, 31(3):545–593, 2018.

[29] Paul Brinkman, Ariane H. Wagener, Pieter-Paul Hekking, Aruna T. Bansal, Anke-Hilse Maitland-van der Zee, Yuanyue Wang, Hans Weda, Hugo H. Knobel, Teunis J. Vink, Nicholas J. Rattray, et al. Identification and prospective stability of electronic nose (enose)–derived inflammatory phenotypes in patients with severe asthma. *Journal of Allergy and Clinical Immunology*, 143(5):1811–1820, 2019.

[30] Hervé Brönnimann, Andreas Fabri, Geert-Jan Giezeman, Susan Hert, Michael Hoffmann, Lutz Kettner, Sylvain Pion, and Stefan Schirra. 2D and 3D linear geometry kernel. In *CGAL User and Reference Manual*. CGAL Editorial Board, 5.0 edition, 2019.

[31] Peter Bubenik. Statistical topological data analysis using persistence landscapes. *The Journal of Machine Learning Research*, 16(1):77–102, 2015.

[32] Peter Bubenik and Nikola Milicevic. Homological algebra for persistence modules. *arXiv:1905.05744*, 2019.

[33] Peter Bubenik and Jonathan Scott. Categorification of persistent homology. *Discrete and Computational Geometry*, 51(3):600–627, 2014.

[34] Peter Bubenik, Vin Silva, and Jonathan Scott. Metrics for generalized persistence modules. *Foundations of Computational Mathematics*, 15(6):1501–1531, 2015.

[35] Mickaël Buchet and Emerson G. Escolar. Realizations of indecomposable persistence modules of arbitrarily large dimension. In *34th International Symposium on Computational Geometry, SoCG 2018*, pages 151–1513. Schloss Dagstuhl, Leibniz-Zentrum für Informatik, 2018.

[36] Mickaël Buchet and Emerson G. Escolar. Every 1D persistence module is a restriction of some indecomposable 2D persistence module. *Journal of Applied and Computational Topology*, 2020.

[37] Wolf Byttner. Classifying RGB images with multi-colour persistent homology. Bachelor's Thesis, Linköpings Universitet, 2019.

[38] Gunnar Carlsson. Topology and data. *Bulletin of the AMS*, 46:255–308, 2009.

[39] Gunnar Carlsson and Vin de Silva. Zigzag persistence. *Foundations of Computational Mathematics*, 10:367–405, 2010.

[40] Gunnar Carlsson, Vin de Silva, and Dmitriy Morozov. Zigzag persistent homology and real-valued functions. In *Symposium on Computational Geometry*, 2009.

[41] Gunnar Carlsson, Tigran Ishkhanov, Vin De Silva, and Afra Zomorodian. On the local behavior of spaces of natural images. *International journal of computer vision*, 76(1):1–12, 2008.

[42] Gunnar Carlsson and Facundo Mémoli. Multiparameter hierarchical clustering methods. In Hermann Locarek-Junge and Claus Weihs, editors, *Classification as a Tool for Research*, pages 63–70. Springer Berlin Heidelberg, 2010.

[43] Gunnar Carlsson and Afra Zomorodian. The theory of multidimensional persistence. *Discrete & Computational Geometry*, 42(1):71–93, 2009.

[44] Gunnar Carlsson, Afra Zomorodian, Ane Collins, and Leonidas Guibas. Persistence barcodes for shapes. *International Journal of Shape Modeling*, 11(02):149–187, 2005.

[45] Mathieu Carriére, Marco Cuturi, and Steve Oudot. Sliced Wasserstein kernel for persistence diagrams. In *Proceedings of the 34th International Conference on Machine Learning*, volume 70, pages 664–673, 2017.

[46] Corrie Jacobien Carstens and Kathy J. Horadam. Persistent homology of collaboration networks. *Mathematical Problems in Engineering*, 2013:7, 2013.

[47] Andrea Cerri, Barbara Di Fabio, Massimo Ferri, Patrizio Frosini, and Claudia Landi. Betti numbers in multidimensional persistent homology are stable functions. *Mathematical Methods in the Applied Sciences*, 36(12):1543–1557, 2013.

[48] Erin Wolf Chambers and David Letscher. *Persistent Homology over Directed Acyclic Graphs*, pages 11–32. Springer International Publishing, Cham, 2018.

[49] Joseph Minhow Chan, Gunnar Carlsson, and Raul Rabadan. Topology of viral evolution. *Proceedings of the National Academy of Sciences of the United States of America*, 110(46):18566–18571, 2013.

[50] Frédéric Chazal, David Cohen-Steiner, Marc Glisse, Leonidas J. Guibas, and Steve Y. Oudot. Proximity of persistence modules and their diagrams. In *Proceedings of the Twenty-fifth Annual Symposium on Computational Geometry*, pages 237–246, 2009.

[51] Frédéric Chazal, David Cohen-Steiner, Leonidas J. Guibas, Facundo Mémoli, and Steve Y. Oudot. Gromov-Hausdorff stable signatures for shapes using persistence. *Eurographics Symposium on Geometry Processing*, 28(5):1393–1403, 2009.

[52] Frédéric Chazal, David Cohen-Steiner, and Quentin Mérigot. Geometric inference for probability measures. *Foundations of Computational Mathematics*, 11:733–751, 2011.

[53] Frédéric Chazal, Vin de Silva, Marc Glisse, and Steve Y. Oudot. *The structure and stability of persistence modules*. Springer International Publishing, 2016.

[54] Frédéric Chazal and Steve Y. Oudot. Towards persistence-based reconstruction in euclidean spaces. In *Proceedings of the twenty-fourth annual symposium on Computational geometry*, pages 232–241, 2008.

[55] Mi Kyung Choe, Manyoel Lim, June Sic Kim, Dong Soo Lee, and Chun Kee Chung. Disrupted resting state network of fibromyalgia in theta frequency. *Scientific reports*, 8(1):1–9, 2018.

[56] Alfred H. Clifford and Gordon B. Preston. *The Algebraic Theory of Semigroups*. Mathematical Surveys and Monographs. American Mathematical Society, 1961.

[57] David Cohen-Steiner, Herbert Edelsbrunner, and John Harer. Stability of persistence diagrams. *Discrete and Computational Geometry*, 37(1):103–120, 2007.

[58] David Cohen-Steiner, Herbert Edelsbrunner, John Harer, and Yuriy Mileyko. Lipschitz functions have $L_p$-stable persistence. *Foundations of Computational Mathematics*, 10:127–139, 2010.

[59] René Corbet. Verallgemeinerte Persistenzmoduln. Master's thesis, Technische Universität Berlin, 2016.

[60] René Corbet, Ulderico Fugacci, Michael Kerber, Claudia Landi, and Bei Wang. A kernel for multi-parameter persistent homology. *Computers & Graphics: X*, 2019.

[61] René Corbet and Michael Kerber. The representation theorem of persistence revisited and generalized. *Journal of Applied and Computational Topology*, 2018.

[62] William Crawley-Boevey. Decomposition of pointwise finite-dimensional persistence modules. *Journal of Algebra and its Applications*, 14(05):1550066, 2015.

[63] Justin Michael Curry. *Sheaves, Cosheaves and Applications*. PhD thesis, The University of Pennsylvania, 2014.

[64] Patrick Dehornoy. *Braids and Self-Distributivity*. Springer, 2000.

[65] Patrick Dehornoy, François Digne, Eddy Godelle, Daan Krammer, and Jean Michel. *Foundations of Garside theory*, volume 22. European Mathematical Society, 2015.

[66] Patrick Dehornoy and Luis Paris. Gaussian groups and garside groups, two generalisations of artin groups. *Proceedings of the London Mathematical Society*, 79(3):569–604, 1999.

[67] Boris Delaunay. Sur la sphère vide. A la mémoire de Georges Voronoï. *Bulletin de l'Académie des Sciences de l'URSS*, (6):793–800, 1934.

[68] Der-Tsai Lee. On k-nearest neighbor Voronoi diagrams in the plane. *IEEE Transactions on Computers*, C-31(6):478–487, 1982.

[69] Tamal K. Dey and Cheng Xin. Computing Bottleneck Distance for 2-D Interval Decomposable Modules. In *Proceedings of the 34th International Symposium on Computational Geometry*, pages 32:1–32:15, 2018.

[70] Tamal K. Dey and Cheng Xin. Computing Bottleneck Distance for Multi-parameter Interval Decomposable Persistence Modules, 2019.

[71] Tamal K. Dey and Cheng Xin. Generalized Persistence Algorithm for Decomposing Multi-parameter Persistence Modules. arXiv:1904.03766, 2019.

[72] Barbara Di Fabio and Massimo Ferri. Comparing persistence diagrams through complex vectors. In Murino V. and Puppo E., editors, *International Conference on Image Analysis and Processing*, pages 294–305. Springer, Cham, 2015.

[73] Paweł Dłotko. The persistence landscape toolbox. Software available at https://www.math.upenn.edu/~dlotko/persistenceLandscape.html.

[74] Pratik Doshi. *Using Topological Data Analysis for Text Classification*. PhD thesis, The University of North Carolina at Charlotte, 2018.

[75] Manfred Droste and Dietrich Kuske. Recognizable languages in divisibility monoids. *Mathematical Structures in Computer Science*, 11(6):743–770, 2001.

[76] Herbert Edelsbrunner. Weighted alpha shapes. Technical report, Champaign, IL, USA, 1992.

[77] Herbert Edelsbrunner. The union of balls and its dual shape. *Discrete & Computational Geometry*, 13(3):415–440, 1995.

[78] Herbert Edelsbrunner. Shape reconstruction with Delaunay complex. In Cláudio L. Lucchesi and Arnaldo V. Moura, editors, *LATIN'98: Theoretical Informatics*, pages 119–132, Berlin, Heidelberg, 1998. Springer Berlin Heidelberg.

[79] Herbert Edelsbrunner. *Geometry and Topology for Mesh Generation*. Cambridge Monographs on Applied and Computational Mathematics. Cambridge University Press, 2001.

[80] Herbert Edelsbrunner and John Harer. Jacobi sets of multiple Morse functions. In F. Cucker, R. DeVore, P. Olver, and E. Süli, editors, *Foundations of Computational Mathematics, Minneapolis 2002*, pages 37–57. Cambridge University Press, 2002.

[81] Herbert Edelsbrunner and John Harer. Persistent homology - a survey. *Contemporary Mathematics*, 453:257–282, 2008.

[82] Herbert Edelsbrunner and John Harer. *Computational topology: an introduction*. American Mathematical Society, 2010.

[83] Herbert Edelsbrunner, John Harer, and Amit K. Patel. Reeb spaces of piecewise linear mappings. In *Proceedings of the 24th Annual Symposium on Computational Geometry*, pages 242–250, 2008.

[84] Herbert Edelsbrunner, David Letscher, and Afra J. Zomorodian. Topological persistence and simplification. *Discrete and Computational Geometry*, 28:511–533, 2002.

[85] Herbert Edelsbrunner and Dmitriy Morozov. Persistent homology: Theory and practice. *Proceedings European Congress of Mathematics*, 2012.

[86] Herbert Edelsbrunner and Georg Osang. The multi-cover persistence of Euclidean balls. In *34th International Symposium on Computational Geometry (SoCG 2018)*. Schloss Dagstuhl-Leibniz-Zentrum fuer Informatik, 2018.

[87] Herbert Edelsbrunner and Raimund Seidel. Voronoi diagrams and arrangements. *Discrete & Computational Geometry*, 1(1):25–44, 1986.

[88] Samuel Eilenberg and Norman E. Steenrod. Axiomatic approach to homology theory. *Proceedings of the National Academy of Sciences*, 31(4):117–120, 1945.

[89] David Eisenbud. *Commutative Algebra: With a View Toward Algebraic Geometry*. Graduate Texts in Mathematics. Springer, 1995.

[90] Brittany T. Fasy, Jisu Kim, Fabrizio Lecci, Clément Maria, David L. Millman, and Vincent Rouvreau. TDA: statistical tools for topological data analysis. Software available at https://CRAN.R-project.org/package=TDA.

[91] Kaspar Fischer, Bernd Gärtner, Thomas Herrmann, Michael Hoffmann, and Sven Schönherr. Bounding volumes. In *CGAL User and Reference Manual*. CGAL Editorial Board, 5.0 edition, 2019.

[92] Patrizio Frosini and Claudia Landi. Size theory as a topological tool for computer vision. *Pattern Recognition and Image Analysis (Advances in Mathematical Theory and Applications)*, 9(4):596–603, 1999.

[93] Ulderico Fugacci and Michael Kerber. Chunk reduction for multi-parameter persistent homology. In *35th International Symposium on Computational Geometry (SoCG 2019)*. Schloss Dagstuhl-Leibniz-Zentrum fuer Informatik, 2019.

[94] Peter Gabriel. Unzerlegbare Darstellungen I. *Manuscripta mathematica*, 6(1):71–103, 1972.

[95] Oliver Gäfvert and Wojciech Chachólski. Stable invariants for multidimensional persistence. *arXiv:1703.03632*, 2017.

[96] Hitesh Gakhar and Jose A. Perea. Künneth formulae in persistent homology. *arXiv:1910.05656*, 2019.

[97] Alfred Geroldinger and Franz Halter-Koch. *Non-Unique Factorizations: Algebraic, Combinatorial and Analytic Theory*. Pure and Applied Mathematics. Chapman and Hall CRC, 2006.

[98] Robert Ghrist. Barcodes: the persistent topology of data. *Bulletin of the American Mathematical Society*, 45(1):61–75, 2008.

[99] Robert Ghrist. *Elementary applied topology*. Createspace Seattle, 2014.

[100] Chad Giusti, Eva Pastalkova, Carina Curto, and Vladimir Itskov. Clique topology reveals intrinsic geometric structure in neural correlations. *Proceedings of the National Academy of Sciences of the United States of America*, 112(44):13455–13460, 2015.

[101] Daniel Goldfarb. An application of topological data analysis to hockey analytics. *arXiv:1409.7635*, 2014.

[102] Gert-Martin Greuel and Gerhard Pfister. *A Singular Introduction to Commutative Algebra*. Springer Publishing Company, Incorporated, 2nd edition, 2007.

[103] Pierre A. Grillet. *Semigroups: An Introduction to the Structure Theory*. CRC Press, 2017.

[104] Wei Guo and Ashis G. Banerjee. Toward automated prediction of manufacturing productivity based on feature selection using topological data analysis. In *IEEE International Symposium on Assembly and Manufacturing*, pages 31–36, 2016.

[105] Stefano Gurciullo, Michael Smallegan, María Pereda, Federico Battiston, Alice Patania, Sebastian Poledna, Daniel Hedblom, Bahattin Tolga Oztan, Alexander Herzog, Peter John, et al. Complex politics: A quantitative semantic and topological analysis of uk house of commons debates. *arXiv:1510.03797*, 2015.

[106] Allen Hatcher. *Algebraic topology*. Cambridge University Press, Cambridge, 2000.

[107] Gregory Henselman-Petrusek. Eirene. Software available at https://github.com/Eetion/Eirene.jl, 2017.

[108] Giseon Heo, Kathryn Leonard, Xu Wang, and Yi Zhou. Interdisciplinary approaches to automated obstructive sleep apnea diagnosis through high-dimensional multiple scaled data analysis. In *Research in Data Science*, pages 81–107. Springer, 2019.

[109] Yasuaki Hiraoka, Takenobu Nakamura, Akihiko Hirata, Emerson G. Escolar, Kaname Matsue, and Yasumasa Nishiura. Hierarchical structures of amorphous solids characterized by persistent homology. *Proceedings of the National Academy of Sciences of the United States of America*, 113(26):7035–7040, 2016.

[110] Christoph Hofer, Roland Kwitt, Marc Niethammer, and Andreas Uhl. Deep learning with topological signatures. In I. Guyon, U. V. Luxburg, S. Bengio, H. Wallach, R. Fergus, S. Vishwanathan, and R. Garnett, editors, *Advances in Neural Information Processing Systems 30*, pages 1634–1644. Curran Associates, Inc., 2017.

[111] Christoph Hofer, Roland Kwitt, Marc Niethammer, and Andreas Uhl. Deep learning with topological signatures. In *Advances in Neural Information Processing Systems*, pages 1634–1644, 2017.

[112] Derek F. Holt. The meataxe as a tool in computational group theory. *London Mathematical Society Lecture Note Series*, pages 74–81, 1998.

[113] Sara Kališnik. Tropical coordinates on the space of persistence barcodes. *Foundations of Computational Mathematics*, 19(1):1–29, 2018.

[114] Lida Kanari, Paweł Dłotko, Martina Scolamiero, Ran Levi, Julian Shillcock, Kathryn Hess, and Henry Markram. A topological representation of branching neuronal morphologies. *Neuroinformatics*, 16(1):3–13, 2018.

[115] Bryn Keller, Michael Lesnick, and Theodore L. Willke. Persistent Homology for Virtual Screening. *chemRxiv preprint*, 2018.

[116] Michael Kerber. Persistent homology: State of the art and challenges. *Internationale Mathematische Nachrichten*, 231:15–33, 2016.

[117] Michael Kerber, Michael Lesnick, and Steve Oudot. Exact computation of the matching distance on 2-parameter persistence modules. In *35th International Symposium on Computational Geometry (SoCG 2019)*. Schloss Dagstuhl-Leibniz-Zentrum fuer Informatik, 2019.

[118] Michael Kerber and Arnur Nigmetov. Efficient approximation of the matching distance for 2-parameter persistence. In *36th International Symposium on Computational Geometry (SoCG 2020)*. Schloss Dagstuhl-Leibniz-Zentrum fuer Informatik, 2020.

[119] Michael Kerber and Hannah Schreiber. Barcodes of towers and a streaming algorithm for persistent homology. *Discrete & Computational Geometry*, 61(4):852–879, 2019.

[120] Dmitry Krasnoshchekov and Valentin Polishchuk. Order-k alpha-hulls and alpha-shapes. *Information Processing Letters*, 114(1-2):76–83, 2014.

[121] Genki Kusano, Yasuaki Hiraoka, and Kenji Fukumizu. Persistence weighted gaussian kernel for topological data analysis. In *International Conference on Machine Learning*, pages 2004–2013, 2016.

[122] Dietrich Kuske. Divisibility monoids: Presentation, word problem, and rational languages. In *International Symposium on Fundamentals of Computation Theory*, pages 227–239. Springer, 2001.

[123] Roland Kwitt, Stefan Huber, Marc Niethammer, Weili Lin, and Ulrich Bauer. Statistical topological data analysis - a kernel perspective. In C. Cortes, N. D. Lawrence, D. D. Lee, M. Sugiyama, and R. Garnett, editors, *Advances in Neural Information Processing Systems 28*, pages 3070–3078. Curran Associates, Inc., 2015.

[124] Tsit-Yuen Lam. *Lectures on Modules and Rings*. Graduate Texts in Mathematics. Springer New York, 1999.

[125] Claudia Landi. The rank invariant stability via interleavings. *arXiv:1412.3374*, 2014.

[126] Hyekyoung Lee, Moo K Chung, Hyejin Kang, Hongyoon Choi, Yu Kyeong Kim, and Dong Soo Lee. Abnormal hole detection in brain connectivity by kernel density of persistence diagram and hodge laplacian. In *2018 IEEE 15th International Symposium on Biomedical Imaging (ISBI 2018)*, pages 20–23. IEEE, 2018.

[127] Jean Leray. Sur la forme des espaces topologiques et sur les points fixes des représentations. *Journal de Mathématiques Pures et Appliquées*, 24, 1945.

[128] Michael Lesnick. Lecture notes for Math 840: Multiparameter persistence. https://www.albany.edu/~ML644186/AMAT_840_Spring_2019/Math840_Notes.pdf. Accessed: 2020-04-04.

[129] Michael Lesnick. The theory of the interleaving distance on multidimensional persistence modules. *Foundations of Computational Mathematics*, 15(3):613–650, 2015.

[130] Michael Lesnick and Matthew Wright (Project Founders). RIVET, visualization and analysis of two-parameter persistent homology. http://rivet.online/. Accessed: 2020-04-04.

[131] Michael Lesnick and Matthew Wright. Interactive visualization of 2-D persistence modules. *arXiv:1512.00180*, 2015.

[132] Michael Lesnick and Matthew Wright. Computing minimal presentations and Betti numbers of 2-parameter persistent homology. *arXiv:1902.05708*, 2019.

[133] Chunyuan Li, Maks Ovsjanikov, and Frédéric Chazal. Persistence-based structural recognition. *IEEE Conference on Computer Vision and Pattern Recognition*, 2014.

[134] Li Li, Wei-Yi Cheng, Benjamin S. Glicksberg, Omri Gottesman, Ronald Tamler, Rong Chen, Erwin P. Bottinger, and Joel T. Dudley. Identification of type 2 diabetes subgroups through topological analysis of patient similarity. *Science Translational Medicine*, 7(311):311ra174, 2015.

[135] Saunders Mac Lane. *Categories for the Working Mathematician*. Springer, 1971.

[136] Clément Maria, Jean-Daniel Boissonnat, Marc Glisse, and Mariette Yvinec. The Gudhi library: Simplicial complexes and persistent homology. In Hoon Hong and Chee Yap, editors, *Mathematical Software – ICMS 2014*, pages 167–174. Springer Berlin Heidelberg, 2014. Software available at https://project.inria.fr/gudhi/software/.

[137] Clément Maria and Steve Y. Oudot. Zigzag persistence via reflections and transpositions. In *Proceedings of the Twenty-sixth Annual ACM-SIAM Symposium on Discrete Algorithms*, SODA '15, pages 181–199, Philadelphia, PA, USA, 2015. Society for Industrial and Applied Mathematics.

[138] John McCleary. *A User's Guide to Spectral Sequences*. Cambridge University Press, 2001.

[139] Ezra Miller. Data structures for real multiparameter persistence modules. *arXiv:1709.08155*, 2017.

[140] Dmitriy Morozov. Dionysus. Software available at http://www.mrzv.org/software/dionysus/.

[141] James R. Munkres. *Topology: a first course*. Prentice-Hall. 1975.

[142] Vidit Nanda. Perseus, the persistent homology software. Software available at http://www.sas.upenn.edu/~vnanda/perseus, 2013.

[143] Joseph Neggers and Hee Sik Kim. *Basic Posets*. World Scientific, 1998.

[144] Monica Nicolau, Arnold J. Levine, and Gunnar Carlsson. Topology based data analysis identifies a subgroup of breast cancers with a unique mutational profile and excellent survival. *Proceedings National Academy of Sciences of the United States of America*, 108(17):7265–7270, 2011.

[145] Partha Niyogi, Stephen Smale, and Shmuel Weinberger. Finding the homology of submanifolds with high confidence from random samples. *Discrete & Computational Geometry*, 39(1-3):419–441, 2008.

[146] Steve Y. Oudot. *Persistence theory: from quiver representations to data analysis*. American Mathematical Society, 2015.

[147] Matthieu Picantin. Garside monoids vs divisibility monoids. *Mathematical Structures in Computer Science*, 15(2):231–242, 2005.

[148] Henri Poincaré. Complément à l'analysis situs. *Rendiconti del Circolo Matematico di Palermo*, (13):285–343, 1899.

[149] Talha Qaiser, Yee-Wah Tsang, Daiki Taniyama, Naoya Sakamoto, Kazuaki Nakane, David Epstein, and Nasir Rajpoot. Fast and accurate tumor segmentation of histology images using persistent homology and deep convolutional features. *Medical image analysis*, 55:1–14, 2019.

[150] Jan Reininghaus, Stefan Huber, Ulrich Bauer, and Roland Kwitt. A stable multi-scale kernel for topological machine learning. In *IEEE Conference on Computer Vision and Pattern Recognition*, pages 4741–4748, 2015.

[151] Vanessa Robins. Towards computing homology from approximations. *Topology Proceedings*, 24, 1999.

[152] José Carlos Rosales and Pedro A. García-Sánchez. *Finitely Generated Commutative Monoids*. Nova Science Publishers, 1999.

[153] Martina Scolamiero, Wojciech Chachólski, Anders Lundman, Ryan Ramanujam, and Sebastian Öberg. Multidimensional persistence and noise. *Foundations of Computational Mathematics*, 17(6):1367–1406, 2017.

[154] Donald R. Sheehy. A multicover nerve for geometric inference. In *Proceedings of the 24th Canadian Conference on Computational Geometry*, 2012.

[155] Donald R. Sheehy. Linear-size approximations to the Vietoris–Rips filtration. *Discrete & Computational Geometry*, 49(4):778–796, 2013.

[156] Gurjeet Singh, Facundo Mémoli, and Gunnar Carlsson. Topological methods for the analysis of high dimensional data sets and 3D object recognition. In *Eurographics Symposium on Point-Based Graphics*, pages 91–100, 2007.

[157] Ann E. Sizemore, Chad Giusti, Ari Kahn, Jean M. Vettel, Richard F. Betzel, and Danielle S. Bassett. Cliques and cavities in the human connectome. *Journal of computational neuroscience*, 44(1):115–145, 2018.

[158] Primoz Skraba, Maks Ovsjanikov, Frédéric Chazal, and Leonidas Guibas. Persistence-based segmentation of deformable shapes. *IEEE Computer Society Conference on Computer Vision and Pattern Recognition Workshop on Non-Rigid Shape Analysis and Deformable Image Alignment*, 2010.

[159] Jian Sun, Maks Ovsjanikov, and Leonidas Guibas. A concise and provably informative multi-scale signature based on heat diffusion. *Computer Graphics Forum*, 28(5):1383–1392, 2009.

[160] Nicolas Tchitchek, Amie J. Eisfeld, Jennifer Tisoncik-Go, Laurence Josset, Lisa E Gralinski, Christophe Bécavin, Susan C. Tilton, Bobbie-Jo Webb-Robertson, Martin T. Ferris, Allison L. Totura, et al. Specific mutations in h5n1 mainly impact the magnitude and velocity of the host response in mice. *BMC systems biology*, 7(1):69, 2013.

[161] Ashleigh Thomas. *Invariants and Metrics for Multiparameter Persistent Homology*. PhD thesis, Duke University, 2019.

[162] Katharine Turner, Sayan Mukherjee, and Doug M. Boyer. Persistent homology transform for modeling shapes and surfaces. *Information and Inference: A Journal of the IMA*, 3(4):310–344, 2014.

[163] Bartel Leendert van der Waerden. *Algebra II*. Springer Berlin Heidelberg, 1993.

[164] Mikael Vejdemo-Johansson. Sketches of a platypus: a survey of persistent homology and its algebraic foundations. *Contemporary Mathematics*, 620, 2014.

[165] Leopold Vietoris. Über den höheren Zusammenhang kompakter Räume und eine Klasse von zusammenhangstreuen Abbildungen. *Mathematische Annalen*, 97(1):454–472, 1927.

[166] Oliver Vipond. Multiparameter persistence landscapes. *arXiv:1812.09935*, 2018.

[167] Boto von Querenburg. *Mengentheoretische Topologie*. Springer Berlin Heidelberg, 2001.

[168] Georgy Voronoi. Recherches sur les paralléloèdres primitives. *Journal für die reine und angewandte Mathematik*, 134:198–287, 1908.

[169] Yuan Wang, Hernando Ombao, and Moo K. Chung. Topological data analysis of single-trial electroencephalographic signals. *Annals of Applied Statistics*, 12(3):1506–1534, 2017.

[170] Friedrich Wehrung. Tensor products of structures with interpolation. *Pacific Journal of Mathematics*, 176(1):267–285, 1996.

[171] André Weil. Sur les théorèmes de de Rham. *Commentarii Mathematici Helvetici*, 26:119–145, 1952.

[172] Kelin Xia and Guo-Wei Wei. Multidimensional persistence in biomolecular data. *Journal of computational chemistry*, 36(20):1502–1520, 2015.

[173] Jaejun Yoo, Eun Young Kim, Yong Min Ahn, and Jong Chul Ye. Topological persistence vineyard for dynamic functional brain connectivity during resting and gaming stages. *Journal of Neuroscience Methods*, 267(15):1–13, 2016.

[174] Mariette Yvinec. 2D triangulation. In *CGAL User and Reference Manual*. CGAL Editorial Board, 5.0 edition, 2019.

[175] Afra Zomorodian. *Topology for Computing*. Cambridge University Press, 2009.

[176] Afra Zomorodian and Gunnar Carlsson. Computing persistent homology. *Discrete and Computational Geometry*, 33(2):249–274, 2005.